Parasitic Influences on the Host Genome Using the Molluscan Model Organism *Biomphalaria glabrata*

A thesis submitted for the degree of

Doctor of Philosophy

By

Halime D. Arican-Goktas

Biosciences, School of Health Sciences and Social Care

Brunel University

September 2013

Abstract

The freshwater snail *Biomphalaria glabrata* is an intermediate host for *Schistosoma mansoni* parasites, causing one of the most prevalent parasitic infections in mammals, known as schistosomiasis (Bilharzia). Due to its importance in the spread of the disease *B. glabrata* has been selected for whole genome sequencing and is now a molluscan model organism. In order to aid the sequencing project and to understand the structure and organisation of *B. glabrata*'s genome at the chromosomal level, a G-banded karyotype has been established. Unlike in any other previous reports, two heteromorphic chromosomes have been identified in the genome of *B. glabrata* and for the first time snail ideograms have been produced. In addition to characterising the snail chromosomes, a methodology for mapping single copy *B. glabrata* genes onto these chromosomes has also been established, and 4 genes have successfully been mapped using fluorescence *in situ* hybridisation.

In the relationship between a parasite and a host organism, it is of fundamental importance to understand the basic biology and interfere with the life cycle to reveal how the parasite controls and elicits host gene expression for its own benefit. This study is also directly addressing this aspect of host – parasite interactions by investigating the effects of schistosome infection on the genome and cell nuclei of the host snail *B. glabrata.* Upon infection with *S. mansoni* miracidia, genes known to be involved in the host response to the parasite are dramatically relocated within the interphase snail nuclei. These events are in conjunction with the up-regulation of gene expression, indicating a parasite induced nuclear event. Moreover, a differential response between the schistosome-resistant and schistosome-susceptible snails is also reported. This is the first time this has been described in a host – pathogen relationship.

The precise organisation of the genome is critical for its correct functioning. The genome is non-randomly organised and this level of organisation is very much influenced by the nuclear architecture. Being a molluscan model organism with the availability of a unique cell line, *B. glabrata* is a remarkable organism for the studies of nuclear and genome biology. For this reason, in this thesis the snail nuclear architecture was also investigated. For the first time PML bodies, transcription factories, and nuclear myosin 1β have been visualised in the snail nuclei. A heat shock system was also developed to study the role of these structures in the snail. Upon heat stimuli gene loci were found to reposition and co-localise with transcription factories, which was in parallel with the up-regulation of gene expression. The mechanism of this genome reorganisation was explored by investigating nuclear motor structures in the snail. By using a motor inhibitor on snail cells, gene repositioning and subsequent expression after heat shock was blocked. This is the first time this has been shown in any organism. Thus, due to the ease of use of the snails with respect to maintenance, handling, and treatments, *B. glabrata* is making a very useful new model organism to study spatial genomic events.

Declaration

I hereby declare that all the work presented in this thesis has been performed by me unless otherwise stated.

Halime D. Arican-Goktas

Acknowledgements

I would like to first of all thank my supervisor, my "PhD mother" Dr Joanna Bridger for her guidance, support, strength, and encouragement throughout my PhD. The pure passion and enthusiasm she conveys has been the keystone for my morale and has kept me going for the last 4 years. I am highly grateful for this special experience that I will always treasure and thank her for giving me this opportunity.

I would like to express my sincere thanks to Dr Margaret Town and Dr Christopher Eskiw for the trainings, support, and advice they have always given me since the beginning of my PhD.

I would like to thank our collaborators from the Biomedical Research Institute-USA, Dr Matty Knight, Dr Wannaporn Ittiprasert, Andre Miller, and Dr Fred Lewis for supplying the *B. glabrata* snails, the Bge cells, and the *B. glabrata* BAC genes. I specially would like to thank Dr Matty Knight and Dr Wannaporn Ittiprasert for their encouragement, advice, support, and training they have given me as well as for the qRT-PCR work they have done on *B. glabrata* genes.

I would also very much like to thank our collaborators Dr Emmanuela Volpi and Dr Mohammed Yusuf for their guidance, assistance, training, and use of equipment when karyotyping the snail.

I would like to express my gratitude to the staff from the Brunel institute for the environment for their helpful comments and assistance pertaining to snail husbandry, in particular to Steven Pash whom sadly is no longer with us today. May he rest in peace.

I am very grateful to Prof. Wendy Bickmore and Dr Paul Perry for the 2D FISH erosion script analysis.

I reserve a special thank you to the members of the CCBG and the PhD office 143 for their helpful advice and support but most of all for their friendship and making my PhD an enjoyable experience.

Also a big thank you to my PhD “sister” Safia Reja, for always being there for me and for such fun times we had together in the tissue culture lab during our PhD’s, which I will always remember.

I would like to say a huge thank you to my Mummy, Daddy, and Brother Enes for there continues love and support. Finally to my friend, my soul mate, my husband Yunus not least for his words of encouragement and support, but for keeping up with all my science and snail talks and keeping me as sane as possible throughout the last push of my research and the thesis writing. I love you all!

Abbreviations

2D	Two-dimensional
3D	Three-dimensional
BB02	Resistant *B. glabrata* snail
BDM	2,3-Butanedione 2-Monoxime
BLAST	Basic local alignment search tool
BSA	Bovine serum albumin
BS90	Brazilian isolate resistant *B. glabrata* snail
cDNA	Complementary DNA
Cy3	Cyanine 3
DAPI	4, 6 di-aminino-2-phenylindole
DIG	Digoxigenin-11-dUTP
DNA	Deoxyribonucleic acid
EBSS	Earle's balanced salt solution
EDTA	Ethylenediaminetetraacetic acid
FISH	Fluorescence *in situ* hybridisation
FITC	Fluorescein isothiocyanate
FBS	Foetal bovine serum
g	Grams
HCl	Hydrochloric acid

HSPs	Heat shock proteins
M	Molar
mg	Milligrams
ml	Millilitres
mM	Millimolar
mRNA	Messenger RNA
NaCl	Sodium chloride
NE	Nuclear envelope
NCS	Newborn calf serum
NM1β	Nuclear myosin 1β
NMRI	Laboratory derived susceptible *B. glabrata* snail
PBS	Phosphate buffered saline
PFA	Paraformaldehyde
PI	Propidium Iodide
PML	Promyelocytic leukaemia
qRT-PCR	Quantitative reverse transcription – polymerase chain reaction
RNA	Ribonucleic acid
RNAP II	RNA polymerase II
SD	Standard deviation

SDS	Sodium dodecyl sulfate
SSC	Saline sodium citrate
Sec	Second
SEM	Standard error of mean (SD / square root of the sample size)
TF	Transcription factory
μg	Microgram
μl	Microliter
μM	Micromolar

Table of Contents

Table of Figures

Table of Tables

Chapter 1

Introduction

Part I

1.1 The molluscan model organism: *Biomphalaria glabrata*

Snails of the genus *Biomphalaria* are of significant medical importance due to their connection with larval trematodes, the causative agents of human schistosomiasis (Bilharzia). The disease disrupts the lives of over 200 million people in 78 countries preventing individuals from an otherwise reasonable expectation of a healthy life. Of these snails the freshwater snail *Biomphalaria glabrata,* the intermediate snail host for *Schistosoma mansoni* in causing schistosomiasis in humans, is one of the most thoroughly studied species due to its importance in the spreading of the disease. Because of this *B. glabrata* has been selected for whole genome sequencing and became a molluscan model organism. Therefore in addition to the impact of *B. glabrata* on public health, these snails have also become interesting targets for the study of other topics such as nuclear biology and immunology. Thus the first section of this chapter will provide an overview of advances in the snail – trematode relationship and the schistosomiasis disease, as well as the importance of *Biomphalaria* snails in genome organisation studies.

1.1.1 Schistosomes and Schistosomiasis

In 1851 Theodore Bilharz described the first species of worm parasites found in the human blood vessels. These worm parasites were identified to belong to the *Schistosoma* genus of the class Trematoda (flat worms) and are commonly referred as schistosomes, blood flukes or bilharzia – in honour of Theodore Bilharz (Hoffmann and Dunne, 2003). It is these schistosomes that cause a 'neglected' tropical disease, schistosomiasis, in mammals.

Schistosome parasites are unique trematodes such that they are dioecious, consisting of both male and female sexes. The adult worms are found in *copulo* within the veins of the definitive host, with the longer and thinner female being held in the gynaecophoric channel of the male's body (Walker, 2011; Gryseels *et al.*, 2006). These parasites have a complex life cycle involving a definitive host and an intermediate host [Fig. 1.1]. The life cycle begins with the release of eggs by the adult female schistosome, infecting the blood vessels of its definitive host (humans or other mammals). On average a single schistosome can produce 300 eggs per day, which are released via urine or faeces. On contact with water, the eggs develop into miracidia (viable for up to 24 hours) and penetrate into the intermediate host, a freshwater snail (Walker, 2011; Gryseels *et al.*, 2006; Grevelding, 2004; Anderson *et al.,* 1982).

After penetrating the head/foot region of the snail, the schistosome miracidia go through asexual reproduction to transform into primary sporocysts, followed by a second generation of daughter sporocysts. They remain in the head foot region for 2-3 weeks, after which they can be found in the digestive gland-gonad (DGG) complex (Rafael Toledo and Fried, 2011). The larval stage, known as cercariae emerges from the snail approximately a month after the initial infection (Walker, 2011; Richards and Shade, 1987). Once released from the snail, the highly motile cercariae are viable in water for up to 72 hours, during which they seek a suitable definitive host. Once a suitable host is found, the cercariae penetrate into the skin and transform into schistosomulae. They enter the circulatory system and migrate in the blood via the lungs into the liver. The schistosomulae mature in the portal vein for 4-6 weeks, prior to migrating to perivesicular or mesenteric veins (depending on the species of the parasite) to mate and release eggs to begin a new life cycle. The average life span of a schistosome in the human body is 3-5 years, however they can live up to 30 years (Gryseels *et al.*, 2006).

Figure 1.1 The life cycle of a schistosome parasite, showing the transmission from the intermediate snail host to the definitive human host. (Source: Centers for Disease Control and Prevention: http://www.cdc.gov/parasites/schistosomiasis/biology.html)

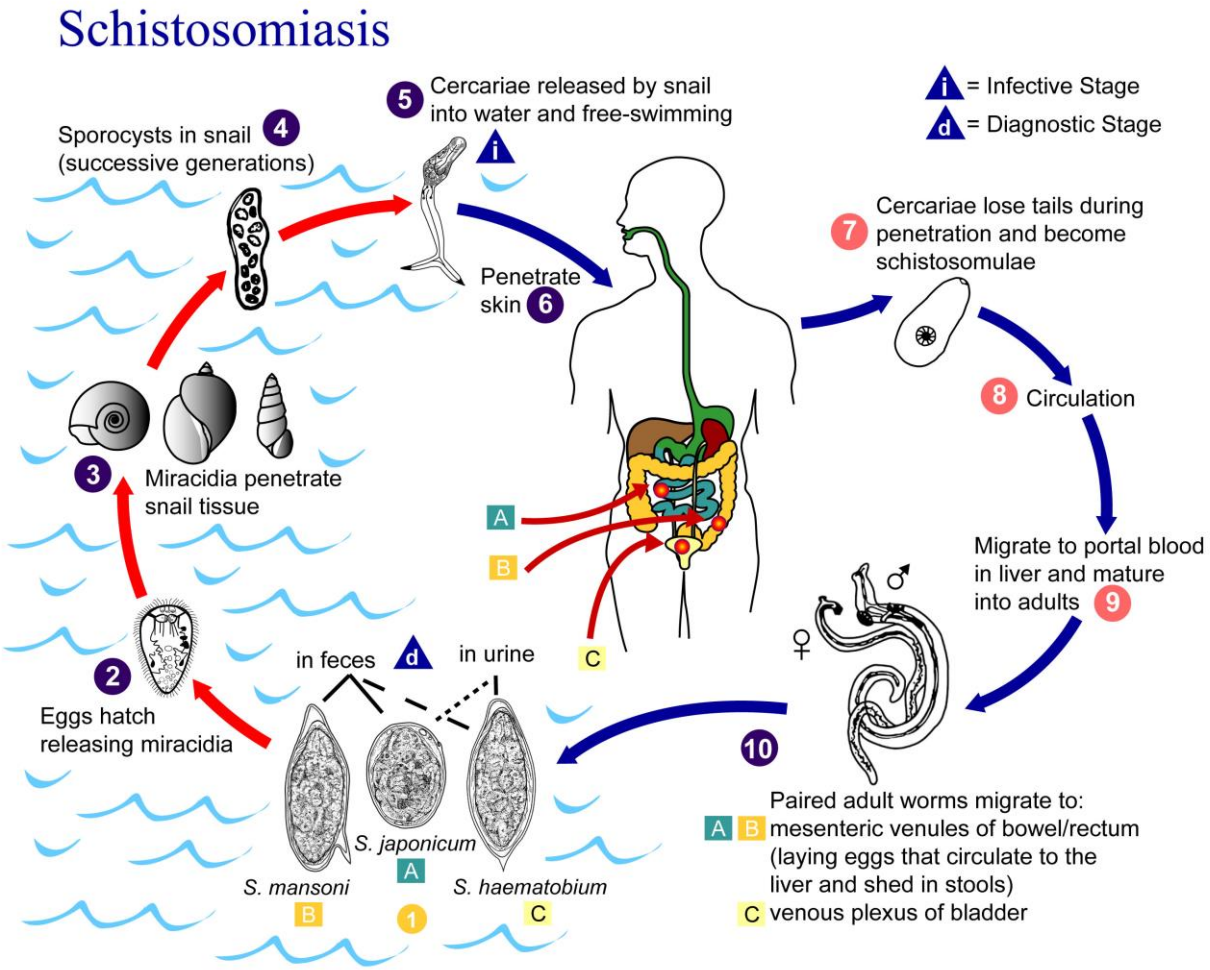

Various species of schistosome are capable of infecting humans [Table 1.1]. However the three most common species causing schistosomiasis are *S. mansoni* and *S. japonicum,* both infecting the blood vessels of the intestines, and *S. haematobium*, which infect the blood vessels of the bladder (Hoffmann and Dunne, 2003). Other than humans the definitive hosts include cats, dogs, goats, horses, pigs, rats, and buffalo. Although rare, infections in baboons and monkeys have also been documented (Blanchard, 2004; Cook and Zumla, 2003).

Table 1.1 Displaying human schistosomes, their intermediate hosts, and regions of endemicity.

Schistosome parasite	Intermediate host snail	Endemic regions
S. mansoni	*Biomphalaria* spp.	Africa, South, America, Caribbean, Middle East
S. haematobium	*Bulinus* spp.	Africa, Middle East
S. japonicum	*Oncomelania* spp.	Asia
S. intercalatum	*Bulinus* spp.	Africa
S. mekongi	*Neotricula aperta*	Asia

The clinical presentation of schistosomiasis is very varied. The acute phase of the disease, known as the Katayama syndrome, occur within 2-6 weeks after exposure (Blanchard, 2004). It is a hypersensitivity reaction against the migrating schistosomulae and can cause fatigue, malaise, cough, and eosinophilia (Gryseels *et al.*, 2006). At this stage, if the disease is left untreated it can progress onto the chronic phase. The chronic infection is not due to the presence of the adult worms but to the eggs trapped in tissues (Gryseels *et al.*, 2006). While the eggs are partially expelled via faeces, approximately half remain in the body and are enveloped by granulomas (Cheever *et al.*, 2002). Pathology is caused by a granulomatous reaction to the eggs, which destroy tissue and causes fibrosis (Blanchard, 2004). A chronic infection with *S. haematobium* results in urinary schistosomiasis. One of the first signs of urinary schistosomiasis is haematuria (blood in urine), with a possible late stage complication of bladder cancer. Progressive damage to the bladder, kidneys and ureters are also observed with urinary schistosomiasis (WHO). Infections with *S. mansoni* or *S. japonicum* cause intestinal schistosomiasis, which leads to progressive enlargement to the liver and spleen, as well as intestinal damage and hypertension. Other signs include abdominal pain, diarrhoea and blood in stool (WHO).

Diagnosis of schistosomiasis involves the examination of excreta for eggs. Owing to their size, shape, and typical lateral or terminal spine, the eggs are easy to detect and identify by microscopy analysis (Gryseels *et al.*, 2006). Serological testing is also used as a screening tool, however schistosomal serology can be negative early in infection and frequently remains positive despite adequate treatment (Meltzer and Schwartz, 2013; Blanchard, 2004). Treatment involves the use of an anti-schistosome drug, praziquentel, which has been the mainstay of treatment over the past 30 years (Meltzer and Schwartz, 2013; Hoffmann and Dunne, 2003). It acts by paralysing the worms and damaging the tegument, leading to their eventual death (Pearce, 2003). Other drugs used to treat schistosomiasis include oxamniquine, corticosteroids, anticonvulsants, and artemisinin derivatives (Gryseels *et al.*, 2006). Drug treatment however have a very limited effect in keeping the disease under control due to people being susceptible to reinfection. There is also the increasing risk of the parasite developing resistance to these drugs (Helleberg and Thybo, 2010; Doenhoff *et al.*, 2002).

According to the figures announced by the World Health Organisation, schistosomiasis affects 243 million people in 78 countries of the tropics and subtropics. It is also estimated that there are more than 200,000 deaths per year due to schistosomiasis, and it is ranked as the second most prevalent parasitic infection after malaria (WHO). Despite the combined use of molluscicides to reduce the snail population along with mass chemotherapy on humans, there is still an estimate of 800 million people in the tropics at risk from developing schistosomiasis. The main reason for this is the agricultural and irrigation projects designed to improve the quality of life. The construction of dams and irrigation schemes expand the aquatic habitat of the snail host, which often results in the spread of the disease into new areas (Knight *et al.*, 1999).

In view of these challenges, alternative methods that will lead to long term prevention for schistosomiasis are being sought. These include the development of an effective, protective vaccine (Siddiqui *et al.,* 2001) as well as the development of novel intervention tools in blocking the transmission of the parasite at the snail's stage of its life cycle (Ittiprasert and Knight, 2012; Rollinson *et al.*, 2009; King *et al.*, 2006).

1.1.2 *Biomphalaria glabrata*

B. glabrata (also known as the blood fluke planorb) is the freshwater snail acting as an intermediate host for the transmission of *S. mansoni* in the Western Hemisphere [Fig. 1.2]. It is a member of the class Gastropoda within the molluscan phylum and is mostly found in South America as well as Greater and Lesser Antilles. Due to its close association with schistosomiasis disease, it is one of the most thoroughly studied host species for schistosomes (Knight *et al.*, 2002).

Figure 1.2 The freshwater snail *Biomphalaria glabrata* (Photograph courtesy of Dr Matty Knight, Biomedical Research Institute, USA).

Biomphalaria snails are found in various aquatic habitats including ponds, lakes, streams, and irrigation channels (Rafael Toledo and Fried, 2011). Their diet consists of aquatic plants and the cyanobacterium*, nostoc*, found in soil and mud (Lewis *et al.*, 1986). *B. glabrata* is the largest *Biomphalaria* species with a shell that can reach up to 40 mm in diameter. Its shell has a counter clockwise spiral and is described as discoid, sinistral with a rounded to oval aperture (Rafael Toledo and Fried, 2011). Transcending the shell of the snail is the mantle, which consists of the muscular head-foot region providing locomotion. *B. glabrata* snails are hermaphrodites with the ability to both self and cross fertilise. Both the egg and sperm are produced in a single organ, known as the ovotestis (Genome: Biomphalaria glabrata). The snails have a short generation time of less than 2 months, and have a life span of up to 18 months (Rafael Toledo and Fried, 2011).

1.1.3 Resistance and susceptibility traits in the snail

B. glabrata snails exist in two forms; while some snails are resistant to the invading parasite other snails are susceptible resulting in the shedding of cercariae, which infect mammals causing the schistosomiasis disease. W. L. Newton first identified this trait in *B. glabrata* when he observed that susceptibility of *B. glabrata* to *S. mansoni* varied in different geographic areas (Newton, 1953). By crossing the non-susceptible albino Brazilian strain with the susceptible pigmented Puerto Rican strain, he noticed that a proportion of the F_1 generation were susceptible to infection with *S. mansoni,* however the snails of albino parental origin were not. When he self fertilised the F_1 albino parental snails, the F_2 progeny had some resistant and highly susceptible snails. Newton was then able to conclude that susceptibility in *B. glabrata* was indeed an inheritable trait, with multiple genetic factors involved (Newton, 1953). Following from Newton's work, in 1973 Richards identified that the resistant trait in the adult snails follow a simple Mendelian nature, governed by a single gene locus with resistance being dominant.

He also noted that resistance in juvenile snails is more complex involving several genes (Richards *et al.,* 1992; Richards, 1973). Furthermore, age related variations in susceptibility were also documented, with susceptible juvenile snails becoming resistant when they reach adulthood (Richards and Minchella, 1987). Aside from these early studies, the development in molecular techniques has now lead to the identification of genetic and molecular basis of the snail - schistosome relationship.

Today numerous strains of *B. glabrata* snails are used in laboratories all over the world, often derived from field isolates or produced via laboratory controlled crosses. The BS90 and BB02 strains are natural field isolates from Brazil. With the BS90 strain snails being totally resistant to *S. mansoni,* BB02 strains are highly susceptible. Another susceptible strain is the laboratory derived albino snails known as NMRI (Miller *et al.*, 2001).

1.1.4 Immunity and parasite destruction in *B. glabrata*

The genetic phenotypes of susceptibility to *S. mansoni* differ among various strains of *B. glabrata.* In the resistant snails, there exists an innate ability to destroy the invading parasites. Molluscs lack an adaptive immune system and appear to use this innate mechanism involving cell mediated and humoral reactions that interact to recognise and eliminate the pathogen (Rafael Toledo and Fried, 2011; Walker, 2006). Molluscs posses a heamolymphatic circulatory system, an equivalent to the fluid and cells making up blood and interstitial fluid. Within the haemolymph are circulating phagocytic cells termed haemocytes, which are dispersed throughout the haemolymph, and bind to invading pathogens leading to their subsequent destruction (Yoshino and Coustau, 2011; Rafael Toledo and Fried, 2011; Raghavan and Knight, 2006; Walker, 2006). Production of haemocytes takes place primarily in an amebocyte producing organ (APO), located in the anterior pericardial wall (Jeong *et al.*, 1983).

In *B. glabrata* and other pulmonates, two distinctive cell types of haemocytes are reported: granulocytes and hyalinocytes (Yoshino and Coustau, 2011; Humphries, 2003). Upon infection with miracidia, the circulating haemocytes aggregate and encapsulate the sporocyst (formed after miracidium infects the snail). Following this encapsulation, the haemocyte-mediated cytotoxicity mechanism of the snail gets activated leading to the destruction and elimination of the parasite (Lockyer *et al.*, 2007). However, in susceptible snails the ability of haemocytes to destroy the invading pathogen seems to have been effectively nullified by the parasite (Humphries, 2003).

Oxygen dependant killing mechanisms play a major role in haemocyte activity and reactive oxygen species (ROS) are involved in cell mediated killing of the invading parasite in *B. glabrata.* Bayne and colleagues have demonstrated that hydrogen peroxide (H_2O_2) and nitric oxide (NO), elaborated from haemocytes of resistant *B. glabrata* are involved in killing of the encapsulated sporocysts (Bayne *et al.,* 2001; Bender *et al.,* 2005). Mechanisms that regulate molluscan haemocyte defence responses include the extracellular signal-regulated kinase (ERK) signalling pathway, which has been found to coordinate the NO and H_2O_2 output (Zahoor *et al.*, 2009; Humphries and Yoshino, 2008; Wright *et al.*, 2006). In fact Cu/Zn-superoxidase dismutase (SOD1) was implicated in having a key role in oxidative killing activity of haemocytes, with SOD1 gene expression and enzyme activity found to be higher in haemocytes of resistant snails than in susceptible snails (Goodall *et al.*, 2004). Goodall *et al* then identified three alleles of SOD1, of which one was significantly correlated with snail resistance (Goodall *et al.*, 2006). This was followed by another study reporting the higher levels of SOD1 transcripts identified in haemocytes from the snails with the resistance associated allele, previously reported by Goodall *et al* (Bender *et al.*, 2007). These results clearly substantiated the contributory role SOD1 has in *B. glabrata* resistance against *S. mansoni.*

Other components of snail defence include the fibrinogen-related proteins (FREPs), encoded by a large gene family first documented in *B. glabrata* (Adema *et al.*, 1997). These proteins are thought to function in the immune response of *B. glabrata* as they are up-regulated following exposure to trematodes (Hertel *et al.,* 2005) and can bind to the surface of miracidia, sporocysts, and their excretory/secretory products (ESPs) (Zhang *et al.,* 2008; Adema *et al.*, 1997). Lockyer *et al* has also shown that elevated levels of FREPs are present in the resistant snails than in the susceptible snails. However an interesting result was that down-regulation was observed in exposed resistant snails (exposed to *S. mansoni*) compared to unexposed resistant snails (Lockyer *et al.*, 2007). This was thought to be the result of parasite manipulation to the normal snail defence response, which has greater effect in the susceptible strain but less significant in the resistant strain, allowing the resistant snails to overcome the challenge. In fact suppression of FREP3 in resistant snails resulted in increased susceptibility to *S. mansoni* infection (Hanington *et al.,* 2012), and FREP3 and FREP12 expression was also found to be greater in haemocytes of resistant snails than in susceptible snail post exposure to the parasite (Lockyer *et al.*, 2012). While FREP3 poses as an important candidate in the resistant phenotype of the snails, it is clear that FREPs in general play a role in immune defence of the snail against the invading pathogen. More recently a cytokine-like molecule, BgMIF (*B. glabrata* macrophage migration inhibitory factory), as well as a β pore-forming toxin (β-PFT) named Biomphalysin, have also been identified to play important roles in immune defence in *B. glabrata* against *S. mansoni* infection (Galinier, 2013; Garcia, 2010).

1.1.5 The host – parasite interactions

Differential expression and regulation of genes of *B. glabrata* in response to schistosomes are being intensively studied to elucidate factors influencing the host – parasite relationship.

This has been achieved via a variety of RNA profiling studies, including subtractive hybridisation, subtraction cDNA cloning, differential display, and microarray (Lockyer *et al.*, 2012; Hanington *et al.*, 2010; Lockyer *et al.*, 2008; Hanelt *et al.,* 2008; Mitta *et al.*, 2005; Lockyer *et al.*, 2004; Miller *et al.*, 2001). As mentioned previously anti-oxidants and lectins play an important role in immune defence of the snail (Hanington *et al.*, 2010; Humphries and Yoshino, 2008; Zhang *et al.,* 2008; Bender *et al.*, 2005; Adema *et al.*, 1997). Aside from these, other differentially regulated genes identified include the heat shock genes, in particular heat shock protein 70 (hsp70). Lockyer *et al* have reported the up-regulation of this gene only in the adult resistant snails and have also confirmed this in resistant snail haemocytes (Lockyer *et al.*, 2012; Lockyer *et al.*, 2004).

In contrast however, Ittiprasert *et al* have reported the induction of *hsp70* in juvenile susceptible snails but not resistant snails in response to parasitic infection (Ittiprasert *et al.*, 2009). The up-regulation of *hsp70* in juvenile resistant snails was also shown to be concurrent with the up-regulation of *B. glabrata* non-LTR retrotranspon, *nimbus* (Raghavan *et al.*, 2007). Although this co-induction may be a specific juvenile susceptible phenotype, the contrary results of the Lockyer study indicate that the age of the snail indeed matters in the regulation of gene expression. Zahoor *et al* also reported a greater reduction of hsp70 protein expression in susceptible snails following *S. mansoni* ESP exposure (Zahoor *et al.*, 2010). As the majority of host-parasite interactions in the snail are studied via RNA profiling looking at gene expression levels, similar protein expression studies in future looking at the protein levels in the snail following infection would allow a more advanced understating of this relationship. Nevertheless, the above discussed studies highlight the importance of stress related mechanisms in snail - schistosome relationship.

Another recent study by Ittiprasert *et al* has also shown that enhancing of stress genes (*hsp70, hsp90,* and reverse transcriptase) in the resistant juvenile snails via heat shock resulted in these snails becoming susceptible to *S. mansoni* infection. Treatment with an hsp90 specific inhibitor prior to heat shock resulted in the snails maintaining their refractory phenotype.

Interestingly however, inhibitor treated susceptible snails also became non-susceptible (Ittiprasert and Knight, 2012). Together, these studies point to stress induction and heat shock genes as an important pathway in *B. glabrata* – schistosome relationship.

In another study from Knight and Bridger, non-random radial positioning of the snail genome was revealed. However upon co-culture with *S. mansoni* miracidia, large scale gene repositioning events in the interphase nuclei of Bge cells was reported (Knight *et al.*, 2011a). Although how the parasite can cause such physical changes in its hosts genome is still unknown, heat shock and stress induction in the snail may be a possible pathway leading to such reorganisation. Given the importance of heat shock proteins in cellular and immune functions, it would be of great value to further elucidate the temporal dynamics of heat shock protein expressions to fully understand the role they play in snail-schistosome relationship.

The antioxidant enzyme peroxiredoxin (*BgPrx4*) is another differentially expressed gene, which is up-regulated in resistant snails and down-regulated in susceptible, following exposure to the parasite (Knight *et al.*, 2009). Given that this enzyme is postulated to function in the scavenging of harmful reactive oxygen species produced by the snail in response to parasitic invasion, it is yet another candidate gene with a possible role in resistance/susceptibility of *B. glabrata*.

From these and similar studies, it is apparent that there exists a parasite mediated transcription regulatory mechanism in controlling gene expression of resistant and susceptible snails. Although identifying these potential genes involved in snail resistance and susceptibility greatly enhances our knowledge on host-parasite interactions, the direct effect of the protein products encoded by most of these genes remains to be elucidated. However with the recent development of a gene silencing technique by RNA interference (RNAi) in the snail (Knight *et al.*, 2011b), identification of genes to target towards the development of parasite transmission blocking strategies in the snail has now been enabled (Rafael Toledo and Fried, 2011).

Other than interfering with the host defence responses, one other plausible explanation for parasite evasion in the snail host is parasite-mediated immunosuppression. This is believed to be achieved through molecular mimicry, with the parasite expressing shared moieties with their host, which benefits the parasite by preventing their recognition as nonself (Damian, 1989; Yoshino and Bayne, 1983). Dissous *et al* whom detected cross reactivity between glycoproteins from the surface of miracidia and from *B. glabrata* provided evidence for such mimicry (Dissous *et al.,* 1986). Thus it is possible that in the susceptible trait of *B. glabrata*, the parasite interferes or avoids the innate response of the snail through these complex interactions. Shared epitopes of carbohydrate moieties have also been reported in this host-parasite system (Yoshino, 2012; Rafael Toledo and Fried, 2011; Yoshino and Coustau, 2011; Lehr *et al.*, 2010). Immunosuppression is also achieved via the parasite interfering the snail cell signalling events involved in haemocyte activation. The *S. mansoni* ESP's were shown to attenuate phosphorylation of ERK in haemocytes from a susceptible *B. glabrata* strain (Zahoor *et al.*, 2008). Since ERK signalling pathway regulates various haemocyte defence reactions, it is thought that this disruption facilitates *S. mansoni* survival in susceptible snails (Walker, 2006).

In conclusion, it is clear that complex interactions that are still not fully understood exist between the snail and schistosome. The completion of the on-going snail genome project along with the *S. mansoni* genome will surely aid for a better understanding of this relationship. The overall message given from these host-parasite studies is that there exists a survival (parasite) and defence (snail) mechanisms, which involves manipulation of the hosts genome. Identification of these genetic factors is fundamental to elucidate this relationship, however what now remains to be answered is *how* does the parasite manipulate the hosts genome, and *what* are mechanisms involved in this process.

1.2 The snail genome project

Due to their role in schistosomiasis disease and transmission, *Biomphalaria* snails have been the targets of researchers for many years. Ever since the pioneering work of Newton and Richards on the heritability of the snail resistance to *S. mansoni,* ideas of preventing schistosomiasis have included the displacement of susceptible snails with the resistant strains (Raghavan and Knight, 2006). The implementation of this idea however relied upon identification of genes involved in the snail's resistance to schistosome parasites, which without knowing the sequence of the organism was exceptionally difficult to achieve. With the availability of the of the genome sequences of *Homo sapiens* (Venter *et al.*, 2001), and the parasites *S. mansoni* (Berriman *et al.*, 2009)*, S. japonicum* (Schistosoma japonicum Genome Sequencing and Functional Analysis Consortium, 2009)*,* and more recently *S. haematobium* (Young *et al.*, 2012), it became imperative the obtain the genome sequence of *B. glabrata*. In 2004 a proposition for complete sequencing of the *B. glabrata* genome was put forward to the National Human Genome Research Institute (NHGRN), and the genome sequencing project for the snail initiated in 2005 at the Washington University Genome Sequencing (WUGS) Centre (Rafael Toledo and Fried, 2011). Although the snail genome project is still on going, steady progress has been made and the sequence is expected to be published soon.

The genome size of *B. glabrata* is 931Mb, which is significantly larger than the genome of *S. mansoni* (270Mb). However when compared to the genomes of other molluscs, *B. glabrata* has one of the smallest genomes, hence why it was selected to have its genome sequenced (Raghavan and Knight, 2006). The genome is organised into 18 haploid chromosomes that are small and monomorphic (Goldman, 1983; Raghunathan, 1976; Narang, 1974). Earlier attempts of karyotyping these chromosomes have failed to obtain distinctive banding patterns due to technical difficulties, and have arranged them mostly according to size and centromere position [Fig 1.3] (Kawano *et al.,* 1987; Goldman *et al.*, 1984; Raghunathan, 1976).

Also available is the *B. glabrata* embryonic cell line, which was established by Eder Hansen in the 1970's (Hansen, 1979). Chromosomal analysis has shown the existence of anomalies within this cell line, with Bge1 containing 64 and Bge2 containing 67 chromosomes (Odoemelam *et al.*, 2010). Being the only molluscan cell line, this tissue culture system has been an important tool in studying the host-parasite relationship. Co-culture experiments with miracidia have shown repositioning of gene loci in the interphase nuclei of these cells (Knight *et al.*, 2011a), giving an insight to the effects a parasitic infection has on the host genome.

Figure 1.3 G-banded karyotype of *Biomphalaria glabrata* NIH strain 6-4-1, performed by Goldman *et al* in 1984. Chromosomes were arranged into nine groups according to size and centromere position. Scale bar = 5μm.

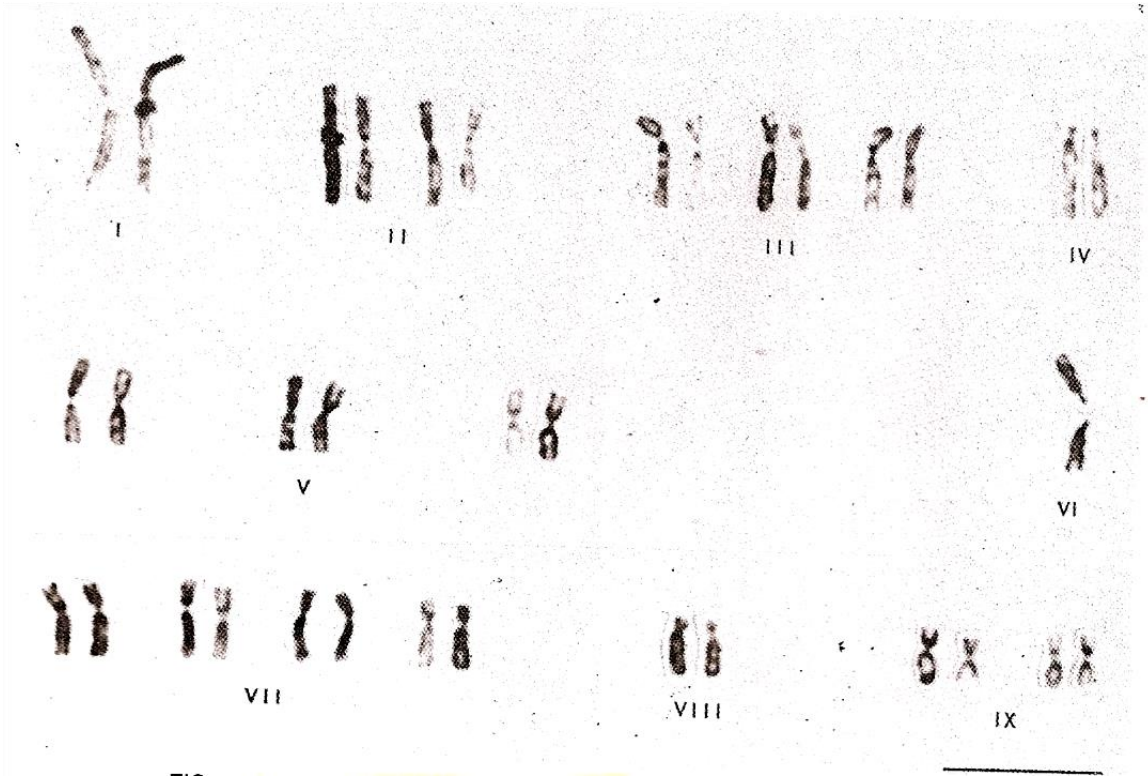

Currently two Bacterial Artificial Chromosome (BAC) libraries are available for *B. glabrata*. One of the BAC libraries was constructed from the wild type susceptible snail, BB02, the same snail stock chosen for whole genome sequencing (Adema *et al.*, 2006). The other BAC library is constructed from the resistant BS90 snail stock (Raghavan *et al.*, 2007). A cDNA microarray has also been constructed for *B. glabrata*, which consists of 2053 clones from the headfoot, ovotestis, haemopoeitic organ and haemocytes. (Lockyer *et al*., 2008). Also present is the fully sequenced *B. glabrata* mitochondrial genome, which was found to be AT rich and highly repetitive (DeJong *et al.,* 2004). Currently on the NCBI databases there are 55,831 nucleotide sequences (54,309 ESTs) and 730 protein entries. However there are no official records of where these gene sequences map on the snail genome, and no information is available regarding the snail chromosomes. Since 2010 a BLAST-able preliminary *B. glabrata* genome assembly database is also available, and more recently annotating efforts have now begun (Bg_Initiative).

So far, small but steady advances have been made to unravel the snail – trematode relationship. The anticipated completion of the whole genome sequencing project for *B. glabrata* will without a doubt lead to major advances in this field. Comparative genomic analysis between the human, parasite, and the snail will also help to reveal important shared elements between these organisms, which hopefully will eventually make it possible to eradicate schistosomiasis.

1.3 *B. glabrata* as a model organism for genome studies

Since the approval of the snail genome project extensive research has begun on *B. glabrata*. In particular this freshwater snail is proving to be a unique model organism for nuclear organisation studies. The development of fluorescence *in situ* hybridisation techniques for snail cells has been the starting point for these studies (Odoemelam *et al.*, 2009).

By incorporating exogenous labelled nucleotides, the presence and non-random distribution of chromosome territories in the Bge cell line was also revealed [Fig. 1.4]. This was achieved by incorporating the thymidine analog 5-bromo-2'-deoxyuridine (BrdU) into cells during DNA synthesis, which resulted in sister chromatid labelling. Further cultivation in normal medium (without BrdU) for several cell cycles then resulted in the random segregation of the labelled and unlabelled sister chromatids into daughter cells. After 5-10 cycles, the interphase Bge cell nuclei were observed to contain few or single chromatid territories. It appears that the snail chromosomes have a size correlated distribution, with large chromosomes having an intermediate position and smaller chromosomes having an internal position within the snail nuclei (Knight *et al.*, 2011a). This study was the first to reveal the occurrence of non-randomly positioned chromosome territories in molluscs.

Figure 1.4 Representative 2-D image displaying the presence and non-random distribution of chromosomes territories in Bge cells. Two separate chromosome territories (green) were revealed by using the incorporation of 5-Bromo-2'-deoxyuridine (BrdU) into newly synthesised DNA of Bge cells. The DNA within the Bge cell nucleus was counterstained with DAPI (blue), and the incorporated BrdU revealed using a primary antibody recognising BrdU and a secondary antibody conjugated to FITC. Scale bar = 5μm. (Source: Knight *et al.,* 2011a)

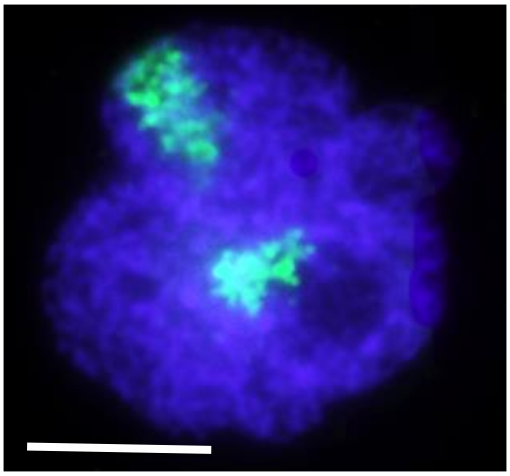

Since the presence of chromosome territories appears to be a conserved feature of functional genome organisation in higher organisms including humans (Boyle *et al.*, 2001), pig (Foster *et al.*, 2005), chicken (Habermann *et al.*, 2001), mice (Mayer *et al.*, 2005), and lower eukaryotic organisms such as *Drosophila* (Marshall *et al.*, 1996), yeast (Bystricky *et al.*, 2005), and plants (Dong and Jiang, 1998), the addition of *B. glabrata* to this list of organisms may provide a model molluscan organism in this field of research. Although it is too early to predict the snail genome organisation in interphase nuclei, the progression of the snail genome sequencing project as well as studies in the intact snail will enable further elucidation of the snail genome organisation.

The level of organisation within the snail genome was also shown to further extend to gene loci. Specific gene sequences from the *B. glabrata* BAC library were extracted and labelled by nick translation for use as probes in FISH experiments. Not only were these gene loci also positioned non-randomly, their positions were altered upon co-culture of Bge cells with *S. mansoni* miracidia. An interesting observation however was that while the *ferritin* gene loci were repositioned from the nuclear periphery to the nuclear interior, the *actin* gene loci were repositioned from the nuclear interior to the nuclear periphery, and both these events were in conjunction with the up-regulation of these genes (Knight *et al.*, 2011a). The repositioning of *ferritin* gene loci to the nuclear interior with its subsequent up-regulation is consistent with the behaviour of actively expressing genes moving to the nuclear interior (Szczerbal *et al.,* 2009; Takizawa *et al.*, 2008a; Foster and Bridger, 2005). However the up-regulation of *actin* with its subsequent repositioning to the nuclear periphery is an interesting observation. As discussed in the upcoming section 1.4.1, the nuclear periphery is associated with inactive chromatin and repositioning of active genes to the nuclear periphery is not so common in vertebrates. However in simpler organisms active genes are known to associate with the nuclear periphery, such as the *var* genes in the malaria parasite *Plasmodium falciparum* (Duraisingh *et al.*, 2005).

The observation of gene repositioning and expression occurring at both the nuclear interior and periphery in a single organism makes *B. glabrata* a unique model organism to study the involvement of various nuclear compartments in genomic regulation.

In terms of the snail – parasite relationship, the Knight *et al* 2011a study was the first to study genomic changes in *B. glabrata* via nuclear organisation. *B. glabrata* and *S. mansoni* research is often led through gene expression studies in *B. glabrata* upon parasitic infection, which is thought to play a role in the snails resistance and susceptibility. Hence, studying this host – parasite relationship in terms of nuclear organisation provides the field with a new avenue of investigation. Indeed, the observations that non-randomly positioned gene loci alter their position upon parasitic infection concomitantly with changes in gene expression are very important findings, and it would be of great importance and interest to take this study a step further and study the effect of the parasite on the genome organisation of the intact snail (Arican-Goktas *et al*, in submission). Genome organisation studies in a molluscan organism would also enable the identification of different types of organisation present within the nucleus that may not be present in the so far studied organisms.

For many years, the ease of maintaining *B. glabrata* in a laboratory environment has made it a popular organism in schistosomiasis research. Although very little is known about the snail nucleus, the aforementioned observations give an insight that *B. glabrata* will slowly but surely become an interesting candidate in nuclear and genomic research. With the additional benefit of the availability of Bge cell line, along with the whole genome sequence, this freshwater snail is the highlight of future studies.

Part II

1.4 The nucleus

"Thus I came to observe the blood of a cod and of a salmon, which I also found to consist of hardly anything but oval figures, and however closely I tried to observe these, I could not make out what parts these oval particles consisted, for it seemed to me that some of them enclosed in a small space a little round body or globule, and at some distance from this body there was round the globule a clear ring and round the ring again a slowly shadowing contour, forming the circumference of a globule…" (Harris, 1999).

The above paragraph is from a letter by Van Leeuwenhoek written on the 3rd of March 1682, describing his findings when visualising the red blood cells of the fish, on the microscope. What the Dutch scientist has described as a 'globule' was probably the first sightings of the control centre of the cell, what we know now as the nucleus.

The eukaryotic nucleus is a membranous organelle, occupying about 10% of the total cell volume (Alberts, 2002) and contains the cellular genetic material in the form of DNA. It is a highly complex organelle with essential functions in co-ordinating a variety of nuclear functions and processes including genome stability, DNA replication, and gene expression (Schirmer and Foisner, 2007). The nucleus also houses various sub-compartments including the nuclear envelope, chromosome territories, nucleoli, nuclear bodies, nuclear matrix, and the nuclear motors, which form the nuclear architecture (Adams and Freemont, 2011; Misteli, 2005; Foster and Bridger, 2005; Strouboulis and Wolffe, 1996). Nuclear integrity is maintained through this architecture in which the different nuclear compartments can interact with each other for efficient functioning of the nucleus.

Any disruption to this organisation can have severe effects and result in disease conditions such as nucleopathies and cancer (Bourne *et al.*, 2013). Thus, the second part of this chapter will shed light on the importance of nuclear organisation, in particular the spatial positioning of the genome, and the interaction of the genome with nuclear compartments such as the nuclear bodies and nuclear motors.

1.4.1 Organisation of the genome within the interphase nucleus

The cell nucleus is a highly dynamic and organised organelle with functional domains accommodating various actions such as DNA replication and repair, gene expression, and transcription. This level of organisation is also persistent in the genome with individual chromosomes occupying distinct regions within interphase nuclei, known as chromosome territories (Cremer and Cremer, 2006).

In 1885, based on his studies of *Proteus* and *Salamandra,* Karl Rabl suggested that chromosomes in an interphase nucleus were organised as separate entities, with centromeres on one side and the telomeres on the other (now known as Rabl configuration) (Foster and Bridger, 2005; Rabl, 1885). This organisation of the interphase chromosomes were then named as 'chromosome territories, by Theodor Boveri (Boveri, 1909). However, despite this discovery it was not until the 1970's that the first scientific evidence for the territorial organisation of chromosomes came. In 1974 Thomas and Christopher Cremer brothers experimentally demonstrated the existence of chromosome territories by laser UV micro beam (Cremer *et al.,* 1974). This was followed by Stack *et al* who also visualised distinct interphase chromosomes in *Allium cepa* and the Chinese hamster nuclei (Stack *et al.,* 1977). Further confirmation of the presence of chromosome territories came from fluorescence *in situ* hybridisation studies using fluorescently labelled sequences (gene or whole chromosomes) to hybridise onto the homologues sequences within the genome.

Although in some student textbooks it still implies that chromatin within an interphase nucleus is a tangled mass of threads, territorial organisation of chromosomes is a generally accepted view [Fig. 1.5] (Bickmore and Van Steensel, 2013; Bourne *et al.*, 2013; Geyer *et al.,* 2011; Meaburn and Misteli, 2007).

The territorial organisation of chromosomes in interphase nuclei is conserved from higher eukaryotes including humans (Parada and Misteli, 2002; Cremer and Cremer, 2001; Bridger and Bickmore, 1998), pig (Foster *et al.,* 2012; Federico *et al.*, 2004), chicken (Habermann *et al.*, 2001), and mouse (Mayer *et al.*, 2005), to lower eukaryotes such as *Drosophila melanogaster* (Marshall *et al.*, 1996), and the snail *B. glabrata* (Knight *et al.*, 2011a). Chromosome territories have also been visualised in the plants wheat, rye, and barley (Dong and Jiang, 1998). However this spatial and morphological organisation of chromosome territories has shown to vary between different organisms. While the Rabl pattern of organisation forming elongated chromosome territories is adopted by *Drosophila*, wheat, rye, and barley, in other eukaryotic organisms the chromosomes are distributed radially across the interphase nucleus (Bolzer *et al.*, 2005; Cremer *et al.*, 2001; Boyle *et al.*, 2001; Croft *et al.*, 1999).

In addition to whole chromosomes, it is therefore not surprising that sub-chromosomal regions and individual gene loci also display preferential nuclear positions during interphase (Misteli, 2005). Although the components that contribute to the nuclear position of a gene are not entirely clear, the activity of a gene is believed to affect its position, with active genes being more internally localised than inactive ones [Fig. 1.5] (Elcock and Bridger, 2010; Deniaud and Bickmore, 2009; Szczerbal *et al.,* 2009; Takizawa *et al.,* 2008b; Williams *et al.*, 2006). Visible demonstration of this spatial reorganisation came from Volpi *et al* where upon induction with IFN-γ in mammalian fibroblasts, the MHC cluster was found away from its chromosome territory on external chromatin loops (Volpi *et al.*, 2000). In mice, during gastrulation the induction of the *Hoxb1* cluster is accompanied by its decondensation and extrusion from its chromosome territory.

In contrast, the non-expressing *Hoxb9* cluster remained within its chromosome territory (Chambeyron *et al.*, 2005; Chambeyron and Bickmore, 2004). Williams *et al* also made a similar observation when they studied the proneuronal regulatory gene, *Mash1,* in embryonic stem cells. *Mash1* is transcriptionally repressed and is located at the nuclear periphery. However upon induction during neuronal differentiation, the gene is up-regulated and the loci repositions to the nuclear interior (Williams *et al.*, 2006). During porcine adipogenesis the nuclear positions of seven adipogenic genes, *PPARG, SREBF1, FABP4, CEBPA, CEBPB, CREB, and GATA2,* and their chromosome territories were also reported to alter. The up-regulation of gene expression was also correlated with these genes becoming more internally localised (Szczerbal *et al.,* 2009). Other examples of repositioned gene loci include the CD4 locus (Kim *et al.*, 2004), CFTR gene (Zink *et al.*, 2004a), and the β-globin locus (Brown *et al.*, 2006; Ragoczy *et al.*, 2006), which all localise to the nuclear interior when transcriptionally active and are found at the nuclear periphery when inactive. Support for a link between radial positioning and gene activity also came from Takizawa *et al* when they observed the location of active and inactive copies of a monoallelically expressed GFAP locus. Data from this study demonstrated that the active GFAP allele preferentially occupied a more internal location when compared to its inactive copy within the same nuclei (Takizawa *et al.*, 2008a). Adding to this, a recent study using mice erythroblasts demonstrated loop formation in the β-globin locus prior to transcriptional activation (Deng *et al.*, 2012) suggesting that chromatin loop formation may underlie gene regulation.

However as a caveat to this dogma, Kim *et al* has shown that in the mouse T-cells the CD8 locus becomes more peripheral upon activation (Kim *et al.*, 2004). Similarly the IFNγ locus in mice locates at the nuclear periphery regardless of its activity (Hewitt *et al.*, 2004). The looping of active genes also does not seem to be a general feature of gene expression, as in the limb bud *Hoxd* gene activation and decondensation of chromatin occurs without any looping out of the chromosome territory (Morey *et al.*, 2007).

Non-random positioning of gene loci is also observed in lower eukaryotes. In the nematode *Caenorhabditis elegans,* tissue specific developmentally regulated promoters were found to be located at the nuclear periphery when silent and shift to an internal position when activated (Meister *et al.*, 2010). Although this may be similar to the mechanism observed in higher eukaryotes, in yeast and *Drosophila,* gene activation and transcription has been associated with the nuclear pore complexes (Brown and Silver, 2007; Casolari *et al.*, 2004). Also in the freshwater snail *B. glabrata,* activated genes were shown to be positioned at both the nuclear interior and the periphery (Knight *et al.*, 2011a).

Traditionally the nuclear periphery in mammalian cells has been associated with inactive chromatin and relatively low gene expression (Meaburn *et al.,* 2007b; Foster and Bridger, 2005; Zink *et al.*, 2004a; Brown *et al.*, 1999; Brown *et al.*, 1997; Ferreira *et al.*, 1997; Strouboulis and Wolffe, 1996). However, similar peripheral positioning of activated genes reported in mammalian cells such as the beta-globin locus (Ragoczy *et al.*, 2006) and the IFNγ locus (Hewitt *et al.*, 2004), suggests that a generally applicable rule is yet to emerge. Nevertheless it is apparent that individual gene loci take on preferential arrangements within the nucleus to optimise gene expression [Fig. 1.5].

Figure 1.5 Representative cartoon of the interphase nucleus demonstrating the possible positions of active and inactive gene loci.

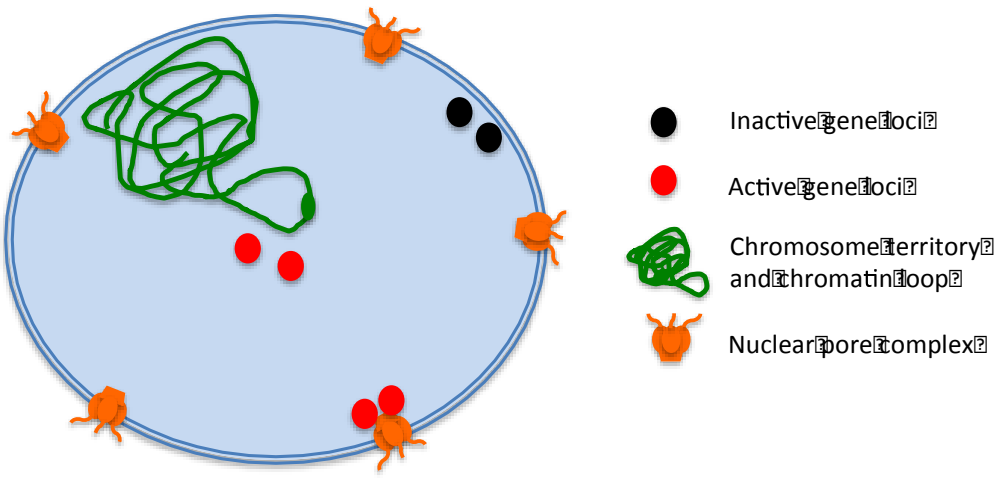

The positions of chromosome territories and gene loci can be functionally and spatially altered upon internal and external stimuli. The first evidence for this came from epilepsy studies demonstrating the altered positions of chromosomes 1, 9, X, and Y in epilepsy patients (Manuelidis and Borden, 1988). Following this, in 2003 Cremer *et al* have demonstrated the loss of radial chromatin order in tumour cell nuclei with the position of chromosome 18 being altered from the nuclear periphery to the nuclear interior (Cremer *et al.*, 2003). Bridger and colleagues have also shown that chromosome territory positions are altered in laminopathy patients, with chromosome 13 and 18 occupying an internal location within the interphase nuclei as opposed to their peripheral location in control cells (Mehta *et al.*, 2011; Meaburn *et al.*, 2007a; Foster and Bridger, 2005). Alterations in interphase genome organisation have also been reported after an infection. Chromosome 17 was shown to reposition from the nuclear periphery to the nuclear interior following an Epstein-Barr virus (EBV) infection on human lymphocytes (Li *et al.*, 2009). Knight *et al* has also shown that after a parasitic infection, genes are repositioned in a molluscan cell line, which is in conjunction with the activation of those genes (Knight *et al.*, 2011a). Other than disease, perturbed positioning of chromosome territories and gene loci have also been reported during physiological processes including cellular proliferation (Mehta *et al.*, 2010; Bridger *et al.*, 2000), and differentiation and development (Solovei and Cremer, 2010; Szczerbal *et al.,* 2009; Solovei *et al.*, 2009; Ragoczy *et al.*, 2006; Foster *et al.*, 2005; Chambeyron and Bickmore, 2004).

It is evident that the spatial organisation of eukaryotic cells is profoundly important to their function. Given that this organisation is altered at various cellular processes and disease, the biological significance of these studies are extremely high. However further research, preferably in live cells, are necessary in order to determine a general mechanism. What also remain to be elucidated are the mechanisms involved in these repositioning events.

1.4.2 The nuclear structures

The eukaryotic nucleus houses a number of important structures that interact with and influence chromatin. These morphologically distinct substructures include the scaffolding proteins that make-up the nuclear lamina found underneath the inner nuclear membrane, the nuclear matrix, the nucleolus, and nuclear bodies situated within the matrix scaffold (Matera, 1999). To date, more than ten of these intranuclear structures have been characterised and are described as coiled bodies, vesicles, spheres, or doughnut like structures (Zimber *et al.,* 2004).

One of the most well characterised nuclear structures are the promyelocytic leukaemia (PML) bodies, formed by the distinct localisation of the PML tumour suppressor protein [Fig. 1.6 A]. These are visualised as discrete foci, 0.2 -1.0 μm wide, and between 1 to 30 bodies are present per nucleus depending on the cell type, cell-cycle phase, and differentiation stage (Bernardi and Pandolfi, 2007). PML nuclear bodies interact with chromatin fibres via their protein based threads, specifically gene rich and transcriptionally active regions. It is believed that through this interaction they are able to regulate transcriptional activity, and conditions that cause chromatin condensation (i.e. stress) result in the detachment of smaller bodies from the main PML body (Eskiw *et al.,* 2004). Similarly, PML nuclear bodies lose their functions in leukaemia's and other solid tumours and can be disrupted upon viral infection (Everett and Chelbi-Alix, 2007). Other functions of PML bodies include tumour suppression, DNA repair (Zhao *et al.,* 2009), as well as regulation of apoptosis, cellular senescence, and neoangiogenesis (Bernardi and Pandolfi, 2007). However despite the central role purported for PML bodies, the PML protein is not very well conserved in lower eukaryotes, and has failed to be identified in the genomes of *S. cerevisiae, D. melanogaster,* and bacteria (Borden, 2008).

The Cajal Body was first identified in neuronal cell nuclei and named after its discoverer Ramon Y Cajal. It is a coiled body consisting of coiled threads of the coilin protein (Morris, 2008) and is about 0.2 – 1.0 μm in diameter [Fig. 1.6 B] (Spector, 2001). Although its functions are still not very clear, the Cajal body is thought to be involved in post-transcriptional modification of newly assembled spliceosomal snRNAs as well as snRNP and snoRNP biogenesis (Spector, 2006). In human cells it associates with specific genetic loci, such as the histone and small nuclear RNA genes (Dundr *et al.*, 2007). Cajal bodies have been observed in many cell types and like PML bodies they vary in number in relation to cell cycle progression, physiological changes, and disease (Zimber *et al.,* 2004). Unlike PML bodies, Cajal bodies are conserved within the lower eukaryotes and have been identified in many organism including amphibians, insects, and plants (Gall, 2003). Although the marker protein coilin has not been identified in the genomes of *C. elegans, S. cerevisiae* and *Drosophila* (Gall, 2003), when grown under certain conditions yeast contain domains resembling Cajal bodies (Verheggen *et al.*, 2002). In *Drosophila* a structure thought to be the equivalent to the mammalian Cajal body has also been identified (Liu *et al.*, 2006).

Figure 1.6 Representative 2-D images displaying the distribution of nuclear structures in mammalian cells. Cells were stained for anti-PML (green) (A), anti-coilin (green) (B), anti-RNA polymerase II (green) (C), and anti-SC35 (green) (D), and were counterstained with either DAPI (blue) or PI (red). (Source: ABCAM: http://www.abcam.com)

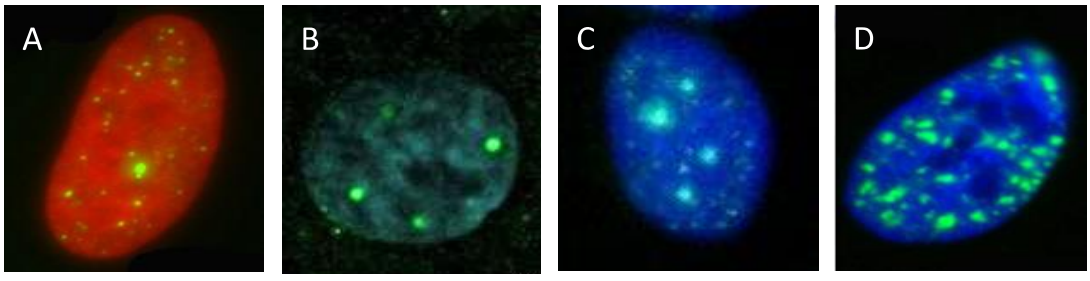

Another functionally important nuclear structure are the nuclear speckles / SC35 domains [Fig. 1.6 D]. These are enriched in splicing small nuclear ribonucleoprotein complexes (snRNPs) (Handwerger and Gall, 2006), and contain proteins for pre-mRNA processing (Spector, 2006). Approximately 25 - 50 nuclear speckle domains can be found in a cell (Zimber *et al.,* 2004) and these regions are thought to be transcriptionally inert (Zhao *et al.,* 2009). Although there are studies suggesting the preferential association of transcriptionally active genes with nuclear speckles (Szczerbal and Bridger, 2010; Brown *et al.*, 2008b; Takizawa *et al.*, 2008a), whether this association occurs as a result of transcriptional activity or the association facilitates transcription is still a matter of debate. Other than mammalian cells nuclear speckles have so far been identified in *Drosophila* and in the amphibian oocyte nucleus (Lamond and Spector, 2003).

The nucleolus, being a clearly defined and prominent sub-nuclear domain, is also considered as a nuclear body (Zimber *et al.,* 2004). It is the site of ribosome biogenesis and a well known example of interchromosomal interactions. Following mitosis, nucleolar organising regions (NORs), which are ribosomal genes found on several chromosomes join together to form the nucleolus, which then recruit RNA polymerase I machinery for ribosome biogenesis (Osborne and Eskiw, 2008).

A similar transcriptional compartment to the nucleolus was put forward by Iborra *et al* after incorporating Br-UTP and biotin-CTP labelled nucleotides into permeabilised cells. They noticed that the resultant labelled nascent transcripts were concentrated at discrete focal sites within the nuclei, which they termed transcription factories [Fig. 1.6 C] (Iborra *et al.*, 1996). These are active transcriptions units, comprising of active, phosphorylated RNA polymerase II and contain newly synthesised RNA (Jackson *et al.*, 1993; Wansink *et al.*, 1993). Further studies utilising *in situ* hybridisation techniques have revealed the association of active genes with these transcription factories (Kang *et al.*, 2011; Schoenfelder *et al.*, 2010; Osborne *et al.*, 2007; Yao *et al.*, 2007; Osborne *et al.*, 2004).

In fact, several gene loci have been observed to share the same transcription factory indicating that these factories may well be coordinating transcription and gene expression within the nucleus (Edelman and Fraser, 2012; Schoenfelder *et al.*, 2010; Osborne *et al.*, 2007; Osborne *et al.*, 2004). By employing chromosome conformation capture (3C), Dhar *et al* has shown that ten genomic loci from nine chromosomes encoding cytochrome c oxidase (COX) subunits, as well as genes from three chromosomes encoding factors required for the transcription of mitochondria encoded COX subunits, all occupy a common transcription factory (Dhar *et al.,* 2009). Other evidence points to similar active gene loci sharing specialised transcription factories. Xu *et al* has shown that 8000 minichromosomes per cell are concentrated in only 20 transcription factories, which is consistent with the transcription of many templates in one factory. Moreover, these factories were found to transcribe particular units, depending on the promoter type and the presence of an intron (Xu and Cook, 2008). Further evidence for specialised factories came from Schoenfelder *et al*, when they revealed that Klf1-regulated mouse globin genes are preferentially transcribed at transcription factories containing large amounts of Klf1 (Schoenfelder *et al.*, 2010).

It is apparent that the structures present within the nucleus are dynamic and are involved in the modulation of numerous nuclear activities. The function and activity of nuclear structures are correlated in the dynamic network of genome function and nuclear organisation. Although remarkable progress has been made in these studies broadening our understanding of nuclear structures and their influence on chromatin, future studies are likely to provide exciting insights in this rapidly growing field.

1.4.3 Interaction of the genome with nuclear structures

The non-random organisation of chromosomes and gene loci, and their ability to move within the nucleus has lead to suggestions of genomic regions interacting with nuclear structures such as transcription factories, nuclear bodies, and the nuclear envelope (Osborne and Eskiw, 2008; Foster and Bridger, 2005; Parada and Misteli, 2002). Indeed various studies have demonstrated the association of gene loci with transcription factories (Kang *et al.*, 2011; Schoenfelder *et al.*, 2010; Dhar *et al.,* 2009; Osborne *et al.*, 2007; Yao *et al.*, 2007; Osborne *et al.*, 2004). An example is the urokinase-type plasminogen activator (uPA) gene locus, which upon induction loops out of its chromosome territory and associates with active transcription factories (Ferrai *et al.*, 2010). It is thought that looping out of active genes from different chromosomes to meet at specialised transcription factories provides the opportunity for what is known as 'chromatin crosstalk' both in *cis* and *trans*, in regulating the genome (Kang *et al.*, 2011; Schoenfelder *et al.*, 2010; Gondor and Ohlsson, 2009; Osborne *et al.*, 2007; Yao *et al.*, 2007; Osborne *et al.*, 2004).

Likewise nuclear bodies such as the PML and Cajal body are also known to interact with the genome. PML bodies recruit genes to their surface, in particular transcriptionally active loci (Zhao *et al.,* 2009; Eskiw *et al.,* 2004; Wang *et al.*, 2004; Eskiw *et al.*, 2003). The actively transcribing major histocompatibility complex I (MHC I) on chromosome 6 have shown to associate with PML bodies (Shiels *et al.*, 2001). Indeed, by interacting with the matrix attachment region (MAR) binding protein, and the special AT-rich sequence binding protein 1 (SATB1), PML bodies were revealed to organise the MHC I locus into loop structures (Kumar *et al.*, 2007). Cajal bodies were also found to associate with chromatin. Upon induction of transcription the transcriptionally silent U2 arrays associate with Cajal bodies by long range directed motion (Dundr *et al.*, 2007). Histone gene clusters as well as the U1 and U2 snRNA genes and the snoRNA genes were also shown to interact with Cajal bodies (Frey *et al.*, 1999; Schul *et al.*, 1999).

The association of genetic loci with SC35 nuclear speckles have also been reported, more specifically gene rich chromosomal regions (Shopland *et al.*, 2003). Activated gene loci during adipogenesis and erythropoiesis have been shown to co-localise with these speckles (Szczerbal and Bridger, 2010; Brown *et al.*, 2008b), and it is suggested that this association may increase the efficiency of RNA splicing and influence gene expression (Ferrai *et al.*, 2010).

The nuclear envelope and the nuclear lamina also influence the organisation of the genome. Various studies have demonstrated the association of specific chromosome loci with the nuclear envelope and the lamina (Guelen *et al.*, 2008; Pickersgill *et al.*, 2006; Marshall *et al.*, 1996). The nuclear lamina in particular, which is a protein meshwork lining the inner nuclear membrane (Burke and Gerace, 1986) and also found within the intra-nuclear space (Bridger *et al.*, 1993; Goldman *et al.*, 1992), is thought to form an internal nucleoskeleton acting as a frame for chromatin compartmentalisation and determining the nuclear organisation (Pickersgill *et al.*, 2006; Barboro *et al.*, 2003; Goldman *et al.*, 2002; Hozak *et al.*, 1995). At the nuclear periphery the integral membrane proteins (IMP) embedded at the nuclear envelope have genome tethering properties. As well as binding to lamins, the IMP's also bind to mitotic chromosomes, histones, and heterochromatin (Schirmer and Foisner, 2007; Foster and Bridger, 2005).

In addition, regions of DNA also interact with nuclear pore complexes (NPC), which are found at intervals within the nuclear envelope joining the inner and outer nuclear membrane (Schirmer *et al.*, 2003). In lower eukaryotes transcriptionally active loci have been found to associate with NPC (Rohner *et al.*, 2013; Brown and Silver, 2007; Casolari *et al.*, 2004). While in mammalian cells the NPC have been associated with silencing epigenetic marks (Brown *et al.*, 2008a), interaction between nucleoporins and gene loci upon activation of transcription has been reported (Casolari *et al.*, 2005). Brown *et al* also demonstrated associations between human chromosomes 5, 7, and 16 with nucleoporin 93 (Brown *et al.*, 2008a).

Together these and similar studies highlight the fact that although chromosomes are organised into distinct territories, they are dynamic structures. Individual chromosomal regions or whole chromosomes can be repositioned with respect to both nuclear structures and other chromosomal regions to control gene expression [Fig. 1.7] (Mehta *et al.,* 2010; Lanctot *et al.,* 2007). The mechanism of this co-ordinated movement within the nucleus is now thought to be result of the presence of an active nuclear motor complex (Bridger, 2011).

Figure 1.7 Representative cartoon of half an interphase nucleus. The nucleus is enclosed by double membrane to separate the nuclear components from the cytoplasm. Embedded within the nuclear membrane are the nuclear pore complexes regulating nucleocytoplasmic transport. Below the nuclear membrane is the nuclear lamina, providing mechanical support as well as participating in nuclear organisation. Chromosomes in an interphase nucleus are arranged into individual chromosome territories. Within the interchromatin space are multiple nuclear bodies, interacting with chromatin fibres and loops.

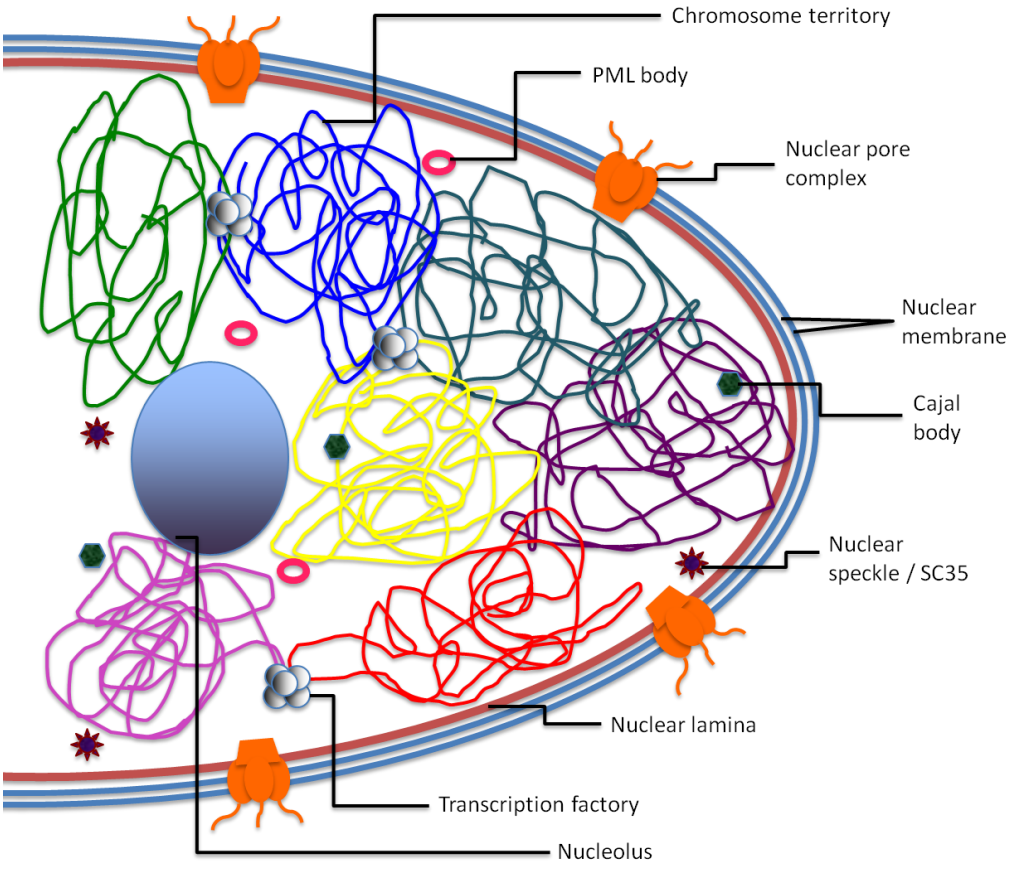

1.4.4 Nuclear motors

Reorganisation of the genome in response to internal and external stimuli is now an accepted concept in the field of nuclear biology. Whether this be long range movement of chromosomes (Mehta *et al.*, 2010; Mehta *et al.*, 2008; Hu *et al.*, 2008; Chuang *et al.*, 2006), movement of individual gene loci or gene clusters away from their chromosome territories (Osborne *et al.*, 2007; Volpi *et al.*, 2000), or the association of gene loci with nuclear structures such as transcription factories or nuclear bodies (Dundr *et al.*, 2007), they all require what appears to be a 'directed' movement. These processes can in fact occur within 15 minutes (Mehta *et al.*, 2010; Volpi *et al.*, 2000), further diminishing the impression of a passive or random movement to nuclear destinations. Thus the presence of a nuclear motor complex, similar to that in the cytoplasm in moving nuclear entities has been hypothesised. Although for many years the presence of such a motor complex within the nucleus has been disregarded as cytoplasmic contamination, with the development of sophisticated biological assays, this hypothesis is now gaining credibility and acceptance (Bridger and Mehta, 2011).

The presence of actin in the nucleus was first suggested in 1969 when it was observed as fibrillar bundles in oocytes treated with actinomycin (Lane, 1969). This was followed by other reports confirming the presence of actin in the nuclei of a range of species (Bridger and Mehta, 2011). However it was not until the last few years that solid evidence for presence of actin in the nucleus was provided. Studies confirming β-actin, G-actin (globular), and F-actin (filamentous) in the nucleus has radically changed the point of view regarding the presence of actin (Schoenenberger *et al.*, 2005; Gonsior *et al.*, 1999; Zhao *et al.*, 1998). The actin polymers present in the nucleus are very different from those found in the cytoplasm and are present as a dynamic mixture of monomeric, oligomeric, and polymeric fibres (McDonald *et al.*, 2006).

Fluorescence staining of actin in the nucleus using anti-actin antibodies has revealed accumulations and a sponge like concentration of actin throughout the nucleoplasm (Jockusch *et al.*, 2006). With respect to the involvement of actin with the dynamic activities within the nucleus, Dundr *et al* has shown that a β-actin dominant negative mutant in cells, blocks the translocation of specific gene loci to Cajal bodies (Dundr *et al.*, 2007).

Myosin's are a large superfamily of motors proteins. Together with actin, they instigate various cytoplasmic processes such as cytokinesis, phagocytosis, and cell trafficking (Hartman and Spudich, 2012). The presence of myosins in the nucleus has also been discussed over the last 25 years when Hagen *et al* revealed a cross reaction with a monoclonal antibody to *Acanthaamoeba castellanii* myosin I (Hagen *et al.*, 1986). Today, various isoforms of myosin's have been identified in the nucleus including NM1β, myosin VI, myosin 16b, myosin Va, and myosin Vb (Bridger, 2011). However, after the pioneering work of Belmont and colleagues regarding motor proteins in transposing chromosomes (Chuang *et al.*, 2006), NM1β became the most investigated myosin candidate. Encoded by the MYO1C gene, NM1β has a unique 16 amino acid residue at the N-terminus, required for its nuclear localisation (Pestic-Dragovich *et al.*, 2000). Within the nucleus it is distributed throughout the nucleoplasm with a concentration at nucleoli (Mehta *et al.*, 2010; Philimonenko *et al.*, 2004; Fomproix and Percipalle, 2004; Pestic-Dragovich *et al.*, 2000).

1.4.5 Evidence for nuclear motor activity in moving genes and chromosomes

The directed movement of individual gene loci and chromosomes, as well as the identification of actin and myosin in the nucleus, have lead to the hypothesis that a nuclear motor mechanism may be present in the nucleus. Within the cytoplasm the movement of myosin filaments over actin filaments generates a force, which facilitates muscle contraction (Coluccio, 2007).

Thus it was thought that these two proteins might also interact within the nuclear environment in moving various nuclear entities. Although this proposition is hindered slightly due to the nuclear isoform of myosin 1C being an unconventional myosin that does not form filaments (Mermall *et al.,* 1998) and the filamentous form of actin being different from the cytoplasmic actin filaments (McDonald *et al.*, 2006), the pioneering work from four major studies is showing otherwise. Initially, by employing mutant cell lines for actin and myosin as well as using drugs that interfere with the polymerisation of these proteins, Chuang *et al* elegantly demonstrated the actin and myosin regulated translocation of a gene locus from the nuclear periphery to the nuclear interior (Chuang *et al.*, 2006). Following this Dundr *et al* demonstrated that the long range linear movement of the U2 gene loci upon transcriptional activation, and its subsequent association with Cajal bodies is distracted in polymerisation deficient actin mutant cell lines (Dundr *et al.*, 2007). By employing specific siRNA against NMI, microinjection of antibodies against NMI, and drugs that interfere with actin and myosin polymerisation, Hu *et al* has also shown that interactions of gene loci present on separate chromosomes are abolished following these treatments (Hu *et al.*, 2008). Finally the Bridger group has shown that movement of whole chromosomes in interphase nuclei is blocked by inhibitors of actin and myosin polymerisation. Moreover, direct evidence for the involvement of NM1β in moving whole chromosomes was provided by using RNA interference to knock down the expression of MYO1C (Mehta *et al.*, 2010).

From the above studies it is clear that active members of molecular motors are responsible for movement of chromatin within the nuclear environment. An attractive model put forward by Hofmann *et al* suggests that NM1β could bind via its tail to the nuclear entity requiring movement. The subsequent binding of actin to the globular head of nuclear myosin I molecule would then form a motor complex. This nuclear motor would be able translocate the nuclear entity along the highly dynamic tracks of nuclear actin (Hofmann *et al.*, 2006). However, more evidence is still required to confirm the presence of such a motor mechanism within the nucleus.

1.5 Overview

Aside from playing a key role in the transmission of the neglected tropical disease schistosomiasis, *B. glabrata* is an important organism for understanding the host-parasite relationship. The existence of two different forms of this snail (resistant and susceptible) has made it a significant target point for schistosomiasis studies. It is evident from these studies that the parasite has the ability to manipulate the snail genome. While the majority of snail studies are unravelling the molecular manipulations i.e. up/down-regulation of genes, very little research is done regarding the effects of the parasite on the physical organisation of the genome i.e. positions of genetic loci. Knowing that the snail genome is highly organised with the presence of individual chromosome territories (Knight *et al.*, 2011a), studying the effects of a parasitic infection on this organisation will most certainly provide invaluable information with regards to both schistosomiasis and nuclear research.

Thus in this thesis the snail genome will be investigated in terms of metaphase chromosomes, affects of infection on interphase genome organisation, and the nuclear structures present in the snail.

1.6 Aims and Objectives

Aims:

- To investigate host-parasite relationships by studying the effects of S. mansoni infection on the interphase genome organisation of the host snail *B. glabrata*.
- To develop a new model system using the snail *B. glabrata* to expand our knowledge and understanding on the dynamics of interphase genome organisation.

Objectives:

- To carry out an initial study on the snail genome by constructing an accurate and a reliable karyotype for *B. glabrata*. This will be achieved by developing robust chromosome spreading and banding protocols for the snail chromosomes.
- To study the effects of infection on the genomes of resistant and susceptible *B. glabrata* strains by developing a FISH protocol suitable for snail cells. Using this protocol specific gene loci will be mapped on to the snail chromosomes. Their positions in the interphase nuclei, before and after infection in the two snail strains, will be revealed using a bespoke erosion analysis.
- To develop a heat shock system using the Bge cell line to study the significance of gene positioning. In particular answers to the destination, cause, and mechanism of gene movement within the interphase nuclei will be sought. This will be achieved by performing FISH, 3D immune-FISH and qRT-PCR experiments.

Chapter 2

The karyotype of the freshwater snail *Biomphalaria glabrata*

The contents of this chapter are in preparation for a publication in the genome sequencing paper of the snail *Biomphalaria glabrata*.

The work undertaken in this chapter was supported by a grant from the National Institute of Health.

2.1 Introduction

The first reference in scientific literature observing *B. glabrata* chromosomes came from Rangel in 1951 (Rangel, 1951). They performed the 'squash' technique to obtain chromosome spreads and identified *B. glabrata* chromosome number as 2n = 36. Following this work various other publications were made confirming a diploid number of 36 chromosomes (Narang, 1974; Burch, 1960; Fraga de Azevedo and Goncalves, 1956). In 1976 Raghunathan was the first to attempt Giemsa staining on the snail chromosomes in an effort to produce a snail karyotype (Raghunathan, 1976). Due to the small nature of these chromosomes the banding was unsuccessful. However the author arranged the chromosomes into 6 groups according to the criteria of Levan *et al* (Levan *et al.,* 1964), also reporting the presence of a homologues pair of satellite chromosomes as well as another pair with secondary constrictions. Following this, in 1984 Goldman isolated chromosomes from young snail embryos using the 'air drying' technique (Goldman *et al.*, 1984). He also attempted G-banding that resulted in several bands. Goldman arranged *B. glabrata* chromosomes into nine groups, which the criterion is as follows:

- **Group I –** largest pair of chromosomes, usually metacentric.
- **Group II –** next two chromosomes in decreasing order by size, generally metacentric.
- **Group III –** next three chromosomes similar in size to group II but less metacentric.
- **Group IV –** single, large, sub-telocentric pair.
- **Group V –** three metacentric chromosomes, smaller than those found in groups II and III.
- **Group VI -** chromosome pair with lightly staining arms.
- **Group VII –** similar to group V but chromosomes generally have a more terminal centromere.
- **Group VIII –** single sub-metacentric pair
- **Group IX –** two smallest metacentric pairs.

The most recent literature available on the karyotype of *B. glabrata* is by Kawano *et al*. However, in this study only silver staining was performed to identify the nuclear organiser regions, and the chromosomes were arranged on the basis of their arm ratios and centromere positions (Kawano *et al.,* 1987).

Despite the efforts for obtaining a better understanding of the cytogenetics of *B. glabrata,* the results obtained by different authors present discrepancies where chromosome classification is concerned. This most certainly is due to technical problems related to cytological preparations. The approval of *B. glabrata* as a non-mammalian sequencing target (Raghavan and Knight, 2006) has now made it an urgent necessity to have an approved karyotype for this organism. Although the Bge cell line was initially considered to be a good starting point, a revised karyotype has shown severe aneuploidy within this cell line (Odoemelam *et al.*, 2009), making it unsuitable for use in the sequencing project. Thus, this chapter will describe the establishment of a robust chromosome spreading and a G-banding protocol for *B. glabrata*, and the construction of the first ever ideograms for chromosomes obtained from whole snails. Also reported is the physical mapping of *B. glabrata* genes onto the snail chromosomes.

2.2 Materials and Methods

2.2.1 Snail husbandry

The snails used in this study were originally obtained from Dr Fred Lewis, Biomedical Research Institute, USA. They were kept in a dedicated snail room with a recirculation system, consisting of 20 tanks maintained at 27˚C with a dark/light cycle of 12 hours. Each tank had a volume of 6.5 litres. The system is mains fed and the water is filtered through a series of sediment filter, carbon block filter and reverse osmosis membrane.

Essential salts were then re-added to the water. Snails were maintained at a density of 30 - 40 snails per tank and fed with fish flake. Faeces, debris and excess egg masses were removed from the tanks every two days. Under these conditions snails reach sexual maturity within 6 - 8 weeks and egg masses are laid at a rate of 2 per day/snail. A single egg mass contains an average of 40 eggs of which 70% - 80% successfully hatch. BS90 (resistant), NMRI (susceptible), and BB02 (susceptible) strains of juvenile and adult *B. glabrata* snails were used for cell extraction and adult BB02 snails were used for karyotyping.

2.2.2 The establishment of cell extraction and chromosome spreading protocol for *B. glabrata*

Various manipulations were applied to the standard chromosomal preparation techniques in order to establish a protocol for *B. glabrata* chromosomes. These are summarised in table 2.1. Below is the finalised cell extraction and chromosome spreading protocol for *B. glabrata.*

The snail cells were arrested in metaphase using the mitotic inhibitor colcemid. Whole snails were incubated in 1% colcemid solution [10μg/ml] for the duration of 3 hours at 27˚C. The snails were then carefully removed from their shells and their ovotestes dissected using a stereomicroscope. The ovotestes were transferred into a 1.5ml Eppendorf tube and macerated in hypotonic potassium chloride solution [0.05M] for 10 minutes until the solution became cloudy. To remove any large tissue pieces left, the suspension was passed through a sieve and incubated in hypotonic solution for a further 20 minutes. The cells were then centrifuged at 163g for 5 minutes and the supernatant removed. The pellet was resuspended and subsequently fixed with methanol acetic acid [3:1] and incubated at room temperature for 10 minutes. The suspension was then centrifuged and fixed three more times. 20μl of this cellular suspension was then applied to a wet glass slide, blown upon and subsequently placed on the wrist for 15 seconds. Slides were allowed to dry at room temperature.

Table 2.1 Summary table displaying the various manipulations made to the standard chromosomal preparation techniques to establish a protocol for the spreading of metaphase chromosomes of *B. glabrata.*

Region of snail exposed to colcemid:	Ovotestis	Whole snail
Colcemid incubation time (hours):	1, 3, 6, 9, 12	
Hypotonic exposure time (minutes):	10, 15, 20, 25, 30	
Hypotonic solution (M):	Potassium chloride [0.075; 0.05]	Tri-sodium citrate dihydrate [0.075; 0.05]
Fixation:	Ethanol – Acetic acid [3:1]	Methanol – Acetic acid [3:1]
Slide condition:	Dry, Wet, Fixative washed	

2.2.3 Establishing the region of the snail with the maximum number of mitotic cells

In an effort to maximise the number of metaphase spreads achieved per slide, the intact snail was dissected into four sections consisting of the head/foot, mantle, liver, and the ovotestis. Prior to dissection the snails were incubated in colcemid solution for 3 hours and cells were extracted from each of the above regions as described in the aforementioned section 2.2.2. The cells were then dropped onto glass slides and stained with the DNA intercalater DAPI (4',6-diamidino-2-phenylindole) (see section 2.2.4).

2.2.4 Slide preparation for 4',6-diamidino-2-phenylindole (DAPI) banding of *B. glabrata* chromosomes

B. glabrata metaphase chromosome spreads on glass slides were stained with the DNA intercalater DAPI (4',6-diamidino-2-phenylindole). 10µl of 2µg/ml DAPI in Vectorshield anti-fade mountant (Vector Laboratories, UK) was applied to the chromosomes and covered with a 22 x 50 mm coverslip.

2.2.5 Slide preparation for denatured DAPI banding of *B. glabrata* chromosomes

Slides prepared in accordance with section 2.2.2 were dehydrated through a 70%, 90% and 100% ethanol series (3 minutes each). They were then subsequently denatured in 70% formamide solution, made up in 2X saline-sodium citrate (SSC), at 70°C for 1.5 minutes. Immediately after denaturation, slides were immersed in 70% ethanol followed by 90% and 100% ethanol series. The slides were then allowed to dry at room temperature and mounted with DAPI as described in section 2.2.4.

2.2.6 Slide preparation for Q-banding of *B. glabrata* chromosomes

The protocol used to attempt Q-banding on the snail chromosomes was derived from Current Protocols in Human Genetics (Haines *et al*., 2001).

Glass slides with *B. glabrata* metaphase chromosome spreads (prepared as described in section 2.2.2) were incubated for 20, 30, and 40 minutes in quinacrine mustard dihydrochloride solution (Sigma). Subsequently they were washed in McIlvaine buffer [0.1M anhydrous citric acid, 0.4M anhydrous sodium phosphate dibasic] for 2 minutes, and mounted with a few drops of McIlvaine buffer. 22 x 50 mm glass coverslips were placed on the slides and sealed with a rubber solution (Halfords).

The following experiments were performed in collaboration with Dr Emanuela Volpi and Dr Mohammed Yusuf at London Centre for Nanotechnology, UCL.

2.2.7 G-banding of *B. glabrata* chromosomes

The protocol used to attempt G-banding was derived from Current Protocols in Cell Biology: Traditional Banding of Chromosomes for Cytogenetic Analysis (Bayani and Squire, 2004a). In order to optimise the banding for *B. glabrata* chromosomes, the protocol was modified in both trypsin and Giemsa stain incubation times.

2.2.7.a. Slide preparation for G-banding

Glass slides of fixed *B. glabrata* cellular suspension were prepared as previously described in section 2.2.2. They were aged in the laboratory at room temperature for a minimum of three days before proceeding with G-banding.

2.2.7.b. Establishing the optimum trypsinisation time for *B. glabrata* chromosomes

Aged slides were incubated at 37°C in 0.025% trypsin solution (Gibco, Invitrogen), made up in 1X Earle's balanced salt solution (EBSS) (Gibco, Invitrogen). Various incubation times were employed, and these were 0.15, 0.30, 0.45, 1, and 1.15 minutes. Following trypsinisation the slides were plunged into 1% Foetal Bovine Serum (FBS) and subsequently rinsed in 1X Phosphate buffered saline (PBS) (Gibco, Invitrogen). They were then stained in Giemsa stain working solution (see section 2.2.7.c.) for 3 minutes and rinsed in ddH_2O. The slides were dried completely at room temperature and mounted with 20µl of DPX mountant (Biotech Sciences Ltd) using 22 x 50 mm coverslips.

2.2.7.c. Establishing the optimum incubation time in Giemsa stain

As a consequence of the results from section 2.2.7.b., aged slides containing metaphase spreads were incubated in 0.025% trypsin for 30 seconds and subsequently taken through FBS and PBS washes. The slides were then incubated in Giemsa stain working solution [1ml Giemsa stain (KaryoMAX, Invitrogen); 50ml dH_2O] for the duration of 1, 2, 3, 4, and 5 minutes. They were subsequently washed and mounted as in the aforementioned section 2.2.7.b.

2.2.8 Image capture of DAPI stained, Q-banded, and G-banded chromosomes

DAPI stained chromosomes were visualised using the Olympus BX41 fluorescence microscope (model: BX41TF) and UPlanFLN 100x/1.30 oil immersion objective. The images of the chromosomes were captured using a grey scale digital camera (Digital Scientific UK) and the Smart Capture 3 software (Digital Scientific UK). For the DAPI karyotyping, images were visualised using the programme Adobe Photoshop CS5. The chromosomes were digitally isolated and arranged according to size, centromere position, and banding pattern (where present).

Quinacrine stained slides were visualised using the Zeiss Axioplan 2 imaging fluorescence microscope. Images were captured with MetaSystems digital camera and analysed with the Ikarus karyotyping system, using a human template.

Giemsa stained chromosomes were visualised using the Olympus BX-51 microscope, and the Olympus UPlanFl 60x/1.25 oil and Olympus UPlanFl 100x/1.30 oil objectives. Images were captured via a black and white fluorescence CCD camera. The acquisition software was the latest Leica Microsystems Gmbh Cytovision Genus v7.1 molecular cytogenetics software for bright field, FISH, and M-FISH image capture, with multi-species karyotyping. Thirty images for *B. glabrata* BB02 strain were analysed in total.

Initially, using a human template the chromosomes were digitally isolated and arranged according to size and centromere position. They were organised into groups of large chromosomes (group A), medium sub-metacentric chromosomes (group B), medium metacentric chromosomes (group C), small sub-metacentric chromosomes (group D), small acrocentric chromosomes (group E), and small metacentric chromosomes (group F). The chromosomes were then paired with their homologues pair according to their banding pattern. Single chromosomes without a designated homologues copy were grouped as 'heteromorphic chromosome pair'.

2.2.9 Constructing ideograms for G-banded *B. glabrata* chromosomes

To create ideograms ten metaphase spreads were used for comparison when measuring chromosomes, as suggested by Francke and Oliver (Francke and Oliver, 1978). Using the software Adobe Photoshop CS5, karyotypes were magnified by a further 100-150% to measure the short arm (p arm) and the long arm (q arm) of each chromosome. These measurements were converted to a percentage of the total haploid autosomal length (HAL) for each cell, as described in Chromosome abnormalities and genetic counselling: Appendix A (Gardner, Sutherland and Shaffer, 2011). The HAL values were then averaged across the respective ten cells to construct an approximate scaled schematic representation for each chromosome. By conferring with the principles outlined in the Human ISCN (Shaffer, Marilyn L. Slovak and Lynda J. Campbell, 2009) and the comparisons made between the ten metaphase spreads, each chromosome arm was divided into regions based on the presence of prominent G-positive or G-negative bands. The landmark bands for each chromosome were then drawn to the schematic representations.

2.2.10 2-D fluorescence *in situ* hybridisation for physical mapping of *B. glabrata* genes onto metaphase chromosomes

B. glabrata cells were extracted and fixed as described in section 2.2.2. The slides were then aged at room temperature for 2 days and stained with the DNA intercalater DAPI (see section 2.2.4). Using automated image acquisition, metaphase spreads were identified, captured, and slide parameters recorded. The coverslips on the glass slides were then removed and the slides were washed in methanol-acetic acid [3:1] and subsequently dried at room temperature. The slides were then dehydrated in 70%, 90% and 100% ethanol series (3 minutes each). They were dried on a hot block at 37°C and subsequently denatured in 70% formamide and 2X SSC solution at 70°C for 1.5 minutes. Immediately after denaturation slides were immersed in ice-cold 70% ethanol followed by 90% and 100% ethanol (3 minutes each), and allowed to dry on a hot block at 37°C. The probe DNA dissolved in 12µl of hybridisation mix [50% formamide, 10% dextran sulphate, 2X SSC, and 1% Tween 20] was also denatured at 75°C for 5 minutes and subsequently incubated at 37°C between 10 and 120 minutes. Probes were derived from clones of *B. glabrata* bacterial artificial chromosome (BAC) libraries (BB02 and BS90 stocks) containing *actin, ferritin, hsp70,* and *piwi* encoding sequences.

Following the denaturing of the slide and the probe, 10µl of the biotin or digoxigenin (DIG) labelled probe was placed onto the slide, covered with 18 x 18 coverslip and sealed with rubber solution (Halfords). Probes were placed on the regions of the slides where a metaphase spread was detected. The denatured probe and slide was left to hybridise in a humidified chamber at 37°C for over four nights. After hybridisation, rubber solution and the coverslips were removed and slides were washed three times in 2X SSC at 42°C for 3 minutes. Subsequently 150µl of 1% BSA in 2X SSC blocking solution was added to each slide and covered with 22 x 50 coverslips. The slides were incubated in a humidified chamber at 37°C for 20 minutes. Slides were then washed in 2X SSC at room temperature for 3 minutes.

150µl of streptavidin conjugated to cyanine 3 or fluorescein isothiocyanate in 0.1% BSA / 2X SSC (1:200 dilution, Amersham Biosciences) was added to each slide and incubated in a humidified chamber at 37°C for 30 minutes, in the dark. They were then washed in 2X SSC at room temperature for 3 minutes, followed by a second wash in 1X PBS with 0.1% Tween 20 for 1 minute. The slides were briefly rinsed in 1X PBS before counterstaining with DAPI [1.5µg/ml] (Vectorshield anti-fade mountant, Vectorlabs).

2.2.11 Image capture and analysis after 2-D FISH

DAPI stained chromosomes were visualised using the motorised microscope AxioImager Z2 (Carl Zeiss, Germany). For image acquisition a high-resolution monochrome megapixel charge coupled device (CCD) camera (CoolCube 1m, MetaSystems, Germany) with a resolution of 1360 x 1024 pixels was used. Automated capturing of metaphase spreads was performed using the Metafer software (MetaSystems, Germany). The denatured metaphase chromosomes with hybridised probes were visualised using the aforementioned microscope system. The image acquisition software was the latest Isis software (MetaSystems, Germany).

2.3 Results

2.3.1 Establishing a protocol to obtain metaphase spreads from *B. glabrata*

Analysis of chromosomes from *B. glabrata* is comparatively under-researched with respect to other model organisms. The established techniques up to now have been particularly difficult to replicate and obtain sufficient numbers to raise trustworthy conclusions. As a consequence, I have been establishing new protocols that result in chromosomes of appropriate standard for analysis.

In standard preparations, mitotic chromosomes are selected due to their compact nature allowing visualisation of the typical 'X' shaped chromosomal structure. In order to collect cells at the metaphase stage of the cell cycle, Levan introduced the use of the spindle inhibitor colchicine, which is still the most common chemical used today to collect the cells in prometaphase (Ronne 1989). Colchicine enables metaphase arrest, however chromosome contraction is not inhibited and prolonged incubation can lead to short and stubby chromosomes. A threshold needs to be identified for the duration of colchicine exposure, which varies among different species.

In accordance with previous studies (Raghunathan, 1976; Narang, 1974), initially only the dissected ovotestis was incubated in colcemid, a commonly used less toxic form of colchicine (Rieder and Palazzo, 1992). However with this method the number of metaphase spreads achieved was no more than 2-3 per snail. In an effort to increase the metaphase yield, live snails were placed in colcemid solution and the ovotestis was dissected after this incubation. The results were seen immediately. After only an hour incubation the metaphase yield was increased to 4-6 per snail. To further maximise this yield, the duration of whole snails in colcemid was increased. Figure 2.1 displays representative images of metaphase chromosomes of *B. glabrata* after different incubation times in colcemid. A prolonged incubation of whole snails for 6 hours in colcemid lead to similar sized, short chromosomes, which were rather difficult to distinguish [Fig. 2.1 A]. This was most probably due to the continuous contraction of chromosomes arrested in metaphase. However, as seen in figure 2.1 B, after 3 hour incubation in colcemid the chromosomes were of a suitable length for analysis, and between 5-8 metaphase spreads were obtained from a single snail, which is a sufficient number for karyotyping and analysis purposes.

Figure 2.1 Representative images of DAPI stained (blue) *B. glabrata* NMRI strain metaphase spreads. Whole snails were incubated in colcemid solution at various time points. The ovotestis was then dissected, macerated to obtain single cells, fixed, and dropped onto glass slides. Panels A and B display metaphase spreads obtained after 6 and 3 hours of incubation in colcemid respectively. Scale bar = 10μm.

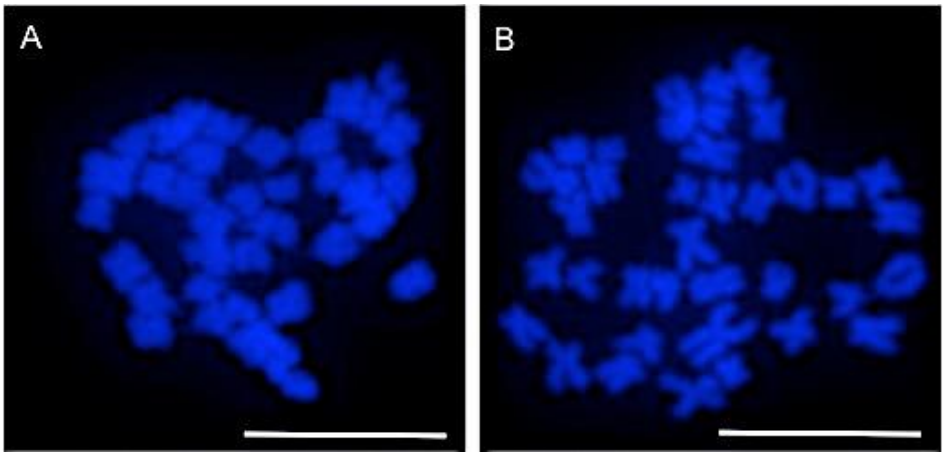

Hypotonic solution and alcohol fixations are also standard procedures in chromosome preparations. The hypotonic salt solution induces swelling of the cells via osmosis, and the alcohol fixation denatures and precipitates proteins by dehydration. The acetic acid in the fixative coagulates nuclear proteins and also causes swelling of the cells, thus counteracting the shrinking effect caused by the alcohol (Ronne, 1989). The degree of dispersion of the chromosomes on the slide is the key element in the preparation of analysable chromosome spreads. Ideally all the chromosomes in a metaphase spread should be in the same optical field on the microscope, with no overlapping chromosomes. This is influenced by the concentration and duration of hypotonic exposure.

Figure 2.2 displays a selection of representative images from the use of different hypotonic solutions, concentrations, and incubation times. Dilute concentrations (0.075M) of sodium citrate solutions are commonly used in animal cytogenetics. However its use with *B. glabrata* leads to under spread and overlapping chromosomes, which were extremely difficult to distinguish from one another and analyse [Fig. 2.2 A].

When the exposure time was extended to 30 minutes, this then resulted in partial spreads occasionally with missing chromosomes. The chromosomal structure was also distorted with the majority of the chromosomes being in an 'S' shape structure, sometimes with surrounding halo [Fig. 2.2 B]. Figure 2.2 C and D display metaphase spreads achieved after hypotonic potassium chloride treatment (KCl) of snail ovotestis cells. After 20 minute incubation in 0.05M KCl [Fig. 2.2 C], chromosome spreads were tightly knotted with quite a few over lapping chromosomes (red arrow). Treatment with 0.075M KCL also resulted in either under or over spread chromosomes. However an increased incubation time of 30 minutes in 0.05M KCl [Fig. 2.2 D] lead to well spread chromosomes with no overlaps or overspreads.

The final step before slide preparation is the preservation of the cells in a stable state by alcohol fixation. In animal cytogenetics ethanol-acetic acid [3:1] is the common method of fixation, while with human cells the preference is methanol-acetic acid [3:1] fixation. Both of these alcohol fixation methods were examined with *B. glabrata* chromosomes and although both can be used to attain metaphase spreads, less clumping of cells and better spreads were achieved with methanol-acetic acid fixation.

When making slides, careful attention to a number of variables increases the chances of successful spreads. After dropping the fixed cell suspension onto a glass slide the fixative is allowed to evaporate. The rate of evaporation is critical to the final dispersion of chromosomes on the glass slide. Humidity, temperature, and the flow of air can be manipulated to produce optimal chromosome spreads. In our laboratory prime metaphase spreads of *B. glabrata* was achieved when the fixed cells were dropped onto wet slides, blown upon, and subsequently placed on the wrist for 15 seconds.

Figure 2.2 Representative images of *B. glabrata* NMRI strain metaphase spreads obtained from ovotestes, and prepared with different hypotonic solutions, concentrations, and incubation times. Panels A and B display metaphase spreads achieved after 20 and 30 minute treatment with 0.075M tri-sodium citrate dehydrate respectively. Images C and D display metaphase spreads after 20 (C) and 30 (D) minute treatment at 0.05M KCl. Chromosomes were counterstained with the DNA intercalater DAPI and subsequently converted to grey scale images. The red arrow indicates chromosomal overlaps. Scale bar = 10µm.

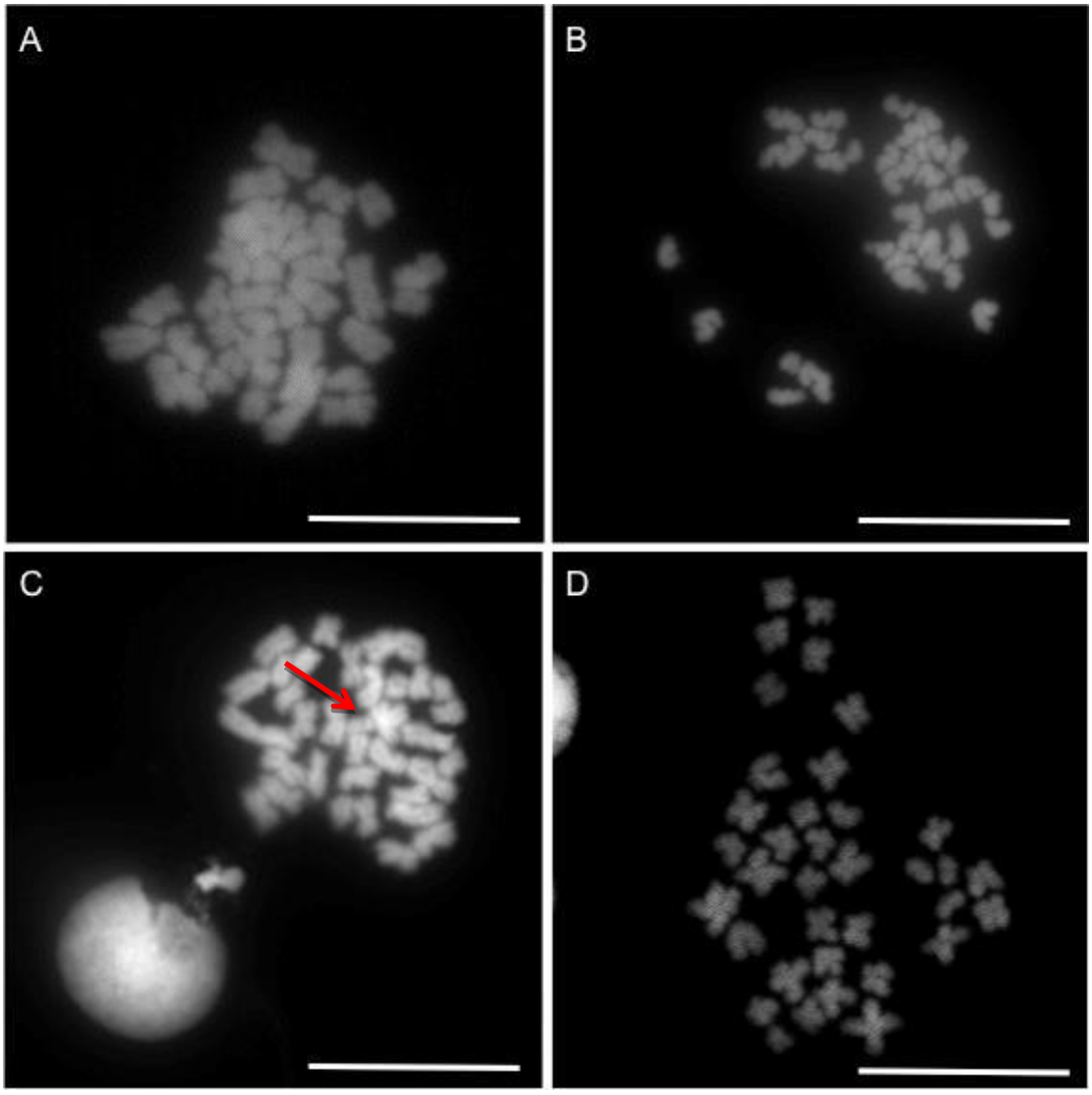

2.3.2 Maximising the number of metaphase spreads achieved from the snail

Incubation of a whole snail in colcemid and subsequent dissection of the ovotestis to obtain a cellular suspension for chromosome spreading resulted in 5-8 metaphase spreads per snail / slide. Although this is a sufficient amount for karyotyping purposes, the use of these chromosomes at a rate of 5-8 per slide would make other studies, such as the physical mapping of genes, extremely difficult to accomplish. To overcome this problem, cellular suspensions were made from other regions of the snail to identify the area with the most mitotic cells. Figure 2.3 displays a graph showing the average number of metaphase spreads acquired from the head/foot, mantle, liver, and ovotestis of the snail. The highest number of metaphase spreads were obtained from the ovotestis (on average 6 per slide), however this figure did not increase even after 12 hour incubation of whole snails in colcemid.

Figure 2.3 Graph showing the average number of metaphase spreads obtained from the head/foot, mantle, liver, and ovotestis of *B. glabrata*, after 3 hour incubation of whole snails in colcemid solution; n = 3. Error bars = S.D.

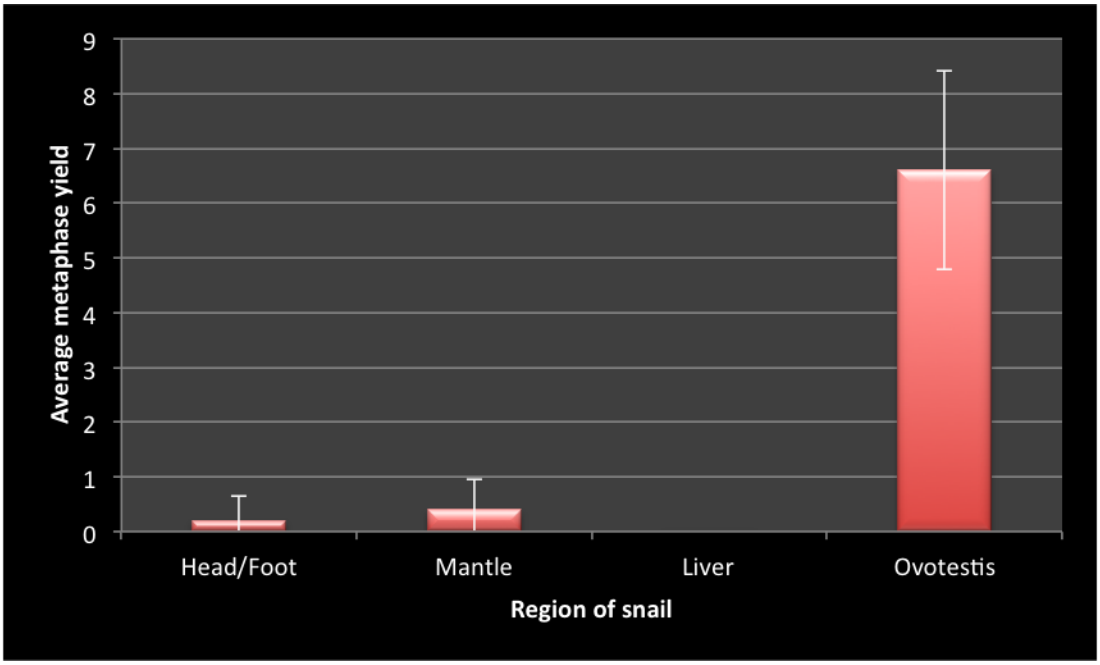

2.3.3 4',6-diamidino-2-phenylindole (DAPI) and denatured DAPI banding of *B. glabrata* chromosomes

4',6-diamidino-2-phenylindole (DAPI) banding is a common technique used in cytological preparations to pair homologues chromosomes requiring minimal slide pre-treatment (Bayani and Squire, 2004b). This type of banding was used when the Bge cell line was karyotyped (Odoemelam *et al.*, 2009). Since previous G-banding efforts on *B. glabrata* chromosomes were not a success, DAPI banding was the first method employed in an effort to produce a karyotype. Despite efforts at experimental and computational optimisation, no bands were achieved when the DAPI stained chromosome images were inverted to grey scale [Fig. 2.4 A]. As dehydration and heat treatment are thought to intensify DAPI bands (Bayani and Squire, 2004a), slides with metaphase spreads were taken through an ethanol series followed by denaturing at 70°C. Although this resulted in some bands [Fig. 2.4 B], the majority of the chromosomes still had solid staining, making it extremely difficult to match the homologues pairs. With both techniques the chromosomes were arranged only on the basis of their size and centromere position and were arranged into nine groups according to the criterion of Goldman *et al* (Goldman *et al.*, 1984), as displayed in table 2.2. However, as a contrary to Goldman's results two acrocentric chromosomes were identified instead of a single large acrocentric chromosome. This second pair was a small acrocentric chromosome and was placed in group VIII, described as a small sub-metacentric chromosome by Goldman. Although the chromosomes were successfully arranged into groups, the lack of banding yielded results of an incomparable standard to that observed in other karyotypes (Dalzell *et al.*, 2009; Couturier-Turpin *et al.*, 1982; Lyons *et al.*, 1977).

Table 2.2 Grouping criterion of DAPI banded *B. glabrata* chromosomes as adapted from Goldman *et al* (1984).

Group	Chromosome description
I	Largest pair of metacentric chromosomes
II	Next two metacentric chromosomes in decreasing order by size
III	Three sub-metacentric chromosomes, similar in size to group II
IV	Single, large acrocentric chromosome pair
V	Three medium sized metacentric chromosomes
VI	Single medium sized sub-metacentric chromosome pair
VII	Three small sub-metacentric chromosomes
VIII	Single small acrocentric pair
IX	Two small metacentric chromosomes

2.3.4 Q-banding of *B. glabrata* chromosomes

As a consequence of the results obtained from DAPI banding, and taking into consideration the previous failure of G-banding attempts (Goldman *et al.*, 1984; Raghunathan, 1976) a new technique was utilised on these chromosomes. Q-banding is another form of fluorescent banding technique used in cytological studies. In an effort to produce a snail karyotype this banding technique was applied to snail chromosomes by staining with quinacrine mustard dihydrochloride. However as with DAPI banding only solid, homogeneous staining was achieved with *B. glabrata* chromosomes [Fig. 2.5], enabling their arrangement only on the basis of size and centromere position. Due to the poor level of staining very limited information was available and thus the chromosomes were not of a standard to construct a karyotype.

Figure 2.4 Representative DAPI banded karyotype images of *B. glabrata* BS90 strain. Metaphase spreads were counterstained with DAPI and then converted into grey scale images. Panel A display a DAPI karyotype with solid bands. Panel B display a DAPI karyotype from a pre-treated and denatured slide. Chromosomes were organised on the basis of their size and centromere position and arranged into nine groups according to the criterion of Goldman *et al* (1984). Scale bar = 5μm.

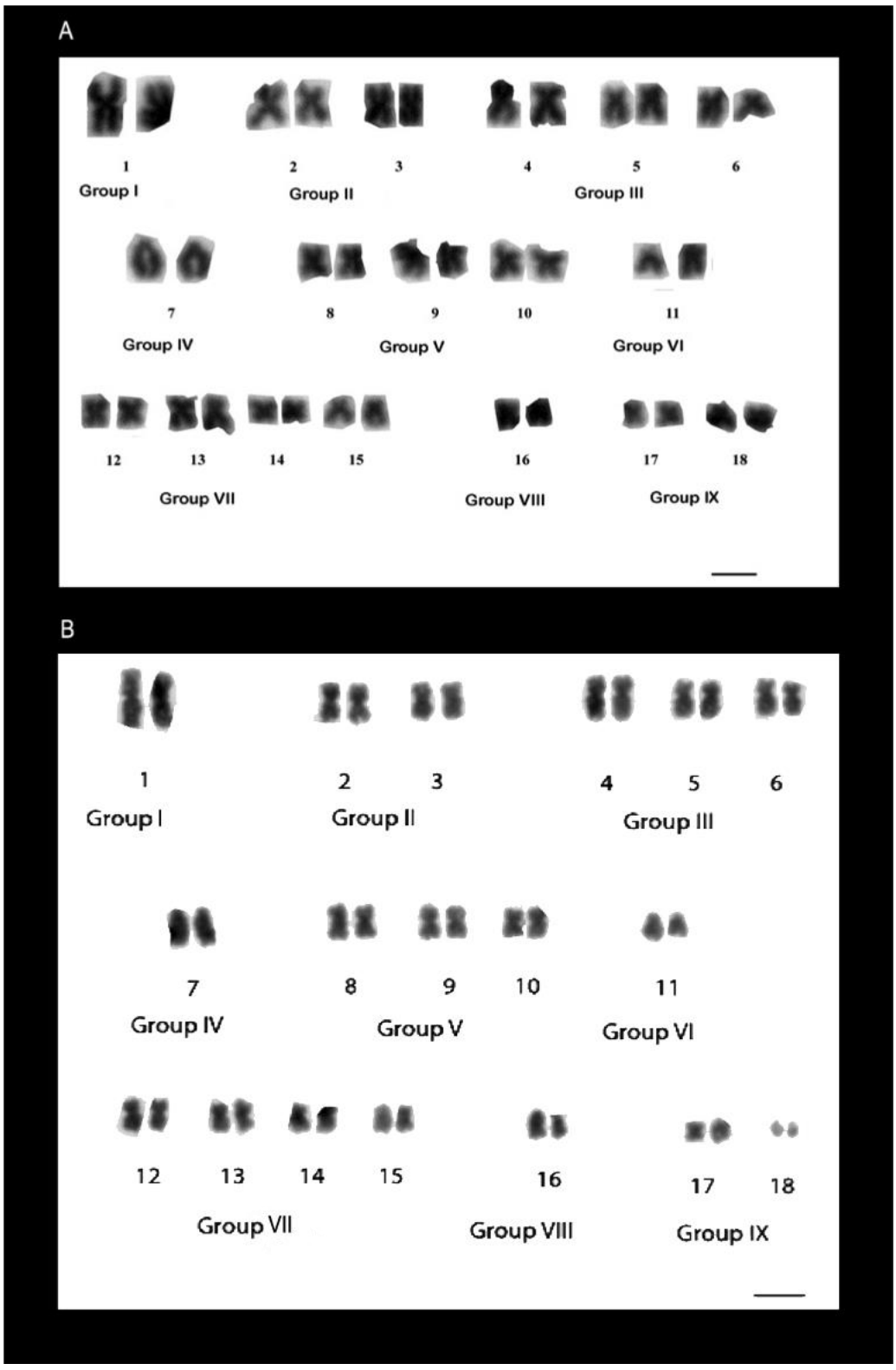

Figure 2.5 Representative images of *B. glabrata* BS90 strain metaphase spreads, stained with quinacrine mustard dihydrochloride. Glass slides with metaphase spreads were incubated in quinacrine solution at various time points and subsequently washed and mounted in McIlvaine buffer. Panel A displays a metaphase spread after 30 minute incubation, and panel B display a spread obtained after 40 minute incubation in quinacrine mustard dihydrochloride solution. Scale bar = 10μm.

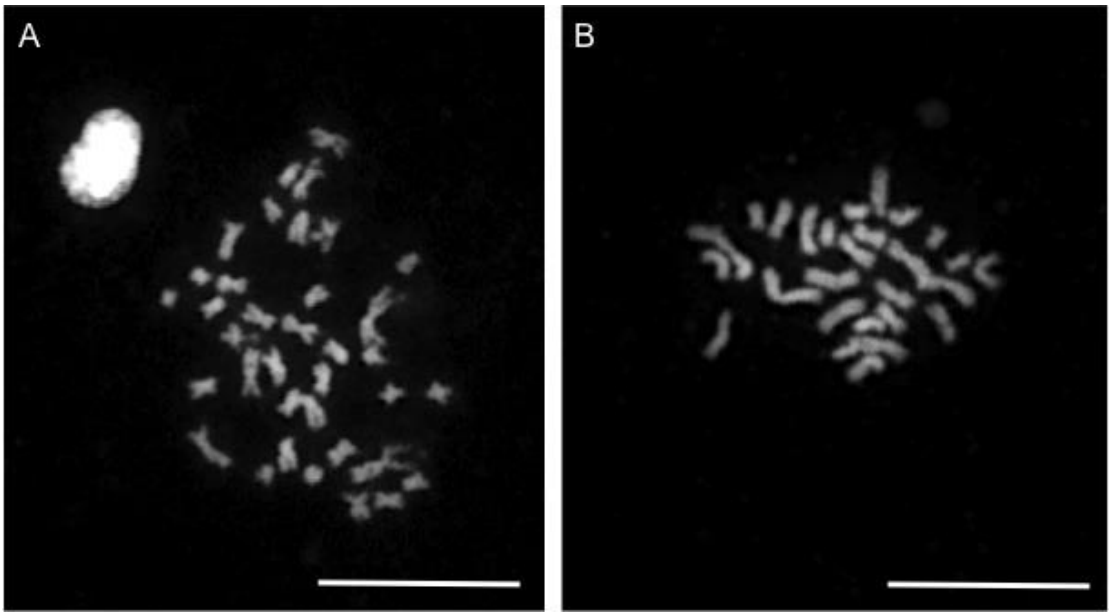

2.3.5 G-banding of *B. glabrata* chromosomes

Due to the variability and poor standard of banding obtained from both DAPI and Q-banding, G-banding was also attempted in an effort to produce a karyotype for *B. glabrata.* To allow access to stain the DNA, G-banding requires sufficient chromosome ageing and enzymatic digestion, which varies among different cell types and organisms (Bayani and Squire, 2004a). To optimise the human G-banding technique for the snail chromosomes, the protocol was modified at critical points to achieve prominent bands. Figure 2.6 displays representative G-banded metaphase chromosomes after different incubation times in trypsin solution. At the lowest incubation time of 20 seconds [Fig. 2.6 A], the morphology of the chromosomes is unaffected by protease activity.

However the chromosomes are mostly homogenously stained with no apparent distinction between G-positive and G-negative regions – a typical indication of insufficient trypsin treatment. After a 30 second incubation in trypsin solution [Fig. 2.6 B] the chromosome morphology was still unaffected, but with clearly defined dark and light regions. This was the optimum time point identified for trypsin treatment in these cells. A prolonged incubation of 40 seconds in trypsin solution resulted in puffy and swollen chromosomes with unsatisfactory stain uptake [Fig. 2.6 C], indicating that for *B. glabrata* chromosomes this time point leads to excessive trypsinisation.

The next step was optimising the incubation time in Giemsa stain solution, using the aforementioned trypsin incubation time. Figure 2.7 displays representative images of trypsinised metaphase spreads stained at various time points in Giemsa stain solution. After 3 minutes of incubation [Fig. 2.7 A], the chromosomes have some stained regions however the staining is insufficient to identify homologues pairs. At 4 minutes [Fig. 2.7 B], chromosomes had prominent dark and light regions, and the bands were clear and distinct for each chromosome. A further 5 minute incubation in Giemsa stain [Fig. 2.7 C] resulted in bands, however some chromosomes had a solid dark stain, which was an indication of excessive staining.

From these experiments it was concluded that for *B. glabrata* chromosomes, stable and effective band resolution is achieved after a 30 second trypsin treatment followed by a 4 minute incubation in Giemsa stain. This results in prominent bands, comparable to those observed in other organisms (Dalzell *et al.*, 2009; Couturier-Turpin *et al.*, 1982; Lyons *et al.*, 1977).

Figure 2.6 Representative bright field images of G-banded *B. glabrata* BB02 strain metaphase spreads after different trypsin incubation times. Panels A, B, and C display representative metaphase spreads after 20, 30, and 40 second incubation in trypsin solution respectively. Scale bar = 10μm.

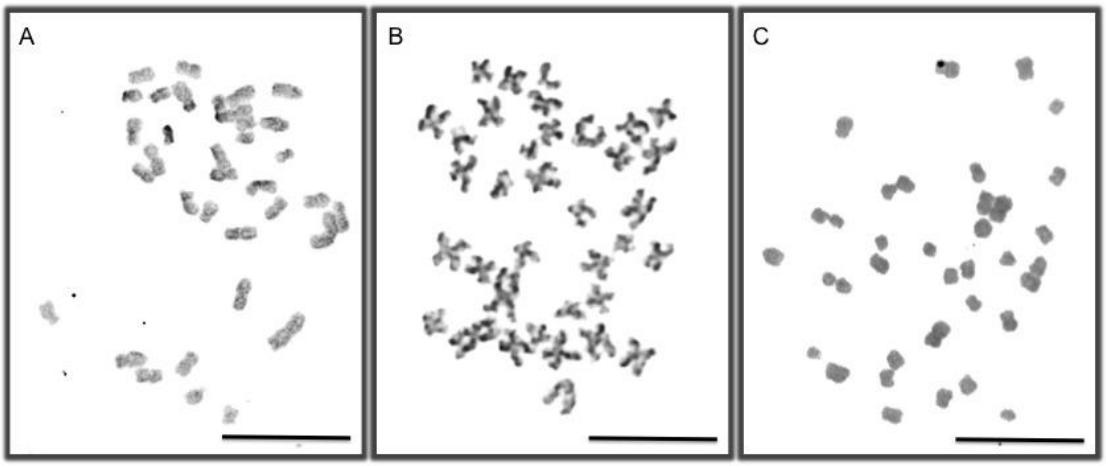

Figure 2.7 Representative bright field images of G-banded *B. glabrata* BB02 strain metaphase spreads stained for different durations in Giemsa solution. Slides with metaphase spreads were incubated in trypsin solution for 30 seconds and subsequently rinsed in FBS and PBS prior to staining with Giemsa solution. Panels A, B, and C display representative metaphase spreads after 3, 4, and 5 minute incubation in Giemsa stain solution respectively. Scale bar = 10μm.

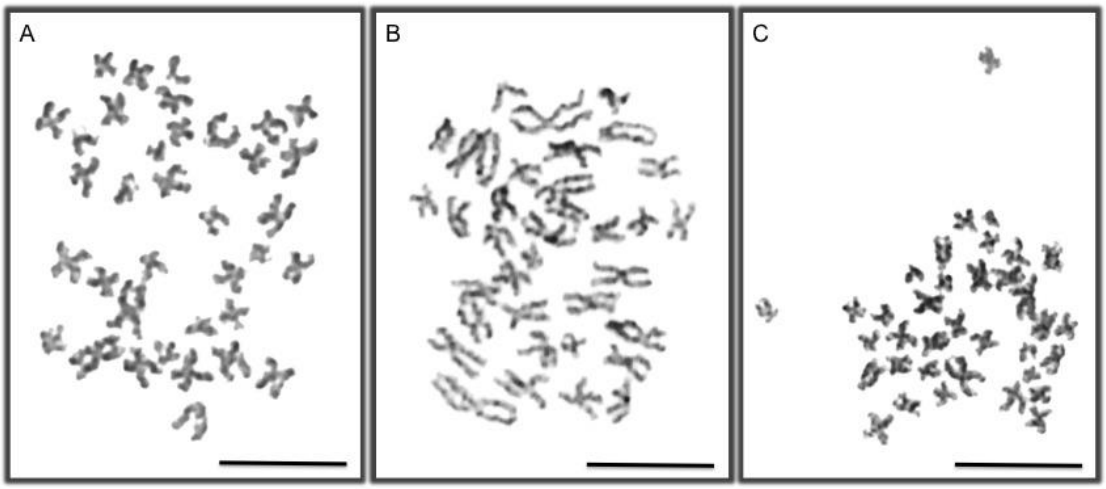

Examination of thirty representative G-banded karyotypes have confirmed the diploid chromosome number of *B. glabrata* to be 2n = 36. Figure 2.8 displays a representative G-banded metaphase spread [Fig. 2.8 A] and a karyotype built from the spread [Fig. 2.8 B]. Chromosomes were arranged into six groups on the basis of their size, centromere position, and banding pattern. Unlike in any other published karyotypes of *B. glabrata*, two chromosomes without a designated homologues pair were identified in all of the karyotypes examined. These were grouped as 'heteromorphic chromosome pair'. Table 2.3 shows a description of the banding patterns for each chromosome, detailing distinguishing features.

To create ideograms, ten representative karyotypes were used to calculate the percentage haploid autosomal length (HAL) for each chromosome [Fig. 2.9] (Gardner *et al.,* 2011). This was then used to construct proportional schematic representation for each chromosome [Fig. 2.8 C]. G-band positive regions are drawn in black and G-band negative regions are in white.

Table 2.3 Description of prominent G-band pattern on each *B. glabrata* chromosome.

Chromosome	Group	Band description
1	A	Largest metacentric chromosome with prominent G-positive regions on both p and q arms
2	A	Largest sub-metacentric chromosome with prominent centromeric band and G-positive bands on the q arm
3	A	Large metacentric chromosome with prominent G-positive bands on both p and q arms
4	A	Large sub-metacentric chromosome with G-positive bands on the q arm
5	A	Large acrocentric chromosome with G-positive bands on the q arm
6	B	Medium sub-metacentric chromosome with G-positive band on the telomeres of the p arm, centromere, and the q arm
7	B	Medium sub-metacentric chromosome with G-positive band on the telomeres of the p arm, centromere, and below the centromere on the q arm

8	B	Medium sub-metacentric chromosome with prominent G-negative bands both above and below the centromere
9	B	Medium sub-metacentric chromosome with large G-negative bands on the p and q arms, and a prominent centromeric band
10	C	Medium metacentric chromosome with G-positive bands on the telomeres of the p and q arms and the centromere
11	C	Medium metacentric chromosome with G-positive bands on the p arm and the centromere
12	C	Medium metacentric chromosome with G-positive bands on the telomeres of the p and q arms
13	C	Medium metacentric chromosome with G-negative bands on the p and q arms and a prominent centromeric band
14	D	Small sub-metacentric chromosome with prominent G-positive bands on the telomeres of the p arm
15	D	Small sub-metacentric chromosome with prominent G-positive bands on the q arm and the centromere
16	E	Small acrocentric chromosome with G-positive bands on the q arm
17	F	Small metacentric chromosomes with G-positive bands above the centromere and on the q arm
18	Heteromorphic	Large sub-metacentric chromosome with large G-positive bands on both p and q arms
19	Heteromorphic	Smallest sub-metacentric chromosome with centromeric band and G-positive bands on the q arm

Figure 2.8 Representative image of a G-banded metaphase spread (A), karyotype (B), and a proposed ideogram (C) for the freshwater snail *B. glabrata* BB02 strain. Chromosomes were organised into groups according to their size, centromere position, and banding pattern. Single chromosomes without a designated homologue are grouped as heteromorphic chromosome pair. On the ideograms G-band positive regions are shown in black and G-band negative regions are in white. Scale bar = 10μm.

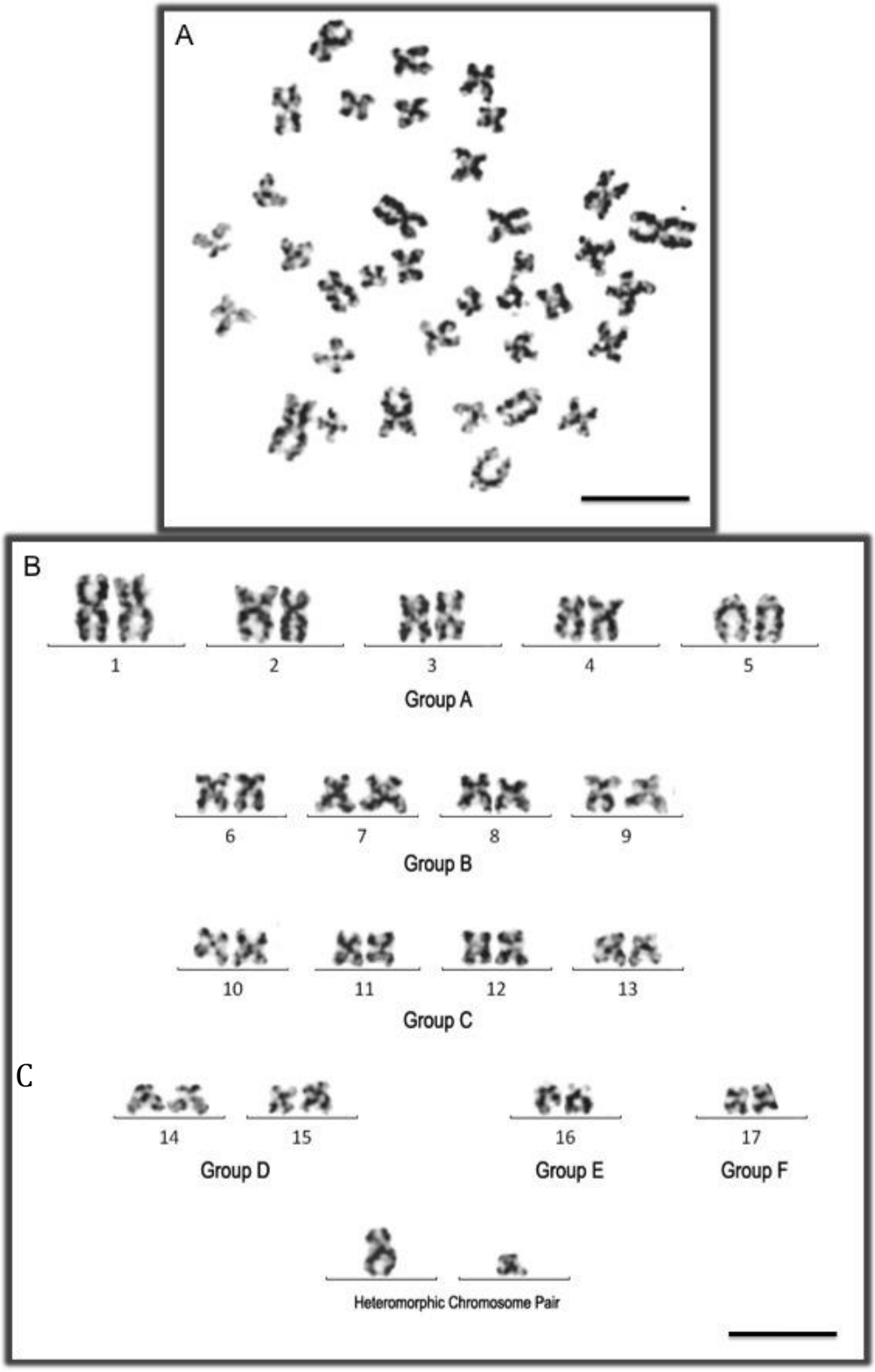

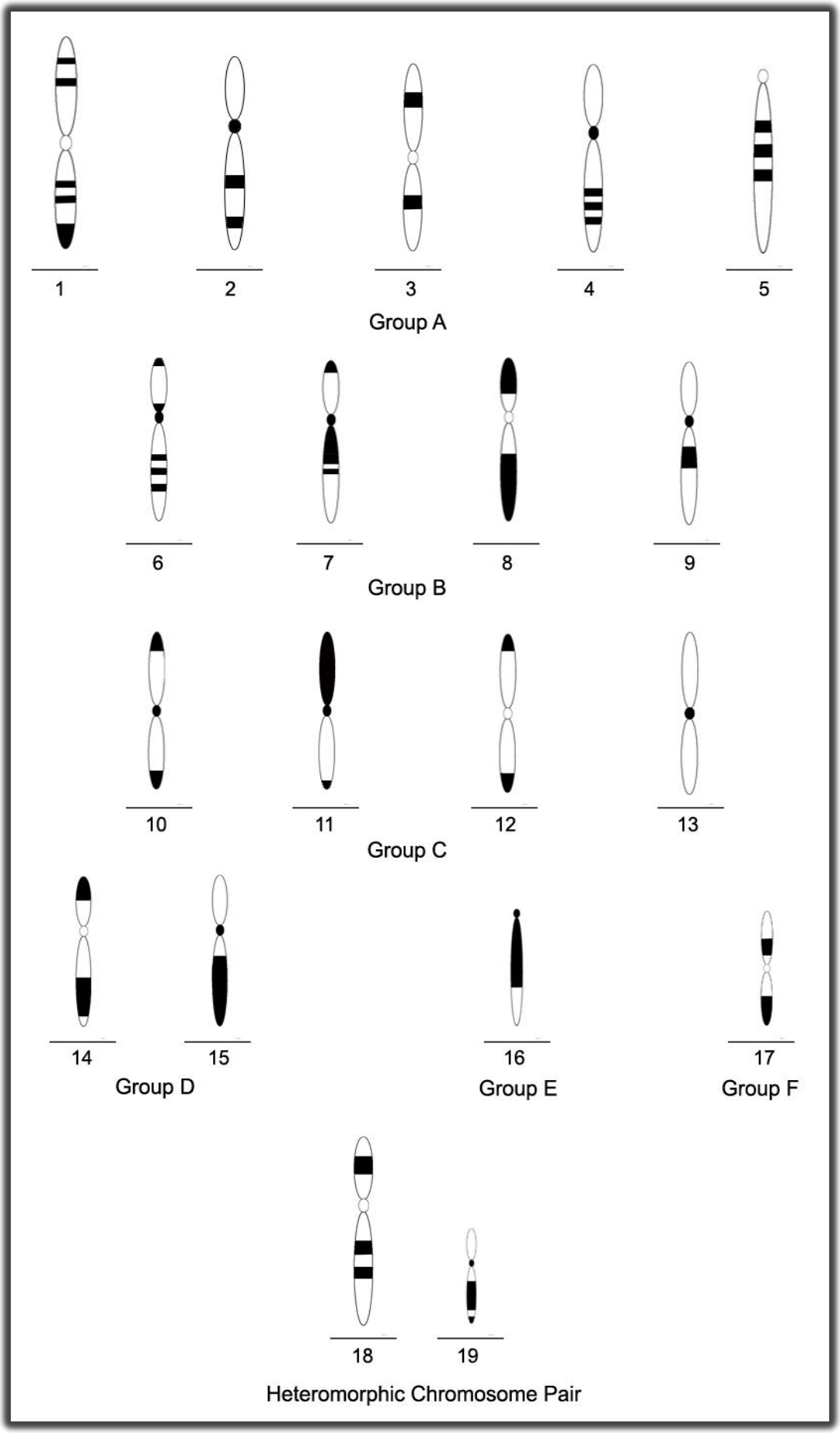
1
2
3
4
5
Group A
6
7
8
9
Group B
10
11
12
13
Group C
14
15
Group D
16
Group E
17
Group F
18
19
Heteromorphic Chromosome Pair

Figure 2.9 Chart showing the average percentage haploid autosomal length (HAL) for *B. glabrata* BB02 strain chromosomes. For each chromosome, the entire chromosomal lengths were measured and averaged across the ten karyotypes. Error bars = S.D.

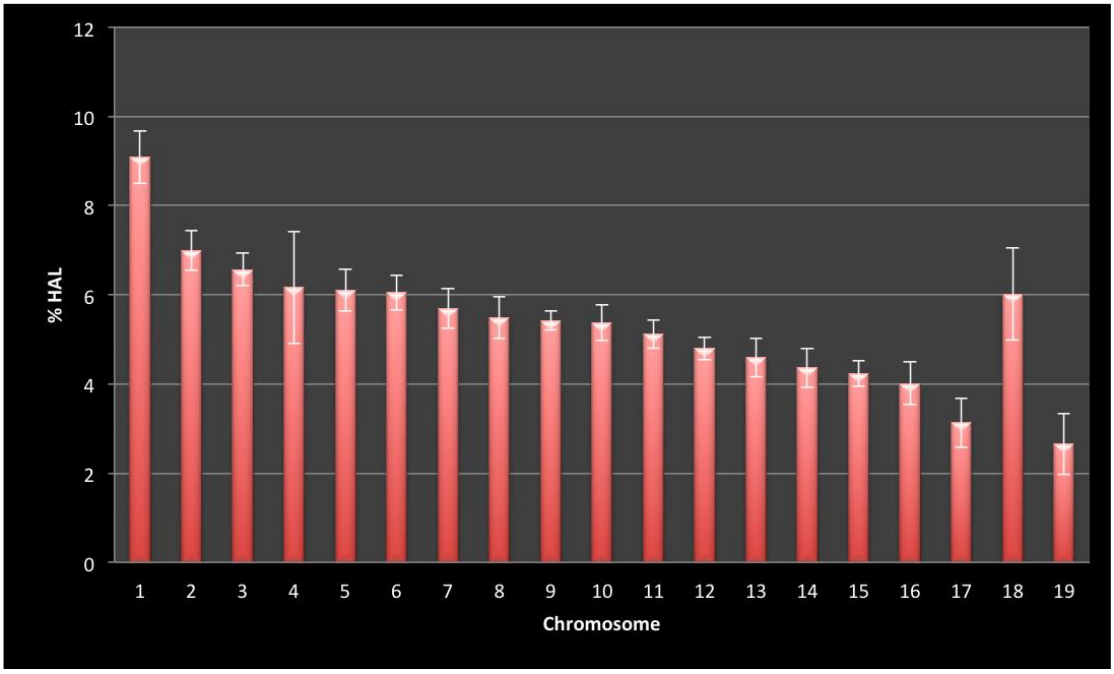

2.3.7 Physical mapping *B. glabrata* genes onto the homologues chromosomes of the snail

Following the construction of a G-banded karyotype, *B. glabrata* genes were mapped onto these chromosomes to assist further identification of the chromosomes. By utilising an established fluorescence *in situ* hybridisation protocol (see chapter 3), effective mapping of *B. glabrata* genes was performed. The four BAC probes used were *actin, ferritin, hsp70,* and *piwi* (for details see chapter 3).

Due to the limited number of metaphase spreads available (5-8 per slide), an initial automated scanning of the slide was performed, which enabled detection of location and parameters of the metaphase spreads on the slide. Probes were then placed on the slide accordingly. Figure 2.10 displays representative images from the mapping of four genes onto homologous chromosomes.

The *actin* probe (A) maps on the large acrocentric chromosome of group A (chromosome 5). *Ferritin* (B) and *hsp 70* (C) probes both map on a p arm of a medium metacentric chromosome in group C. Finally the *piwi* (D) gene maps on a small chromosome, located distally from the centromere. Dual colour 2-D FISH was performed in an effort to clarify that *ferritin* and *hsp70* genes are not mapping onto the same chromosome in group C. The results from this experiment have shown that the two genes map on different chromosomes in group C [Fig. 2.11].

Figure 2.10 Representative images of *B. glabrata* metaphase spreads after 2-D fluorescence *in situ* hybridisation of BAC vectors containing *B. glabrata* genes onto homologues chromosomes of the snail. The four genes, *actin* (A), *ferritin* (B), *hsp70* (C), and *piwi* (D) were labelled with biotin and detecting using streptavidin conjugated to cyanine 3 (red). All *four* genes map onto two homologues chromosomes from *B. glabrata.* The chromosomes were counterstained with DAPI (blue). Arrows indicate the location of genes on the chromosomes. Scale bar = 10μm.

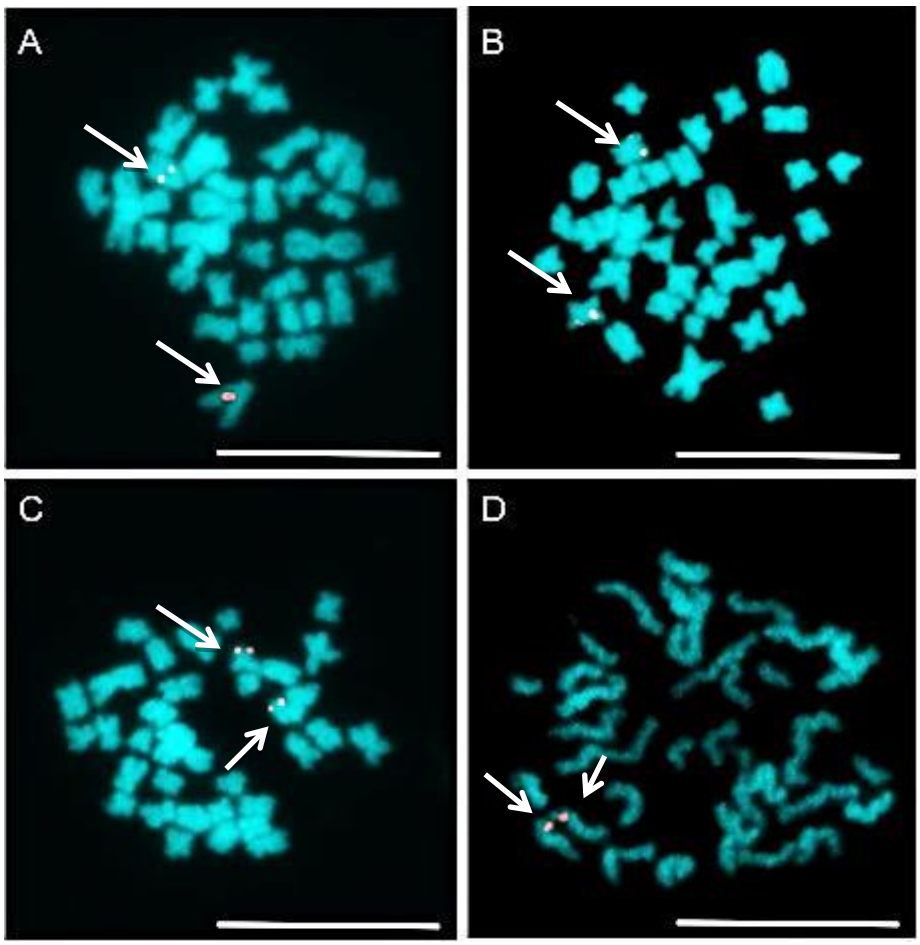

Figure 2.11 Representative images of *B. glabrata* metaphase spreads after dual colour 2-D FISH. Chromosomes were fixed and hybridised with DNA from BAC clones containing the encoding sequences for *ferritin* and *hsp70* genes. The *ferritin* gene was labelled with biotin and detecting using streptavidin conjugated to cyanine 3 (red). *Hsp70* gene was labelled with digoxigenin and subsequently detecting using streptavidin conjugated to fluorescein isothiocyanate (green). The chromosomes were counterstained with DAPI (blue). Arrows indicate the location of genes on the chromosomes. Scale bar = 10μm.

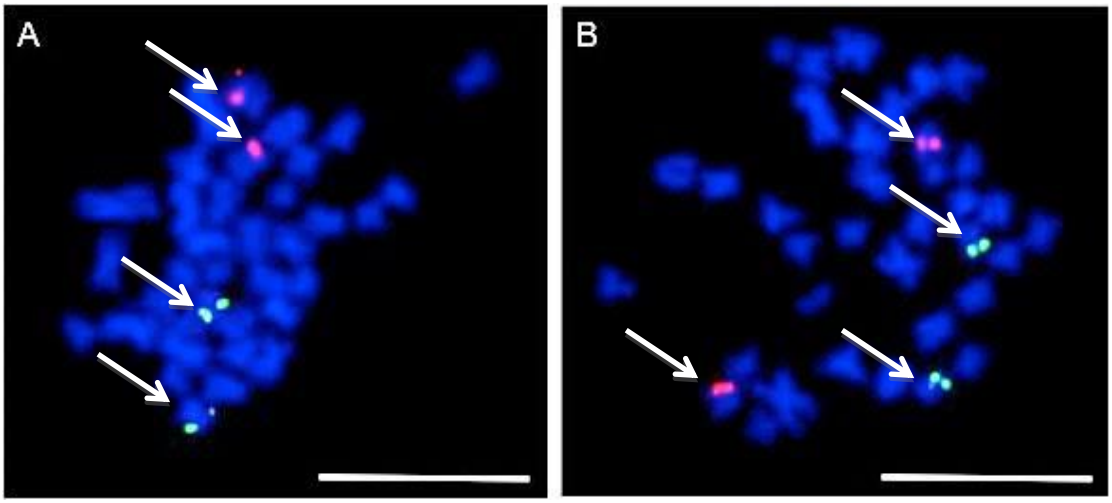

2.4 Discussion

For decades the freshwater snail *B. glabrata* has been an interesting target for countless reports from evolutionary to medical studies. As a major intermediate host for *S. mansoni* parasite in causing schistosomiasis, one of the most prevalent parasitic infections, it has been chosen to have its genome sequenced and became a model organism representing the molluscan phylum. For this reason studies on the genome of this snail has increased over the past few years. With regards to cytogenetic studies of *B. glabrata*, reports have been made in the past in an effort to understand the snail-parasite relationship and chromosomal evolution of this snail (Kawano *et al.,* 1987; Goldman *et al.*, 1984; Raghunathan, 1976; Narang, 1974; Fraga de Azevedo and Goncalves, 1956).

In these studies however, chromosome spreads were obtained either by employing the 'squash' technique using whole snail, or by the 'air drying' technique using snail embryos. Both methods were very challenging, tedious, and time consuming, bringing a hindrance for cytological studies of the snail. With the snail genome project approaching completion (Bg_Initiative) it was crucial to overcome this problem.

In this chapter, a robust and effective chromosome spreading protocol has been established for *B. glabrata.* The snail ovotestis was used to obtain a cellular suspension fixated in methanol-acetic acid, which can be prepared in large quantities and stored at -20°C for prolonged use. Using this new method, between five to eight good quality metaphase spreads can be achieved per snail / slide. Unfortunately, despite the use of the ovotestes where absolute cell division is expected, and prolonged exposure to colcemid solution, the number of metaphases per slide could not be increased. A possible explanation for this bizarre situation came from Fraga de Azevedo *et al*, whom in 1956 reported the very limited number of dividing cells found in histological studies of the ovotestis. They reported that the majority of the cells were in a state of maturity and advanced quiescence (Fraga de Azevedo and Goncalves, 1956). However, application of state-of-the-art technology to snail research has by far made snail chromosomal studies feasible. With the aid of automated scanning and capturing, metaphase chromosomes of *B. glabrata* can be now be analysed regardless of their limited number. Likewise, technical improvements in banding techniques have made it possible to construct a snail karyotype and the first snail ideograms. As a standard representation for chromosomes, the ideograms will most certainly be an invaluable tool for future snail genome studies, in particular when describing the location of genes on chromosomes.

In accordance with previous reports, the G-banded karyotype of *B. glabrata* contains a diploid chromosome number of 2n = 36. In spite of this, unlike in any other karyotype reports of *B. glabrata* and other hermaphrodite organisms, two heteromorphic chromosomes were identified. It is thought that these two chromosomes could be the snail sex chromosomes.

Sex determination in another hermaphrodite organism, the nematode C. elegans, is governed by an X-dosage system. While the hermaphrodites have two X chromosomes (XX), a spontaneous loss of the X chromosome during self-fertilisation can generate the rare male with a single X chromosomes (XO). The males contain equal amounts of X-bearing gametes and nullo-X gametes (gametes that lack an X chromosome) and half their cross progeny will also be males (Hodgkin, 1987; Herman, 2005). However whether *B. glabrata* has a similar system to the nematode, or an XY sex determination system as in humans, a ZW system seen in birds, reptiles and some insects (Ellegren, 2011), or even a new unknown system remains to be elucidated.

Construction of physical genetic maps is essential for a better understanding of an organisms genome organisation. It also allows thorough characterisation of chromosomes, which is vital for an understudied organism such as *B. glabrata.* Since the representation of the Bge cell line of *B. glabrata* is now a matter of debate, it was imperative to develop protocols for snail *ex vivo* cells to be used in future mapping experiments. Given that only a very limited number of metaphase spreads can be gained from whole snails, the task was not simple. Large quantities of FISH probes were required to be able to get gene signals on the broadly distributed metaphases, which was a very expensive method. Automated scanning of slides and identifying areas of the slide containing metaphase spreads prior to FISH experiments overcame these problems. Thus, a fast and efficient technique has now been identified for *B. glabrata,* enabling rapid analysis of its chromosomes. The four genes studied have all successfully mapped onto two homologues chromosomes. Three of these genes, *actin, ferritin,* and *hsp70* were previously found to be up-regulated after an infection with *S. mansoni* (Ittiprasert *et al.*, 2009). It would therefore be interesting to analyse the mapping of these genes between the resistant and susceptible snail genomes.

The P-element induced wimpy testis (*piwi*) gene was selected due to its role in germ cells (Wang and Elgin, 2011). The prospect of this gene mapping onto one of the heteromorphic chromosomes was another reason for its choice, which would have clarified the existence of these unpaired chromosomes.

However as displayed in figure 2.10 D, the gene mapped onto a small pair of homologues chromosomes. Nevertheless, to investigate the possibility of the presence of snail sex chromosomes, future studies should aim to search for sex-specific genes in the *B. glabrata* database and map them onto the snail *ex-vivo* chromosomes.

Understanding of snail cytogenetics is vital to study chromosomal aberrations and to even gather past evolutionary events. In terms of *B. glabrata* and the sequencing project, it would allow the initial physical studying of the difference between the susceptible and resistant snail chromosomes to identify chromosomal insertions, translocation, and/or deletions that may be present in the genome leading to that particular phenotype of the snail. To close this gap in the snail studies, a technique has now been developed, which results in good quality metaphase spreads. Successful G-bands have also been obtained on these chromosomes enabling the identification of homologues pairs to form a snail karyotype. The presence of prominent and landmark G-bands has also enabled the construction of the first snail ideograms, enabling researchers to rapidly identify each individual snail chromosome. Finally, for the first time physical mapping of genes onto chromosomes from *B. glabrata* have also been achieved. Knowledge of *B. glabrata* genome is a future stepping stone for the development of new control measures to help eliminate the spread of schistosomiasis. The genome is an unknown to all, which inevitably means that time will be taking in optimising many techniques to suit the *B. glabrata* genome. This chapter describes the first steps taken to achieve this goal.

Chapter 3

Analysis of *Biomphalaria glabrata* genome organisation upon parasitic infection

The contents of this chapter are in preparation for a publication in PLOS Pathogens: 'Spatial repositioning of activated genes in *Biomphalaria glabrata* snails infected with *Schistosoma mansoni*' - Halime Derya Arican, Wannaporn Ittiprasert, Joanna M Bridger, Matty Knight.

The work undertaken in this chapter was supported by a grant from the National Institute of Health and Burroughs Wellcome Fund.

3.1 Introduction

Fluorescence *in situ* hybridisation (FISH) is a cytogenetic technique allowing the study of nucleic acids in their cytological context. Since the establishment of the early *in situ* hybridisation system via radioactive labelling (Gall and Pardue, 1969), many variations of the procedure have been developed, the most common being fluorescence *in situ* hybridisation. FISH is a widely used technique enabling the detection of unique sequences as distinct colours with the aid of fluorescently labelled probes. The probe can be labelled directly by the incorporation of fluorescent nucleotides or by indirect labelling using reporter molecules such as hapten, which can then be detected using enzymatic or immunological detection systems. The basic principles of FISH technique involve heat denaturation of the labelled probe and the target sequence on a slide to obtain single strands of DNA molecules. Under specialised conditions, complementary strands of the labelled probe are permitted to hybridise and anneal to its counterpart sequence on the target sample. The ability of the DNA helix to renature provides the molecular basis for this hybridisation. Following hybridisation slides are taken through several washes to remove any excess unbound probe, and can be visualised *in situ* by fluorescence microscopy analysis.

The unique ability of FISH to provide an intermediate degree of resolution between DNA analysis and chromosomal investigations while retaining information at the single cell level, has made its application very appealing (Volpi and Bridger, 2008). Today it is commonly used as a clinical diagnostic tool to identify and localise the presence or absence of specific DNA sequences on chromosomes and nuclei in diagnosing congenital syndromes. It is also widely used in research investigating chromosomal and nuclear architecture. FISH plays a primary role when mapping genes onto metaphase chromosomes, providing important positional data. However its application in interphase cytogenetics allows the analysis of the genome in its three-dimensional context, which is discussed below.

When utilising the FISH technique for the first time, manipulations to the standard procedure may be required to suit a particular organism, tissue, cell, or chromosomes. There are many crucial components before, during, and after hybridisation that can affect the success of a FISH assay. In this chapter I describe the 2-D FISH technique optimised for *ex vivo* cells and chromosomes of *B. glabrata* for effective hybridisation of gene signals. For the first time, the mapping of *B. glabrata* genes onto interphase nuclei of the actual snail is demonstrated.

The eukaryotic cell nucleus is a highly organised structure. Interphase chromosomes are compartmentalised within the nuclei and form individual entities known as chromosome territories (Meaburn and Misteli, 2007; Cremer and Cremer, 2006). Likewise, genes also harbour non-random positioning during interphase (Misteli, 2005). This dynamic organisation of chromosome territories and gene loci within the nucleus plays an integral role in controlling gene expression (Green *et al.*, 2012; Kumaran and Spector, 2008). Changes in spatial positioning of chromosome territories and/or gene loci have been reported during physiological processes such as differentiation and development (Szczerbal *et al.,* 2009; Foster *et al.*, 2005), disease (Meaburn *et al.*, 2009; Meaburn and Misteli, 2008; Zink *et al.,* 2004b; Cremer *et al.*, 2003), and cellular proliferation (Mehta *et al.*, 2010; Bridger *et al.*, 2000). Moreover, studies using mammalian models correlate the activation of a gene with its movement towards the nuclear interior (Elcock and Bridger, 2010; Deniaud and Bickmore, 2009; Szczerbal *et al.,* 2009; Takizawa *et al.,* 2008b) and the nuclear periphery as a site for down regulation of gene activity and gene silencing (Shaklai *et al.*, 2007). However, an increasing number of studies are now providing evidence for the presence of active genes at the nuclear edge, and some active genes relocating to the nuclear periphery (Kim *et al.,* 2004; Deniaud and Bickmore, 2009). Transcriptionally active genes in yeast and the fruit fly *Drosophila* have also been found located around the nuclear pore complexes (Brown and Silver, 2007).

Indeed, in the Bge cell co-culture system, gene expression was observed to be taking place both when the genes relocated to the nuclear interior and to the nuclear periphery (Knight *et al.*, 2011). As described in this chapter, a similar mechanism is also found in the intact snail *B. glabrata*.

Biomphalaria snails vary in their compatibility as a schistosome host such that some display resistance to infection while others are susceptible (Richards and Shade, 1987). Research investigating the transcriptional modulation of genes upon infection has elucidated genetic factors including fibrinogen related proteins (FREPs) and the cellular stress response proteins ferritin and hsp70, which influence resistance and susceptibility in the snail (Lockyer *et al.*, 2012; Ittiprasert *et al.*, 2010; Ittiprasert *et al.*, 2009; Lockyer *et al.*, 2008; Hertel *et al.,* 2005; Miller *et al.*, 2001). The development of an *in vitro* tissue culture model to support the intra-molluscan stages of *S. mansoni* has also aided the investigations into *B. glabrata's* relationship with *S. mansoni* parasites (Castillo and Yoshino, 2002; Yoshino and Laursen, 1995; Basch and DiConza, 1977). Using such a model the Bge cell *in vitro* co-culture system has been utilised to determine the spatio-temporal affects on specific genes in the nuclei of Bge cells that have been co-cultured with *S. mansoni* miracidia (Knight *et al.*, 2011). Both chromosome territories and genes were found to have a non-random radial position within the interphase nuclei of Bge cells (Odoemelam *et al.*, 2009). Furthermore, large scale gene repositioning which correlated to temporal kinetics of gene expression levels in Bge cells co-cultured with normal miracidia were reported. Co-culturing with irradiated miracidia failed to elicit similar gene expression and gene loci repositioning, indicating that normal but not attenuated schistosomes provide stimuli that evoke host responses (Knight *et al.*, 2011).

In summary, it is evident that parasitic infection alters the transcriptional activity of *B. glabrata* genes. Although the Bge cells provide a responsive *in vitro* model system in which to study molluscan host-parasite interactions, they show extensive aneuploidy to the extent that the total chromosome number greatly exceeds the original cell lines diploid number of 36 chromosomes (Odoemelam *et al.*, 2009).

In this chapter *B. glabrata* fluorescence *in situ* hybridisation technique has been utilised using the snail *ex vivo* cells to determine spatio-temporal affects of three genes in the resistant and susceptible snails that have been infected with *S. mansoni* miracidia. Since the alterations in transcriptional activity have been correlated with spatial reorganisation of gene loci in other organisms, the role a parasitic infection plays in the genome of *B. glabrata* is addressed.

3.2 Materials and Methods

3.2.1 *B. glabrata* stocks and parasite exposure

The following parasite exposure protocol was performed at the Biomedical Research Institute in Maryland, USA, supported by the Sandler Burroughs Wellcome Fund Travel award.

Adult *B. glabrata* snails from the susceptible line (NMRI) and the resistant line (BS90) were incubated overnight in sterile distilled water containing 100ug/ml ampicillin at room temperature in an attempt to reduce contaminating resident bacteria in the snails. Individual snails were exposed to either normal or attenuated miracidia (10 miracidia per snail) at four different time points (0.5, 2, 5, and 24 hours). Using a micropipette and a dissecting microscope, 10 miracidia were counted as they were drawn up into the glass pipette. The miracidia were then placed into each well of 12-well plates, and 2ml of sterile distilled water was added to each well prior to placing the snail into the well. Attenuated miracidia were obtained by irradiation (20 Krad) using Mark 1 cesium-^{137} irradiator at the National Institute of Health (Bethesda, Maryland, USA), as described by Ittiprasert *et al* (Ittiprasert *et al.*, 2009).

Following parasite exposure the snail ovotestes were dissected and incubated in hypotonic potassium chloride solution (0.050M) for 30 minutes, during which time the tissues were macerated with a needle to obtain single cells.

The cells were then centrifuged at 163g for 5 minutes and fixed with methanol and acetic acid as described in chapter 2, section 2.2.2. The cellular suspension was stored at 4°C until further use.

3.2.2 Bge cell culture

Bge cells used in this study were derived from Hansen's original Bge cell line (Hansen, 1979), obtained from the laboratories of Dr E.S. Loker (Bge SL) and Dr. C. Bayne (Bge CB).

Bge cells were grown at 27°C in the absence of carbon dioxide in medium comprised of 22% Schneider's Drosophila medium (Invitrogen, UK), 0.45% lactalbumin hydrolysate (Invitogen, UK), and 0.13% galactose (Invitrogen, UK). The medium was filtered and sterilised through a 0.22µm pore filter (Fisher Scientific, UK), followed by the addition of the antibiotic gentamicin [50µg/ml] (Invitrogen, UK). The medium was made complete by adding 10% FBS (Sigma, UK), which had previously been inactivated at 56°C for 30 minutes. Cells were grown to approximately 80% confluence in T75 cm^3 flasks (Fisher Scientific, UK) before they were reseeded at 1:12 dilution. Due to trypsinisation leading to loss of viability and death, cells were released by firm tapping motions.

3.2.3 Preparation of Bge cell genomic DNA for suppression of repetitive sequences in *B. glabrata* genome.

Bge cells were cultured as described in the aforementioned section 3.2.2. Cells were collected after centrifugation at 400g at room temperature. The pellet was resuspended in 400µl of digestion buffer (100mM Tris [pH 8.0], 5mM EDTA, 200mM NaCl, 0.2% SDS), and 40µl of Proteinase K [20mg/ml], and incubated at 55°C for 2 hours. The suspension was then vortexed and subsequently centrifuged at 170g for 5 minutes at 4°C.

The supernatant was removed to a fresh tube and the DNA precipitated by adding 10% 3M sodium acetate and 2 volumes of ice-cold ethanol, and incubated on ice until the DNA became visible. Using a Pasteur pipette, the DNA was transferred to 1.5ml Eppendorf tubes containing 70% ethanol (two changes). The DNA was then dissolved in 500µl of deionised distilled water and sonicated to obtain fragments ranging between 200 - 500bp. The concentration of the sonicated DNA was measured using the NanoDrop spectrophotometer ND-1000 (Thermo Scientific, UK).

3.2.4 Preparation, labelling, and denaturing of probes to be used in the FISH experiments

The DNA for probes were isolated from BAC clones obtained from *B. glabrata* (BS90) BAC DNA library as described by Raghavan *et al* (Raghavan *et al.*, 2007). Bacterial cells comprising *actin, ferritin*, and *hsp70* BAC DNA were grown as streaks on Luria Bertani (LB) agar plates (1% NaCl, 1% tryptone, 0.5% yeast extract, 1.5% agar technical, and 12.5µg/ml chloramphenicol). The colonies were then inoculated and expanded in liquid culture LB broth (1% NaCl, 1% tryptone, 0.5% yeast extract, and 12.5µg/ml chloramphenicol). DNA was extracted as described in Fluorescence in situ Hybridisation Protocols and Applications: FISH, Basic Principles and Methodology (Garimberti and Tosi, 2010). BACs containing the three genes *actin, ferritin,* and *hsp70* were labelled with Biotin-14 – dATP via nick translation (Langer, Waldrop and Ward, 1981). This was achieved by using a nick translation kit (BioNick™, Invitrogen, UK), which produced probes ranging from 200 - 500bp in size. The products were analysed on a 2% agarose gel and subsequently purified from unincorporated nucleotides using a MicroSpin G50 column (GE Healthcare, UK).

For each slide 250ng of probe solution, combined with 40ng of Bge genomic DNA, 3µg of herring sperm DNA, and one-tenth volume of 3M sodium acetate, were precipitated in 2.25 volumes of 100% ice-cold ethanol.

This mixture was incubated at -20°C for a minimum of 1 hour followed by centrifugation at 400g for 30 minutes at 4°C. The pellet was then washed with ice-cold 70% ethanol and subsequently centrifuged at 400g for 15 minutes at 4°C. The supernatant was removed and the probe was allowed to dry at room temperature. The probe DNA was dissolved in 12µl of hybridisation mix (50% formamide, 10% dextran sulphate, 2X SSC and 1% Tween 20) overnight at room temperature. The probes were then denatured at 75°C for 5 minutes and subsequently incubated at 37°C between 10 and 120 minutes.

3.2.5 Preparation and pre-treatment of slides to be used in 2-D FISH

Slides containing *B. glabrata ex vivo* cells were prepared as described in chapter 2, section 2.2.2, and were aged for two days at room temperature. They were then taken through two pre-treatment methods as described in table 3.1, both individually or combined. The slides were then dehydrated in 70%, 90% and 100% ethanol series (3 minutes each). They were allowed to dry on a hot block at 37°C and subsequently denatured in 70% formamide in 2X SSC solution at 70°C for 1.5 minutes as previously established by Odoemelam *et al* (Odoemelam *et al.*, 2009). Immediately after denaturation slides were immersed in ice-cold 70% ethanol followed by 90% and 100% ethanol (3 minutes each), and allowed to dry on a hot block at 37°C.

Table 3.1 Table showing the slide pre-treatment methods used with *B. glabrata ex vivo* cells.

Treatment	Protocol
RNase A	1 hour incubation at 37°C with RNase A [100µg/ml in 2X SSC], followed by two washes in 2X SSC (5 minutes each).
Pepsin	10 minute incubation at 37°C with pepsin solution (1% 1N HCl, 0.1% pepsin, made up in ddH_2O), followed by a brief rinse in 1X PBS and subsequent dehydration in 70% and 100% ethanol (5 minutes each).

3.2.6 Hybridisation, washing, and counterstaining

Following the denaturing of the slide and the probe, 10µl of the biotin labelled probe was placed onto the slide, covered with 18 x 18 coverslips and sealed with rubber solution (Halfords). The denatured slide and probe was then left to hybridise for 12 – 36 hours in a humidified chamber at 37°C.

Washing of the hybridised slides involved the use of the following two protocols:

Protocol A

This protocol was the standard FISH washing procedure used in our laboratory.

Following hybridisation, the rubber solution and the coverslips were removed and the slides were washed three times for 5 minutes in 50 % formamide and 2X SSC solution (pH7) at 45°C. Slides were then transferred to a Coplin jar containing pre-warmed 0.1X SSC at 60°C, which was then transferred to a 45°C water bath. They were washed in this solution three times for 5 minutes, before being transferred into a solution of 4X SCC at room temperature for 10 minutes. Subsequently 100µl of 4% Bovine serum albumin (BSA) in 4X SSC blocking solution was added to each slide and covered with 22 x 50 cover slips. The slides were left at room temperature for 10 minutes. Coverslips were removed and 100µl of streptavidin conjugated cyanine 3 in 1% BSA / 4X SSC (1:200 dilution, Amersham Biosciences) was added to each slide and a new coverslip applied. The slides were incubated at 37°C for 30 minutes in the dark and then washed three times for 5 minutes in 4X SSC with 0.1% Tween 20 at 42°C in the dark. They were briefly rinsed in deionised distilled water before counterstaining with DAPI [1.5µg/ml] (Vectorshield anti-fade mountant, Vectorlabs).

Protocol B

This protocol was an adapted version of the FISH washing protocol used in the Molecular Cytogenetics laboratory at Wellcome Trust Centre for Human Genetics, Oxford (Moralli and Monaco, 2010).

After hybridisation the rubber solution and the coverslips were removed and the slides were washed three times in 2X SSC at 42°C for 3 minutes. Subsequently 150µl of 1% BSA in 2X SSC blocking solution was added to each slide and covered with 22 x 50 cover slips. The slides were incubated in a humidified chamber at 37°C for 20 minutes. Slides were then washed in 2X SSC at room temperature for 3 minutes and 150µl of streptavidin conjugated to cyanine 3 in 0.1% BSA / 2X SSC (1:200 dilution, Amersham Biosciences) was added to each slide and incubated in a humidified chamber at 37°C for 30 minutes, in the dark. They were then washed in 2X SSC at room temperature for 3 minutes, followed by a second wash in 1X PBS with 0.1% Tween 20 for 1 minute. The slides were briefly rinsed in 1X PBS before counterstaining with DAPI [1.5µg/ml] (Vectorshield anti-fade mountant, Vectorlabs).

3.2.7 Image capture and analysis after 2-D FISH

Nuclei were observed using the Olympus BX41 fluorescence microscope and UPlanFLN 100x / 1.30 oil immersion objective. Digital images were captured using a Grey scale digital camera (Digital Scientific UK) and the Smart Capture 3 software (Digital Scientific UK). Fifty images of nuclei for each gene (*actin, ferritin, hsp70*) were captured and the positions assessed using a bespoke erosion script analysis (Croft *et al.*, 1999). Statistical analyses were performed by using unpaired, two-tailed Student's t-test.

3.2.8 Quantitative reverse transcription PCR analysis of gene transcripts

RNA samples of individual resistant (BS90) and susceptible (NMRI) snails exposed to either normal or irradiated miracidia at different time points (0, 0.5, 2, 5, and 24 hours) were used. Quantitative reverse transcription PCR (qTR-PCR) was performed using Full velocity SYBR Green qRT-PCR Master Mix (Stratagene, Agilent) in a one-step reaction, according to the manufacturer's instructions and run by using the ABI 7300 Real Time PCR system (Applied Biosystems, USA). A final reaction volume of 25µl qRT-PCR mixture contained 80ng of DNase treated RNA, 200nM of each gene specific primer, 300nM reference dye, 1X Full velocity SYBR Green QRT-PCR Master Mix, SYBR Green I dye, $MgCl_2$, and nucleotides.

The primers used were: Actin (F: 5'-GGAGGAGAGAGAACATGC-3'; R: 5'-CACCAATCTGCTTGATGGAC-3'), Ferritin (F: 5'-CTCTCCCACACTGTACCTATC-3'; R: 5'-CGGTCTGCATCTCGTTTTC-3'), and Hsp70 (F: 5'-AGGCGTCGACATTCAGGTCTA-3'; R: 5'-TGGTGATGTTGTTGGTTTTACCA-3'). A parallel reaction was performed using 50nM of the constitutively expressed, housekeeping myoglobin gene (F: 5'-GATGTTCGCCAATGTTCCC-3'; R: 5'-AGCGATCAAGTTTCCCCAG-3'). qRT-PCR reactions included an initial cDNA synthesis at 48°C for 45 minutes followed by a 95°C denaturation for 10 seconds, and annealing/amplification at 58°C for 1 minute. The fluorescent product was detected at the end of the amplification period and all amplifications were run in triplicate. Fluorescent threshold value (Ct) was determined using the 7300 System v1.3.1 SDS software (Applied Biosystems). The differences in gene transcript levels were calculated by the delta-delta Ct (ΔΔCt) method (Livak and Schmittgen, 2001), using the myoglobin housekeeping gene to normalise the quantification of targets. Fold change in transcription was calculated using the following formula:

$$\text{Fold change} = 2^{-\Delta\Delta Ct}$$

$$= 2^{-[(Ct_{\text{gene, exposed}} - Ct_{\text{myoglobin, exposed}}) - (Ct_{\text{gene, unexposed}} - Ct_{\text{myoglobin, exposed}})]}$$

In order to determine the significance of differences ($P < 0.05$ or $P < 0.01$) in gene expression for the different time points, the *P*-value was calculated by comparing delta-delta Ct values using the Student's *t*-test between the exposed and non-exposed snails within each stock.

These experiments were performed together with collaborators from the Biomedical Research Institute in Maryland, USA.

3.3 Results

The cell nucleus is a highly organised and compartmentalised structure, and chromosomes in interphase nuclei occupy individual entities known as chromosome territories (Cremer *et al.,* 2006). This dynamic organisation of chromosome territories and gene loci within them is thought to play an integral role in controlling gene expression (Kumaran *et al.,* 2008). Evidence suggests that spatial positioning of genes in interphase nuclei could be another level of regulating gene expression. This mechanism is now becoming an accepted concept. To investigate this in molluscs, FISH procedure has been optimised for *B. glabrata* cells. For the first time, three genes known to be expressed after parasitic infection have been mapped on to the interphase nuclei of the snail. Results from these experiments confirm the use of a similar mechanism for gene regulation by molluscs.

3.3.1 Slide pre-treatment to acquire optimum gene signals in interphase nuclei of *B. glabrata* cells

Preparation of good quality slides is vital for FISH studies as it can affect the quality of the chromosome / gene signals visualised. High levels of cytoplasmic material can lead to background fluorescence, which in some cases can resemble false signals. Nuclei can mostly be cleaned from cytoplasmic debris by increasing the number of washes in fixative during slide preparations.

However due to the limited number of cells available when using a whole organism, a compromise is given in fixative washes in an attempt to have a sufficient number of cells for analysis, which was the case with *B. glabrata.* In these circumstances slide pre-treatment is crucial to achieve good quality FISH results. Figure 3.1 displays representative images of *B. glabrata* nuclei after using various slide pre-treatment methods. Untreated slides [Fig. 3.1 A] have very high levels of background fluorescence making it extremely difficult to visualise any gene signals. Pre-treatment with either pepsin [Fig. 3.1 B] or RNase A [Fig. 3.1 C] reduced the level of background fluorescence present around the nuclei but contamination was still present within the nuclei. Bright signals were present at this stage however it was difficult to establish these as false positive or negative signals. Only when pepsin pre-treatment was combined with RNase treatment [Fig. 3.1 D] two bright gene signals were clearly visualised through the microscope.

Figure 3.1 Representative images of interphase nuclei of *B. glabrata* BS90 strain after 2-D FISH. The images show nuclei stained with DAPI (blue) and the gene loci for *actin* (red). Slides were either untreated (A), or pre-treated with pepsin (B), RNase A (C) or both (D). Scale bar = 5μm.

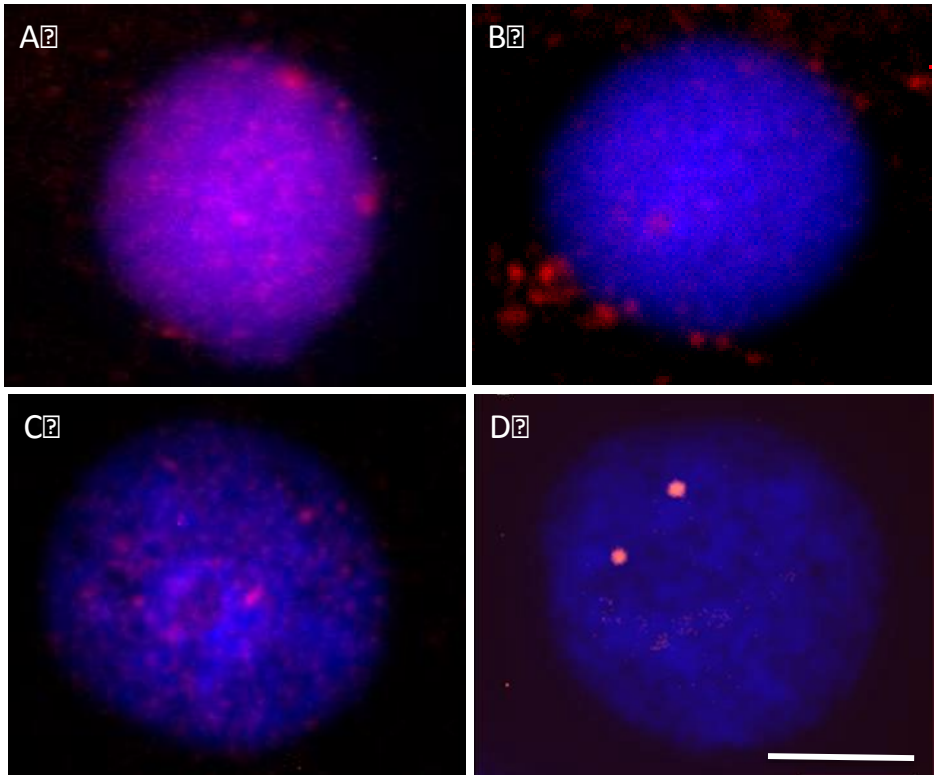

3.3.2 Establishing the optimum post-hybridisation wash protocol for *B. glabrata* cells

Post-hybridisation washes are an important step in the FISH procedure to remove non-specifically bound labelled probe. These washes are typically carried out at a higher stringency than the conditions during the hybridisation. This is achieved by raising the temperature of the wash solutions, which essentially can remove the entire hybridised probe. Probes for small unique sequence targets, such as the ones used in these experiments, require careful washing in order to maintain the signal intensity. Bearing this in mind, two different post-hybridisation wash protocols were assessed. Protocol A included several stringency washes at 45°C and 60°C, which resulted in signals in some cells [Fig. 3.2 A]. The intensity of the gene signals was significantly low which is possibly due to loss of too much of the hybridised probe during the washing steps. Alternatively protocol B had fewer washing steps with a single stringency wash at 42 °C. This protocol resulted in clear and bright gene signals in every cell [Fig. 3.2 B].

Figure 3.2 Representative images of interphase nuclei of *B. glabrata* BS90 strain after post hybridisation washes. Images A and B are showing interphase nuclei after washes with protocol A and protocol B respectively. Nuclei are stained with DAPI (blue) and hybridised with the *actin* gene (green in A/red in B). Scale bar = 5μm.

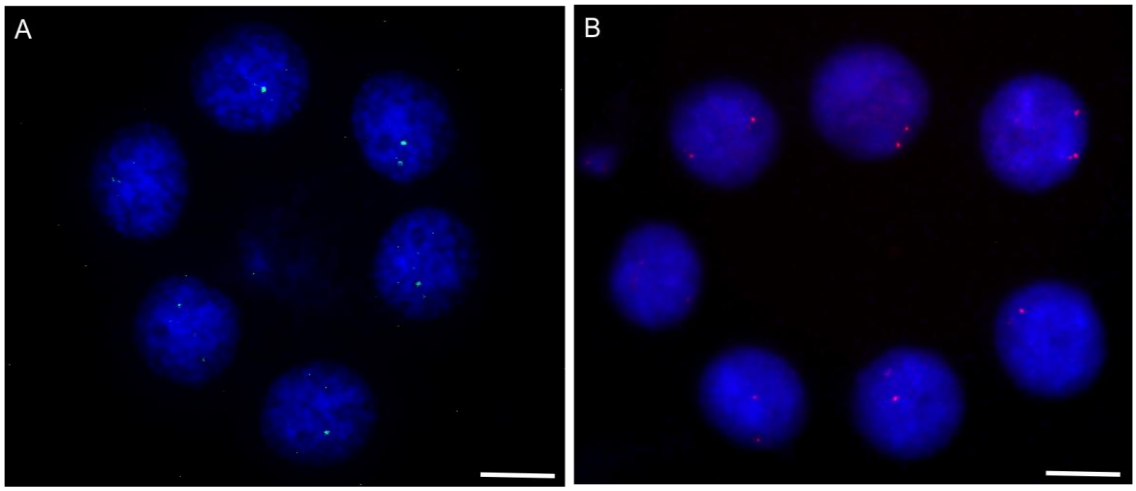

3.3.3 Non-random positioning of gene loci in interphase nuclei of *B. glabrata*

By utilising the results attained in sections 3.3.1 and 3.3.2 genes were effectively mapped in interphase nuclei of *B. glabrata* cells. Three genes were delineated in interphase nuclei from the susceptible (NMRI) and the resistant (BS90) snail lines. The three genes, *actin, ferritin,* and *hsp70* were previously found to be up-regulated after an infection with *S. mansoni* miracidia (Lockyer *et al.,* 2004; Lockyer *et al.,* 2008; Ittiprasert *et al.*, 2009). All were revealed in interphase *B. glabrata* cell nuclei, displaying two gene signals [Fig. 3.3].

Fifty images of nuclei for each gene were captured and the positions assessed using the erosion script analysis (Croft *et al.*, 1999) [Fig. 3.4]. The script outlines the (DAPI) staining of the nuclei creating five concentric shells of equal area. It subsequently measures the intensity of fluorescent signals from the DNA and records these. In order to normalise the data, the percentage of gene signal in each shell is divided by the DAPI signal for the corresponding shell. These data for gene loci are then plotted as a bar chart. The bar charts presented in figure 3.5 displays the radial distribution of the aforementioned *B. glabrata* genes in the interphase nuclei of the snail *ex vivo* cells from the BS90 and NMRI strains. All three gene loci display non-random radial positioning in interphase nuclei. *Actin* and *ferritin* genes are located towards the nuclear interior [Fig. 3.5 A-B, D-E], and *hsp70* is located at an intermediate position within the nucleus [Fig. 3.5 C, F]. The positions of the genes did not alter between the NMRI and BS90 snail strains.

Figure 3.3 Representative 2-D FISH images of hybridised *B. glabrata* genes in the interphase nuclei of *B. glabrata* BS90 strain *ex vivo* cells. The gene signals have been pseudo-coloured green and there are only two distinct signals within each representative nucleus The images show the nuclei stained with DAPI (blue) and gene loci for *actin* (A), *ferritin* (B), and *hsp70* (C). Scale bar = 5µm.

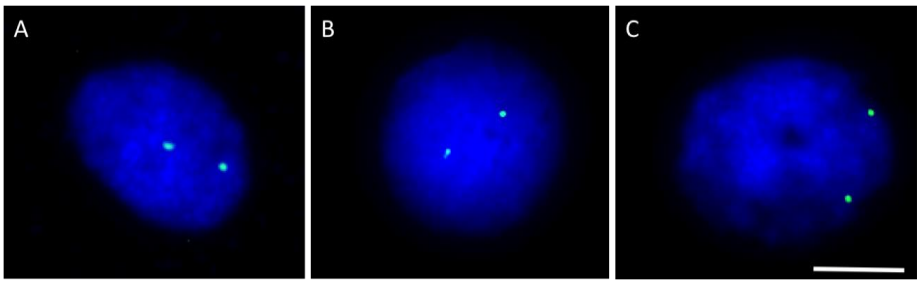

Figure 3.4 Representative images of the erosion script analysis. Image A displays a composite cartoon of the nucleus where the computer script has outlined the DAPI signal staining DNA (blue) and creating five shells of equal area. The script measures the intensity of the fluorescent signals from both the genes (green) and the DAPI and records these. In order to normalise the data, the percentage of gene signal in each shell is divided by the DAPI signal for the corresponding shell. The data can then be plotted as a bar chart. Images B, C, and D are displaying genes having peripheral, intermediate, and internal positions respectively. Scale bar = 5µm.

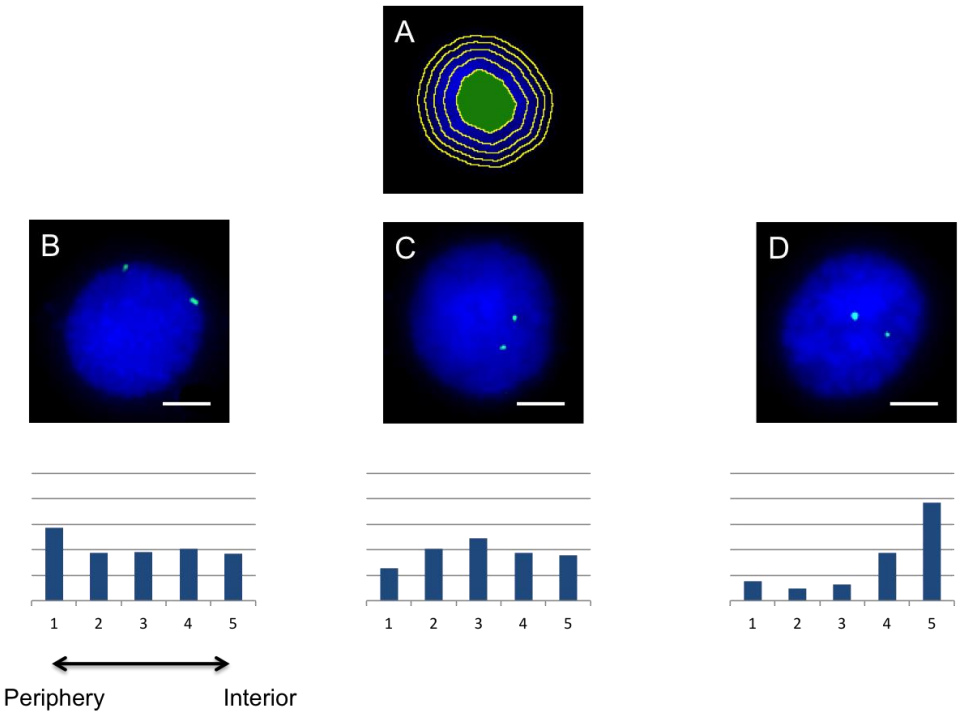

Figure 3.5 Bar charts showing the radial positioning of *B. glabrata* genes in the interphase nuclei of *B. glabrata ex vivo* cells. Genes are non-randomly positioned in the interphase nuclei of *B. glabrata* cells. Fifty images of nuclei for each gene (A-F) were captured and the gene position assessed using the erosion script analysis (see Fig. 3.4). All genes are non-randomly positioned with *actin* (A, D), and *ferritin* (B, E) being located towards the nuclear interior, and *hsp70* (C, F) at an intermediate position within the nuclei. The positions of the genes did not alter between the NMRI and BS90 snail strains. Statistically significant differences, as assessed by two-tailed Student's t-test, between normalized gene signal in each shell are indicated by an asterisk ($P<0.05$). Error bars = S.E.M.

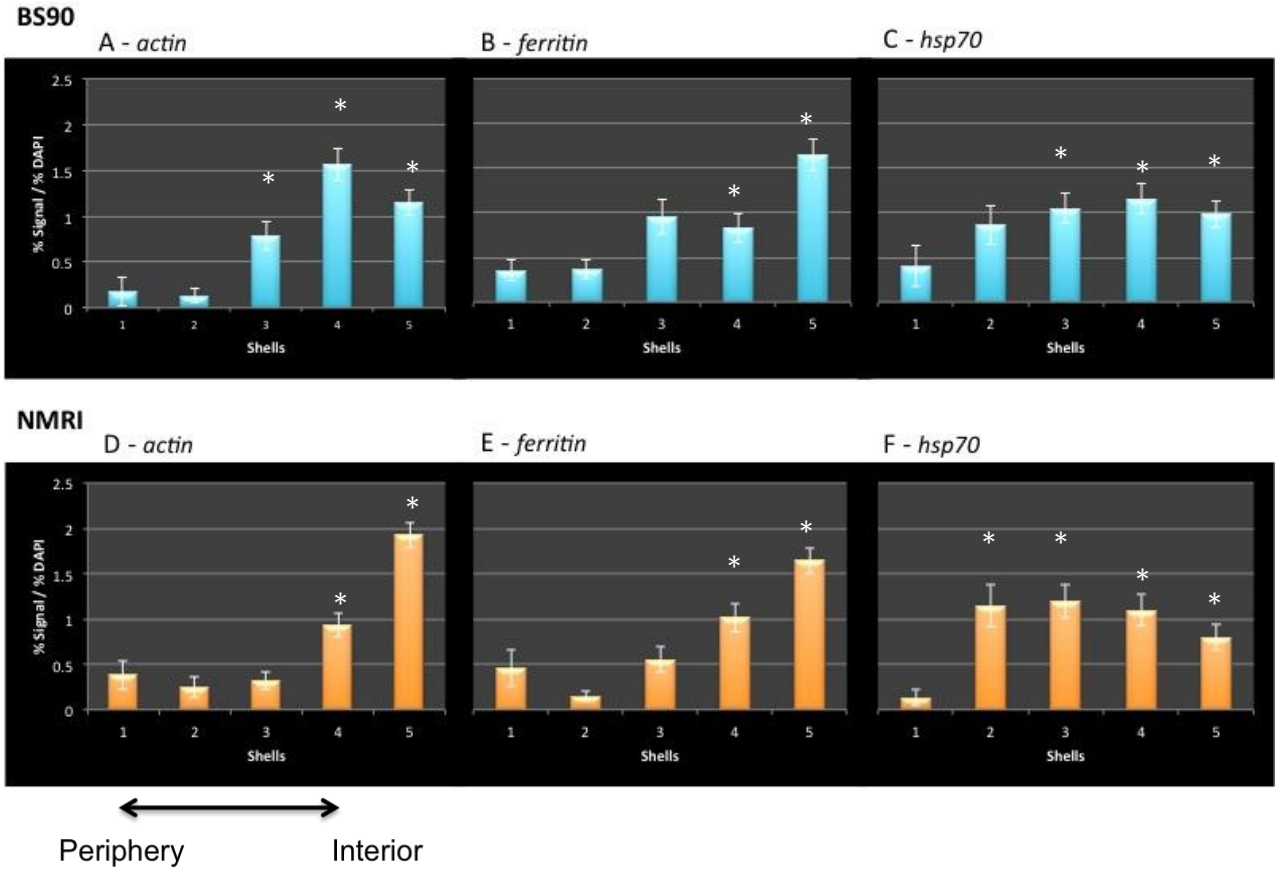

3.3.4 Gene positioning is altered in *B. glabrata* after an infection with *S. mansoni* miracidia and is correlated with gene expression

Infection of *B. glabrata* with *S. mansoni* miracidia modulates host gene expression resulting in the up regulation of certain genes including *actin, ferritin,* and *hsp70* (Lockyer *et al.,* 2004; Lockyer *et al.,* 2008; Ittiprasert *et al.*, 2009). Previously *actin* and *ferritin* were shown to be repositioned in co-culture experiments with Bge cells (Knight *et al.*, 2011). A further step has now been taken in this study to analyse the behaviour of these genes *in vivo*, after infection in the susceptible and resistant snail lines. Considering that genes and chromosomes can move within a matter minutes to hours within the nuclear environment (Bridger, 2011; Mehta *et al.*, 2010; Hu *et al.*, 2009; Volpi *et al.*, 2000), time points were taken at 0, 0.5, 2, 5, and 24 hours after introduction of the parasite to the host snail. To correlate the alteration in the spatial positioning with gene expression, qRT-PCR was performed using RNA isolated from infected snails for the same time points. In order to determine whether changes observed in gene positioning and gene expression are purely due to the infection process rather than an injury mediated response associated with intra-dermal penetration of the parasite into the snail, nuclei and RNA samples were collected from snails that had been infected with irradiated miracidia. Tables 3.2 and 3.3 shows a summary of these exposure experiments in the NMRI and BS90 snails.

3.3.4.a. *Actin* and *hsp70* display a differential response with respect to gene repositioning between the susceptible and resistant snail lines

As demonstrated in section 3.3.3, *actin* and *hsp70* genes were located non-randomly within the interphase nuclei of *B. glabrata ex vivo* cells. Using 2-D FISH, the two genes were hybridised onto interphase nuclei derived from *B. glabrata* after exposure to *S. mansoni* miracidia. 50 images of both *actin* and *hsp70* gene loci were analysed using the previously mentioned erosion script analysis (Croft *et al.*, 1999). This analysis was performed on *ex vivo* nuclei derived from NMRI and BS90 snails after 0.5, 2, 5, and 24 hour exposure to miracidia.

Figure 3.6 displays the radial positioning results of *actin* gene pre and post exposure to the parasite, in the two snail strains. Upon exposure to miracidia, in the NMRI (susceptible) snails [Fig. 3.6 A] the *actin* gene loci changes position and moves from the nuclear interior towards a more intermediate position within the nuclei at 30 minutes. The gene loci then subsequently moves back to the nuclear interior 5 hours after exposure. Interestingly however, the *actin* loci have an intermediate position in the BS90 (resistant) snails, and do not alter its nuclear position after infection [Fig. 3.6 B]. The repositioning of *actin* in the NMRI snails is correlated with a 16-fold increase in its expression at 2 hours after infection and 1.5 hours after gene repositioning. In the BS90 snails there is 22-fold increase in expression only after 30 minutes of infection. No repositioning of gene loci or change in expression was observed for *actin* in snails infected with irradiated miracidia for either snail strain.

Figure 3.7 displays the data for the radial positioning of *hsp70* gene in timed samples prepared for FISH. Infection with normal miracidia in the NMRI snails caused a shift in the position of the gene 2 hours after infection, from an intermediate position towards a more internal position within the nuclei [Fig. 3.7 A]. This repositioning event of *hsp70* gene loci is directly correlated with the up-regulation of gene expression as shown by qRT-PCR. In the BS90 snails, although there are no dramatic changes in the position of *hsp70* gene loci, a shift toward the nuclear periphery is observed 24 hours after infection. However the qRT-PCR data has shown no significant changes in the expression of gene at any of the time points [Fig. 3.7 B]. No evidence for the relocation of the *hsp70* gene loci and no induction of *hsp70* expression were detected by qRT-PCR when the two snail lines were infected with irradiated miracidia.

Figure 3.6 Charts displaying the *in vivo* radial positioning and expression profile of *B. glabrata actin* gene in the interphase nuclei of cells derived from NMRI (A) and BS90 (B) snail strains, pre and post exposure to *S. mansoni* miracidia. *B. glabrata* snails were infected with miracidia, dissected, fixed, and subjected to 2-D FISH. 50 images were collected for each time point (0, 0.5, 2, 5, and 24 hours) and analysed by the erosion script analysis (Croft *et al.*, 1999). In the NMRI strain snails *actin* is repositioned within interphase nuclei after infection and this is correlated with changes in gene expression (A). No repositioning is observed in the BS90 strain snails, however the gene is expressed 30 minutes after infection (B). No repositioning of gene loci or change in expression was observed for *actin* in snails infected with attenuated miracidia. Statistically significant differences, as assessed by two-tailed Student's t-test, between normalized gene signal in each shell of control nuclei compared with infected snail nuclei are indicated by an asterisk (P<0.05). Error bars = S.E.M.

A – NMRI (susceptible)

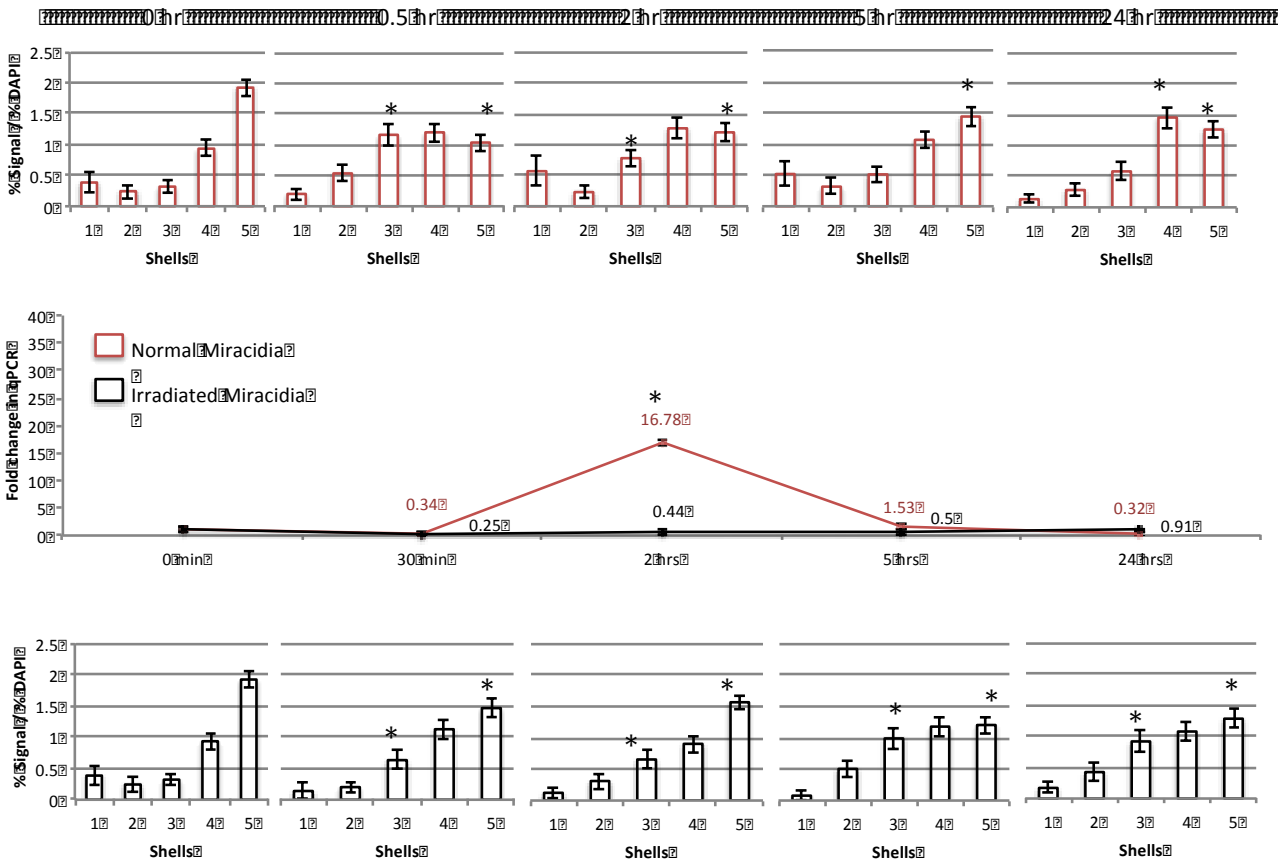

B – BS90 (resistant)

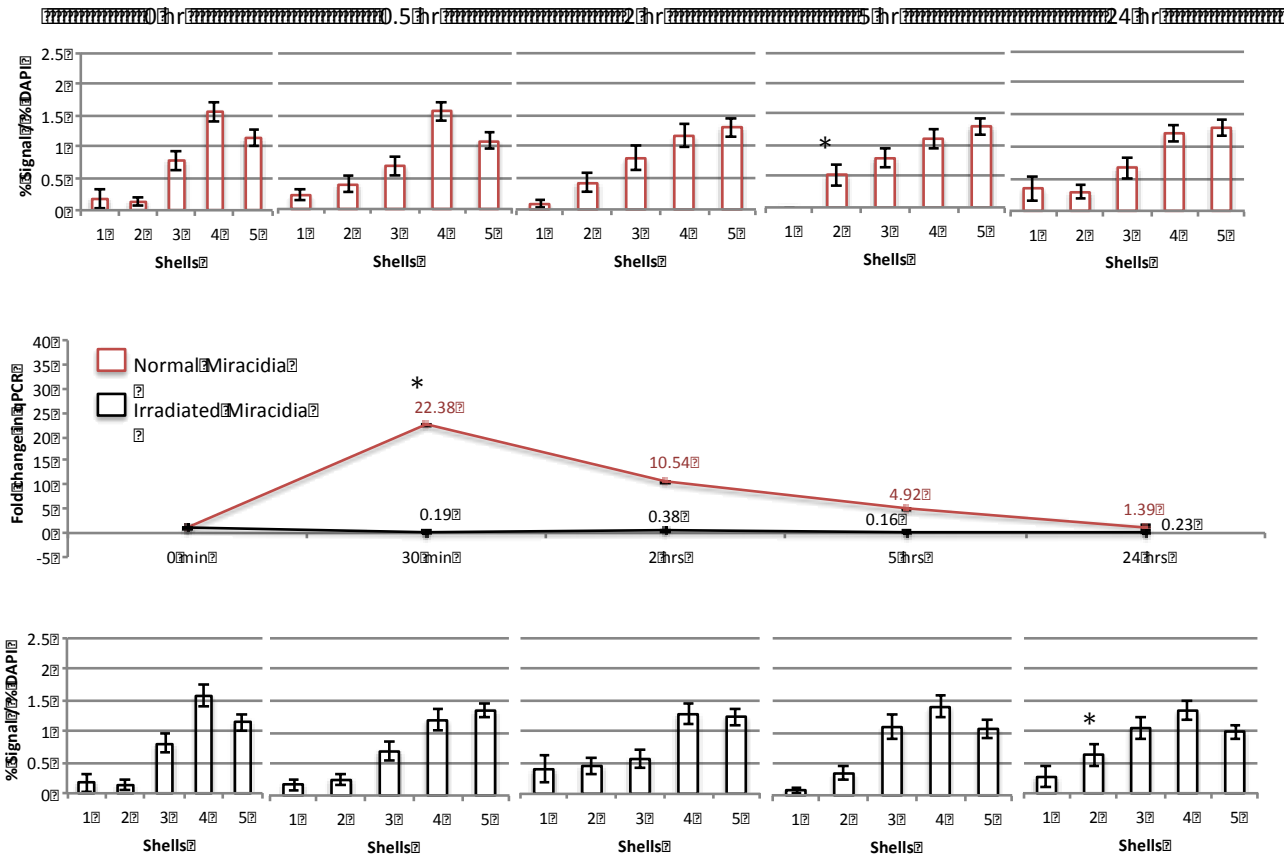

Figure 3.7 Charts displaying the *in vivo* radial positioning and expression profile of *B. glabrata hsp70* gene in the interphase nuclei of cells derived from NMRI (A) and BS90 (B) snail strains, pre and post exposure to *S. mansoni* miracidia. *B. glabrata* snails were infected with miracidia, dissected, fixed, and subjected to 2-D FISH. 50 images were collected for each time point (0, 0.5, 2, 5, and 24 hours) and analysed by the erosion script analysis (Croft *et al.*, 1999). In the NMRI strain snail's *hsp70* gene is repositioned after infection from an intermediate position to a more internal position within the nuclei. This repositioning is directly correlated with changes in gene expression 2 hours after infection (A). No repositioning or change in expression is observed in the BS90 strain snails (B). No evidence for the relocation of the *hsp70* gene loci and no induction of *hsp70* expression were detected by qRT-PCR when the two snail lines were infected with irradiated miracidia. Statistically significant differences, as assessed by two-tailed Student's t-test, between normalized gene signal in each shell of control nuclei compared with infected snail nuclei are indicated by an asterisk ($P<0.05$). Error bars = S.E.M.

A – NMRI (susceptible)

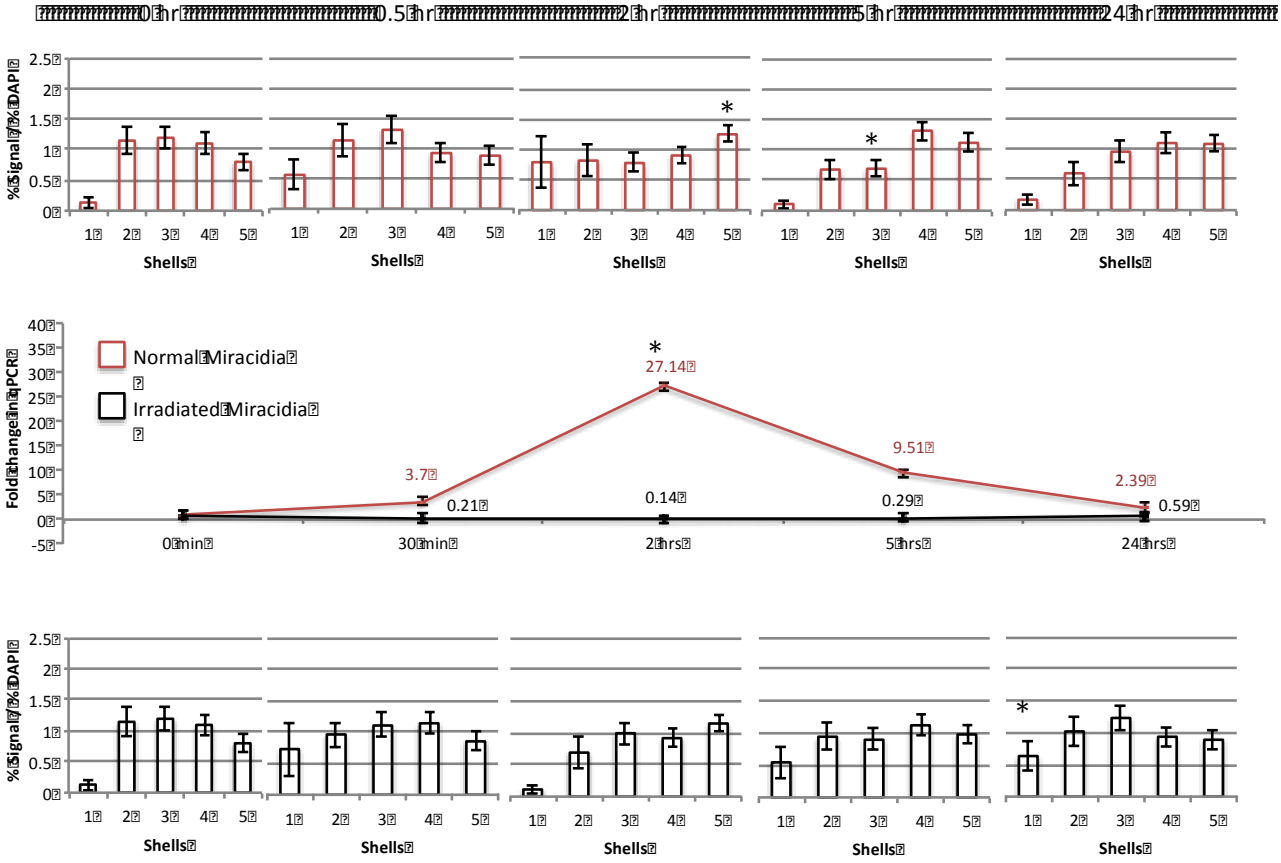

B – BS90 (resistant)

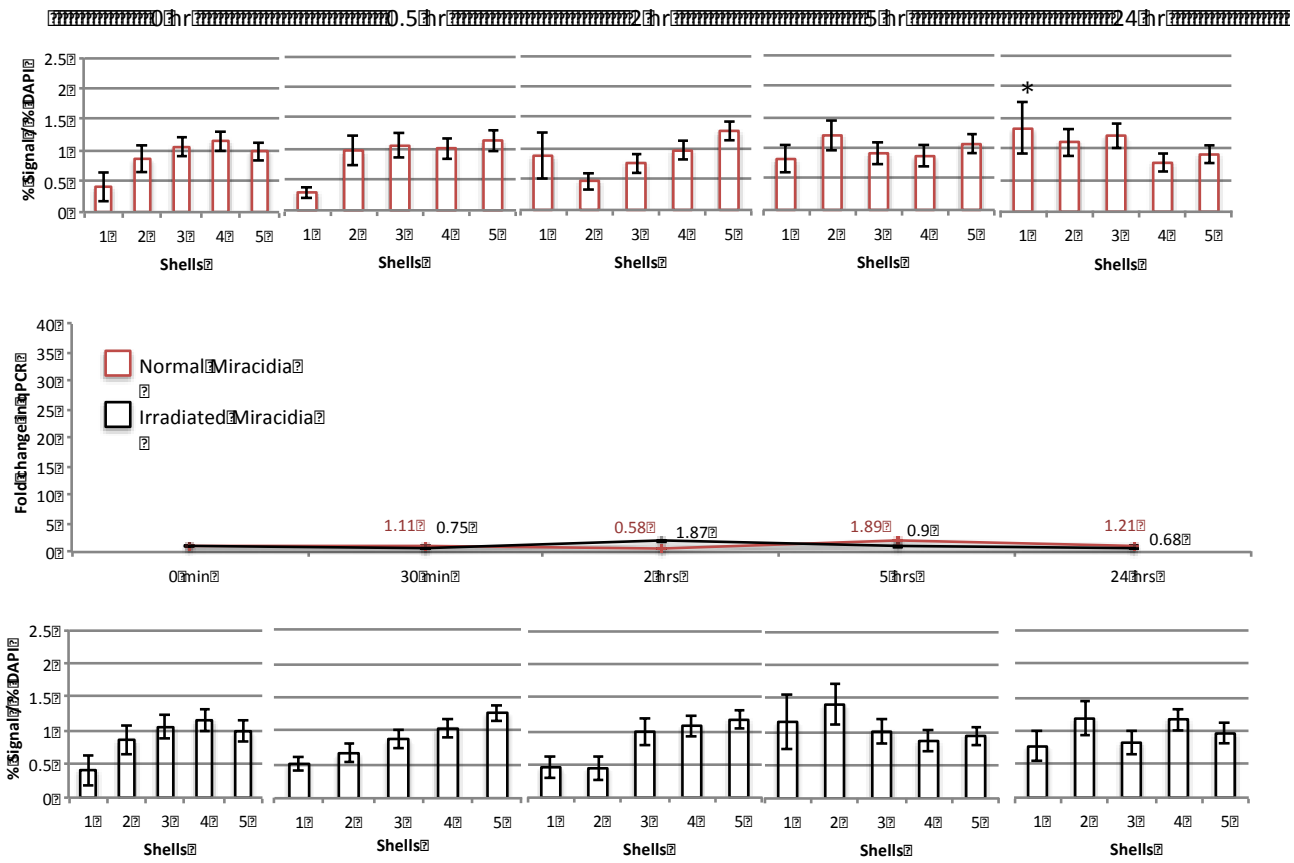

3.3.4.b. Ferritin may not be involved in the infection process but acts as an injury mediated response gene

By utilising 2-D FISH the *ferritin* gene probe was successfully mapped onto the interphase nuclei of snail *ex* vivo cells and was observed to be positioned non-randomly (see section 3.3.3). Using the same technique, the *ferritin* gene was hybridised onto interphase nuclei derived from *B. glabrata* after exposure to *S. mansoni* miracidia. Figure 3.8 displays the radial positioning of the *ferritin* gene loci in these nuclei. In the NMRI strain *ferritin* was repositioned from the nuclear interior to a more intermediate position at 30 minutes [Fig. 3.8 A]. Interestingly, *ferritin* gene loci are also repositioned at 30 minutes in snails infected with the irradiated miracidia, and this is correlated with a 37-fold increase in the expression of *ferritin.*

A similar response is seen in the BS90 snails infected with irradiated miracidia [Fig. 3.8 B]. *Ferritin* is repositioned to the nuclear periphery and this is once again correlated with increase in its expression as determined by qRT-PCR. A dramatic alteration is also observed in the position of genes in BS90 snails infected with normal miracidia. The majority of gene loci were detected in shell 2 of the erosion analysis 30 minutes after infection, which is indicating a shift from the nuclear interior towards the nuclear periphery. This is again correlated with an 8-fold increase in the expression of *ferritin*. Although a differential response for *ferritin* is observed between the susceptible and the resistant snail lines, relocation of *ferritin* gene loci and the induction of gene expression in snails infected with irradiated miracidia suggests that this a response to the presence of the miracidia rather than a response to an active infection mechanism elicited by the parasite.

Figure 3.8 Charts displaying the *in vivo* radial positioning and expression profile of *B. glabrata ferritin* gene in the interphase nuclei of cells derived from NMRI (A) and BS90 (B) snail strains, pre and post exposure to *S. mansoni* miracidia. *B. glabrata* snails were infected with miracidia, dissected, fixed, and subjected to 2-D FISH. 50 images were collected for each time point (0, 0.5, 2, 5, and 24 hours) and analysed by the erosion script analysis (Croft *et al.*, 1999). In the NMRI strain *ferritin* is repositioned in snails infected with both normal and irradiated miracidia. However the gene is up-regulated only in snails infected with irradiated miracidia (A). Repositioning of *ferritin* gene loci is observed in the BS90 strain snails infected with normal and irradiated miracidia, and this is correlated with up-regulation of its expression (B). Statistically significant differences, as assessed by two-tailed Student's t-test, between normalized gene signal in each shell of control nuclei compared with infected snail nuclei are indicated by an asterisk ($P<0.05$). Error bars = S.E.M.

A – NMRI (susceptible)

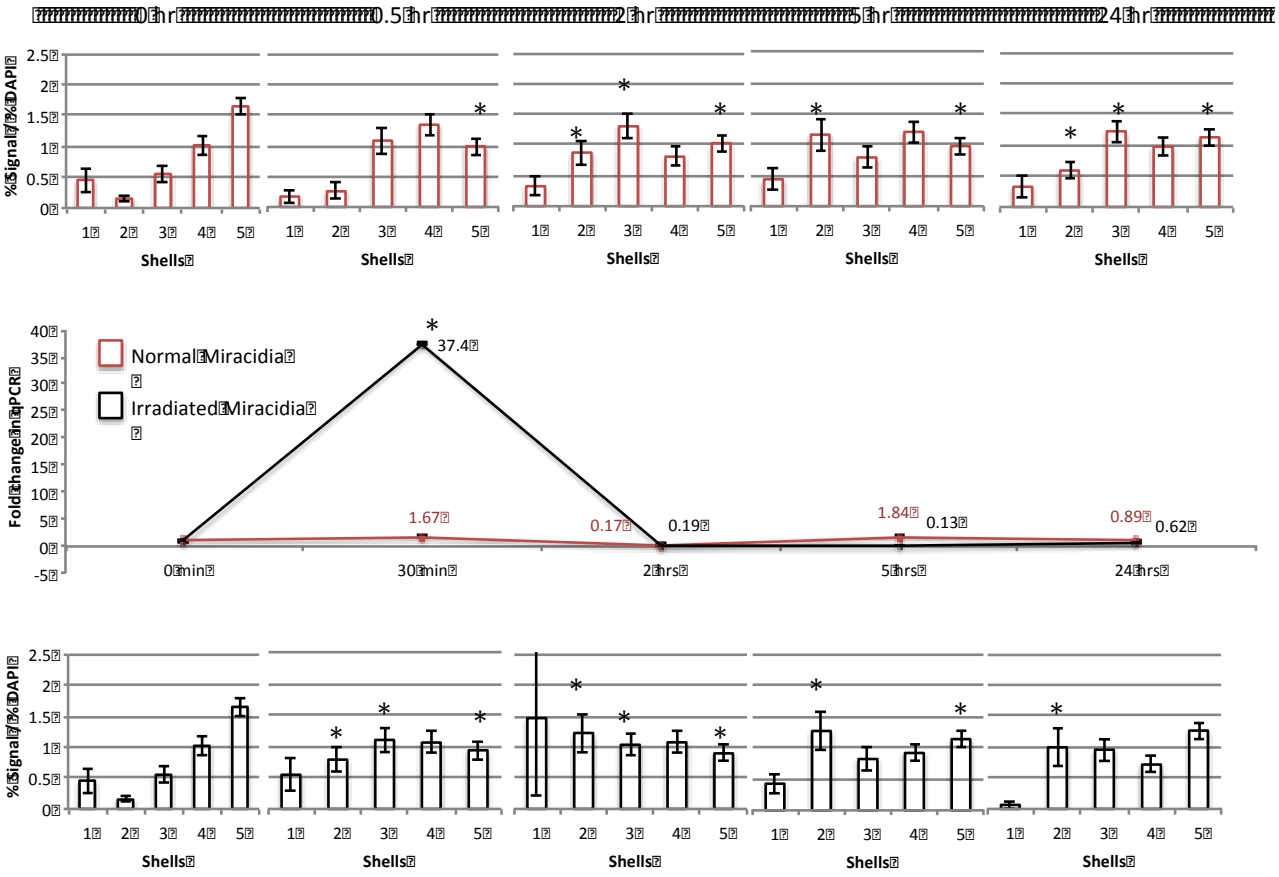

B – BS90 (resistant)

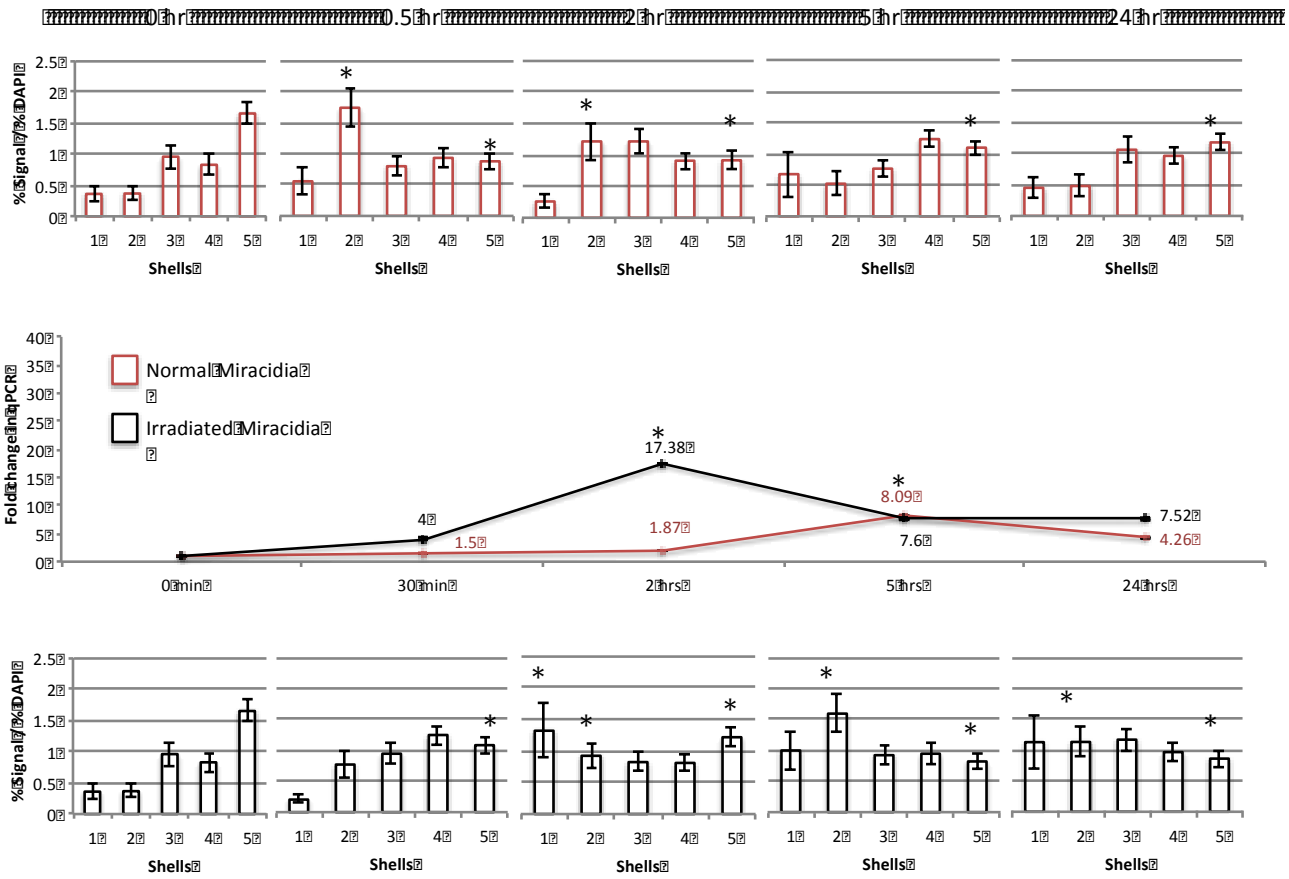

Table 3.2 Table showing a summary of the parasite exposure experiments in *B. glabrata,* NMRI strain.

NMRI (susceptible)	*Actin*		*Ferritin*		*Hsp70*	
	Gene loci	Expression	Gene loci	Expression	Gene loci	Expression
Normal parasite	Moves	✓	Moves	✓	Moves	✓
Irradiated parasite	Stationary	**X**	Moves	✓	Stationary	**X**

Table 3.3 Table showing a summary of the parasite exposure experiments in *B. glabrata,* BS90 strain.

BS90 (resistant)	*Actin*		*Ferritin*		*Hsp70*	
	Gene loci	Expression	Gene loci	Expression	Gene loci	Expression
Normal parasite	Stationary	✓	Moves	✓	Stationary	**X**
Irradiated parasite	Stationary	**X**	Moves	✓	Stationary	**X**

3.4 Discussion

Following the initiation of the snail genome project (Raghavan and Knight, 2006), interests in the snail *B. glabrata* have greatly increased. Whilst the majority of these studies concentrate on the molecular biology of the snail to understand the host snail – parasite relationship, to date only a single study has examined the genome organisation in the snail using the *in vitro* co-culture assay employing Bge cells and schistosome miracidia (Knight *et al.*, 2011). In this chapter I have taken a step further and utilised the *B. glabrata* fluorescence *in situ* hybridisation technique using the snail cells to determine spatio-temporal affects on three genes in the resistant and susceptible snails after infection with *S. mansoni* miracidia. Since the experimental design involved the use of whole organisms, the task itself was not simple. Modifications to the previously established 2-D FISH protocol for Bge cell line (Odoemelam *et al.*, 2010) was required to adapt it for its use with cells extracted from *B. glabrata*. This was achieved by the application of slide pre-treatment methods, as well as a new post-hybridisation wash protocol to maintain signal intensity. Culmination of these experiments revealed major gene repositioning events in the interphase nuclei of *B. glabrata* cells, which deviated between the resistant and susceptible snail strains. The repositioning of these genes was also correlated with up regulation of their expression.

The *actin* gene loci repositioned from the nuclear interior to an intermediate position between the nuclear interior and periphery in the NMRI (susceptible) strain snails, but did not alter its position in the BS90 (resistant) strain. The repositioning of gene loci in the NMRI snails correlated with the expression of the gene 1.5 hours after the repositioning event. To our knowledge, this is the first evidence of gene movement prior to a change in expression. In the BS90 snails there was a rapid response to infection with a large fold increase in the expression of *actin* after 30 minutes. Although in the BS90 snails no repositioning was observed for the gene loci at any of the time points, alterations in the organisation of interphase nuclei can be a very rapid process of less than 15 minutes after a change in status in a cell (Mehta *et al.*, 2010). Therefore it may well be that the gene was repositioned and has moved back to its original position within 30 minutes. Also in the NMRI snails the gene loci moves to shells 4 and 3 in the erosion analysis (intermediate position). However, since *actin* in the BS90 snails already has an intermediate position before infection, this may be another explanation for the stability of these gene loci in BS90 strain snails. Actin protein is a major constituent of the cytoskeleton and is involved in a number of cellular processes (Bernal and Stahel, 1985). Increase in the expression of *actin* has been reported in plant-fungal pathogen interactions (Jin *et al.*, 1999). Thus the rapid increase in expression observed in the BS90 snails could be due to rearrangements in the host cytoskeleton, which the susceptible (NMRI) snails fail to respond as efficiently.

The distribution of *hsp70* appeared slightly more random than the others but the majority of the signals were found in shell 3, revealing an intermediate distribution. A similar differential response was also observed with *hsp70* gene loci, which in the NMRI snails was repositioned to the nuclear interior 2 hours after infection. However in the BS90 snails *hsp70* did not alter its nuclear position, which is supported by the qRT-PCR data showing no alteration in gene expression profile of this gene. These results support a previous study by Ittiprasert *et al* reporting induction of *hsp70* only in susceptible juvenile snails (Ittiprasert *et al.*, 2009).

Reduction in hsp70 protein expression was also reported in snails following *S. mansoni* larval ESP exposure, with a greater reduction in susceptible snails (Zahoor *et al.*, 2010). Since the nuclear interior is associated with transcriptionally active loci (Elcock and Bridger, 2010; Deniaud and Bickmore, 2009; Takizawa *et al.,* 2008b), repositioning of *hsp70* to the nuclear interior and the subsequent increase in its expression in NMRI snails may be a mechanism adopted to overcome the effects of substantial decrease in hsp70 protein levels after infection. In another study *hsp70* was found to be constitutively expressed in unstressed resistant and susceptible snails (Ittiprasert *et al.*, 2009). This also may be an explanation for the intermediate position of this gene in uninfected control snails.

Out of the three genes studied, *ferritin* was the one gene to show a response after infection with irradiated miracidia. Given the role of ferritin as a major iron binding protein and protectant against oxidative damage, previous studies have all concluded a possible immune relevant role for *ferritin* against the invading parasite (Knight *et al.*, 2011; Lockyer *et al.*, 2007; Raghavan *et al.*, 2003). In agreement with these studies, a differential response of *ferritin* gene between the resistant and susceptible snails has also been observed in this study. However, as a control measure snails were also infected with irradiated miracidia. The irradiated parasites are alive and can penetrate into the snail, however they fail to develop in the susceptible snails and thus are good controls to use in experiments to eliminate an effect observed in response to an injury rather than to the developing parasite. The results from these control experiments have all shown that *ferritin* responds to irradiated miracidia both in terms of gene expression and gene repositioning. Thus it is evident from these experiments that although *ferritin* may still be a gene involved in immune response in molluscs, it does not have a role in the resistibility of *B. glabrata* snails against the invading parasite.

The dynamics of repositioning of gene loci for *actin, ferritin,* and *hsp70* are correlated with up-regulation of gene expression as determined by qRT-PCR. However, *hsp70* is the only gene that moved to the nuclear interior after infection and was up-regulated at the same time point, which is consistent with previous studies correlating the expression of genes with their movement to the nuclear interior (Szczerbal *et al.,* 2009; Takizawa *et al.*, 2008a). In contrast, both *actin* and *ferritin* genes were up-regulated when they migrated from the nuclear interior towards a more intermediate / peripheral position within the nucleus. While repositioning towards the nuclear periphery with gene expression has not been seen in higher organism, association of activated genes with the nuclear pore complexes at the nuclear periphery are reported in yeast (Brown and Silver, 2007; Taddei *et al.*, 2006; Brickner and Walter, 2004), *Drosophila* (Mendjan *et al.*, 2006; Pickersgill *et al.*, 2006), and in the malaria parasite *Plasmodium falciparum* (Duraisingh *et al.*, 2005). Thus the findings in this study may indicate a novel snail specific response similar to that seen in simpler organisms. In addition, the observations of gene expression occurring both at the nuclear interior and at the nuclear periphery could make *B. glabrata* a model organism in studying the involvement of different nuclear compartments in genomic regulation.

When comparing the results attained in this study to the results from the Bge co-culture studies, discrepancies can be seen between the two data sets (Knight *et al.*, 2011). In the Bge cells both *hsp70* and *ferritin* gene loci have a peripheral position within the nuclei, and only ferritin relocates towards the interior after infection. In comparison, this study has shown that in the snail cells *hsp70* has an intermediate position while *ferritin* has an internal position, and upon parasitic infection both genes are repositioned (*hsp70* only in NMRI snails). The repositioning of *hsp70* gene loci in this study is also in conjunction with its up-regulation. In the co-culture studies, the gene was up-regulated with no change in its nuclear localisation. Furthermore, when the Bge cells were co-cultured with irradiated miracidia, no evidence for the relocation of *ferritin* gene loci and induction of its expression was detected, which is in complete opposition to the data reported here.

The reasons behind these discrepancies however are apparent. The Bge cells comprise severe aneuploidy within their genome and how much they represent the snail is now a matter of debate. Therefore it is not surprising that such inconsistencies are observed between the results from the intact snail and the cell line. The only data sets from the two experiments that correlated with each other came from *actin,* which is positioned internally in both studies and is repositioned towards the nuclear periphery (only in NMRI snails). The gene is also up-regulated in both the Bge cells and the NMRI snails precisely 2 hours after infection. However, since *actin* is the only gene from this study to correlate with the Bge co-culture studies, how well the Bge cells provide an *in vitro* model system in the study of host-parasite interactions should be questioned.

Unlike what is still implied in some student textbooks, chromosomes and genes in an interphase nuclei are not in spaghetti like tangled mass of threads but rather harbour non-random positions (Foster and Bridger, 2005). Although the components that contribute to the nuclear position of a gene are not entirely clear, the activity of a gene is thought to affect its position (Meaburn and Misteli, 2007). In this chapter further evidence for this has been provided from the mollusc *B. glabrata.* The nuclear location of a gene is thought to influence the machinery responsible for specific nuclear functions such as splicing and transcription (Parada and Misteli, 2002), and this spatial organisation is shown to be altered in several situations including differentiation (Szczerbal *et al.,* 2009; Foster and Bridger, 2005), disease (Meaburn *et al.*, 2009; Meaburn and Misteli, 2008; Zink *et al.,* 2004b; Cremer *et al.*, 2003), and viral infection (Li *et al.*, 2009). A number of proteins are known to be involved in the spatial organisation of the genome including lamins, CCCTC-binding factor (CTCF), and RNA polymerase II, and interactions with these proteins have shown to be affecting transcriptional activity (Holwerda and de Laat, 2012). One of the more attractive theories is the migration of genes to pre-existing transcription factories (RNA pol II clusters) (Fraser and Bickmore, 2007). In this chapter it has been shown for the first time that spatial organisation of the genome is also altered after a parasitic infection and movement of genes is correlated with changes in their transcriptional status.

Also for the first time evidence has been provided for the movement of the *actin* gene loci prior to an alteration to its transcriptional activity, which was 1.5 hours after its movement. Movement of chromosome and genes can be inhibited using drugs (Mehta *et al.*, 2010; Chuang *et al.,* 2006; Dundr *et al.,* 2007; Hu *et al.,* 2008). Thus it would be very interesting to observe the effects of movement inhibition on the transcriptional activity of a gene.

Chapter 4

Understanding the significance of spatial gene positioning in interphase nuclei

what, where, how, and why?

The contents of this chapter are in preparation for a publication in PNAS: 'Gene repositioning and subsequent expression after heat shock is blocked by a nuclear motor inhibitor in snail cells' - Halime Derya Arican, Margaret Town, Christopher Eskiw, Matty Knight, Joanna M Bridger.

Part of the work undertaken in this chapter was supported by a grant from the Malacological Society of London.

4.1 Introduction

The nucleus is a highly organised organelle that houses the genome and helps control its behaviour and regulation. It is now well accepted that the eukaryotic genome is spatially organised in interphase nuclei as individual chromosome territories, and these territories along with gene loci within them exhibit non-random radial positioning (Meaburn and Misteli, 2007; Cremer and Cremer, 2006). In chapter 3, non-random organisation of the snail *B. glabrata*'s genome, and for the first time subsequent reorganisation after a parasitic infection was also demonstrated. The movement of snail gene loci additionally correlated with the up-regulation of gene expression. Various studies in the past have exposed the destination of the moving genes, revealing an association with a facilitating nuclear structure (Szczerbal and Bridger, 2010; Eskiw *et al.*, 2010; Dundr *et al.*, 2007; Osborne *et al.*, 2007; Osborne *et al.*, 2004). This spatial reorganisation and subsequent association with nuclear structures may be another level of regulating gene expression and nuclear organisation.

The nucleus houses a number of important structures that interact with and influence chromatin. These structures include the scaffolding proteins that make-up the nuclear lamina subjacent to the inner cell membrane, the nuclear matrix, the nucleolus, and various morphologically distinct substructures situated within the matrix scaffold collectively known as nuclear bodies. To date, more than ten of these intra-nuclear structures have been characterised and are arranged as coiled bodies, vesicles, spheres, or doughnut like structures (Zimber *et al.,* 2004).

One of the most thoroughly studied nuclear structures is the transcription factory (TF), comprising of the enzyme RNA polymerase II and containing newly synthesized RNA (Jackson *et al.*, 1993; Wansink *et al.*, 1993). Iborra *et al* identified TF after incorporating a pulse of a Br-UTP and biotin-CTP labelled nucleotides into permeabilised mammalian cells. The resulting labelled nascent transcripts were noted to be not distributed throughout the nucleus, but concentrated in discrete focal sites, which they termed transcription factories (Iborra *et al.*, 1996).

Studies utilising *in situ* hybridisation techniques have revealed the association of active genes with TF's (Kang *et al.*, 2011; Schoenfelder *et al.*, 2010; Osborne *et al.*, 2007; Yao *et al.*, 2007; Osborne *et al.*, 2004). Several gene loci from different chromosomes have also been reported to share the same TF (Dhar *et al.,* 2009). There is also evidence for the presence of specialised TF's that contain the specific apparatus required for the transcription of certain genes, such as the preferential transcription of Klf1-regulated mouse globin genes at TF's containing large amounts of Klf1 (Schoenfelder *et al.*, 2010; Xu and Cook, 2008). Equally, activated genes have also been reported to associate with nuclear speckles / SC35 domains (Shopland *et al.*, 2003), which are sites comprising pre-mRNA splicing machinery (Spector and Lamond, 2010). During porcine adipogenesis, activated and repositioned genes were found to co-localise with these domains (Szczerbal and Bridger, 2010). Although co-localisation studies provide a good basis for identification and observing of nuclear structures associated with chromatin, further research is required for a direct evidence of gene loci being located in these structures.

Other nuclear bodies associating with active chromatin include the Cajal and promyelocytic leukaemia (PML) bodies. The Cajal body is thought to be involved in post-transcriptional modification of newly assembled spliceosomal snRNAs, and is also correlated with the expression of genes (Dundr *et al.*, 2007). PML bodies also interact with chromatin fibres via their protein based threads, specifically gene rich and transcriptionally active regions (Bernardi and Pandolfi, 2007; Kumar *et al.*, 2007; Wang *et al.*, 2004; Shiels *et al.*, 2001). Besides the majority of these nuclear structures interacting with the genome, it is also evident that these structures are certainly involved with the three-dimensional interphase organisation the nucleus. Thus, it is of a great interest to study the active repositioning of gene loci to these nuclear structures and the temporal effects this may have on the activity of a gene.

Activation related gene repositioning is suggested to be mediated by actin-myosin motors complexes (Bridger, 2011; Chuang *et al.*, 2006). The identification of the presence of actin (Schoenenberger *et al.*, 2005; Bettinger *et al.,* 2004; Pederson and Aebi, 2002; Nakayasu and Ueda, 1985), and isoforms of myosin (Pranchevicius *et al.*, 2008; Hofmann *et al.*, 2006; Vreugde *et al.*, 2006; Pestic-Dragovich *et al.*, 2000) in the cell nucleus have aided the implications of the presence of an active nuclear motor complex in moving genes and chromosome territories (Bridger, 2011; Mehta *et al.*, 2010; Mehta *et al.*, 2008; Hu *et al.*, 2008; Chuang *et al.*, 2006; Hofmann *et al.*, 2006). One of the most investigated myosin's for transposing chromatin around the nucleus is nuclear myosin 1β (NM1β), encoded by the gene MYO1C (Bridger and Mehta, 2011; Mehta *et al.*, 2010). With its unique 16 amino acid residue at the N-terminus, required for its nuclear localisation (Pestic-Dragovich *et al.*, 2000), NM1β also has an implicated role in nucleo-cytoplasmic transport (Obrdlik *et al.*, 2010). By utilising the *B. glabrata* embryonic (Bge) cell line and the heat shock system as external stimuli for genome reorganisation, in this chapter issues regarding gene movement are investigated. These include the significance of gene repositioning, the destination of repositioned genes, and the mechanism of gene movement within the nucleus.

The heat shock response is a universal mechanism adopted by all organisms in response to a challenge to survival (Richter *et al.,* 2010). A slight increase in temperature can have deleterious effects on the cell, from unfolding of proteins to morphological defects (Toivola *et al.*, 2009; Welch and Suhan, 1985). The highly conserved heat shock proteins (HSPs) play a critical role in maintaining protein integrity and preventing the aggregation of misfolded proteins in the cell, to maintain normal cell function in an event of cellular injury (Lindquist and Craig, 1988). This is achieved by dramatic induction in the expression of HSPs upon stress, which can be between 10-1000 fold (Lindquist, 1986). Reorganisation of the genome after heat shock has been reported in lower complexity model organisms. In a recent study, Rohner *et al* has shown the induction and reorganisation of a trans gene, hsp16, in the nematode *Caenorhabditis elegans* after a heat shock (Rohner *et al.*, 2013).

In contrast however, the heat shock gene loci in *Drosophila melanogaster* were observed to be stable after heat shock. In this chapter the repositioning of two genes, *actin,* and *hsp70,* in the Bge cell line and the subsequent changes in expression upon heat shock treatment is reported. Also reported is the inhibition of gene repositioning and subsequent expression after heat shock, following a nuclear motor inhibitor treatment.

4.2 Material and Methods

4.2.1 Bge cell culture

Bge cells used in this study were cultured as described in chapter 3, section 3.2.2.

4.2.2 Growing cells on coverslips

Bge cells were grown on sterile 13 mm circular coverslips placed in 90 mm petri dishes. The petri dish was seeded at a density of 2.5 X 10^5 and cells were grown in Bge medium for over two nights.

4.2.3 Fixation of cells for indirect immunofluorescence

Bge cells grown on coverslips were washed once with 1X phosphate buffered saline (PBS) [4.3mM sodium phosphate dibasic, 137mM sodium chloride, 2.7mM potassium chloride, 1.4mM potassium phosphate, pH 7.0]. They were subsequently fixed with either methanol-acetone [1:1] for 10 minutes on ice or with 4% paraformaldehyde (PFA) in 1X PBS at room temperature. The cells were washed three times with 1X PBS followed by the addition of 0.5 % Triton-X-100 in 1X PBS to cells fixed with PFA. PFA fixed cells were then left at room temperature for 10 minutes and washed with three changes of 1X PBS.

4.2.4 Antibody staining for indirect immunofluorescence

Following fixation cells were transferred to a humidified chamber. 10μl of primary antibody (see table 4.1) diluted with newborn calf serum (NCS) in 1X PBS was added to the coverslips and incubated for 1 hour at room temperature. The coverslips were then washed 27 times with 1X PBS before the addition of the secondary antibody. 10μl of the appropriate fluorochrome-conjugated secondary antibody (see table 4.2) diluted with 1% NCS in 1X PBS was added to the coverslips and incubated in the dark for 1 hour at room temperature. The coverslips were subsequently washed 27 times with 1X PBS, followed by a final wash in ddH_2O. They were then counterstained with the DNA intercalater DAPI [1.5μg/ml] (Vectorshield anti-fade mountant, Vectorlabs).

Table 4.1 Primary antibodies used with their appropriate dilution factor (according to manufacturer's instructions).

Primary antibody	**Dilution factor**
Mouse anti-RNA pol II (Chemicon)	1:200
Rabbit anti-PML (Chemicon)	1:200
Mouse anti-coilin (Abcam)	1:200
Mouse anti-SC35 (Abcam)	1:1000
Rabbit anti-nuclear myosin 1β (Sigma)	1:50

Table 4.2 Secondary antibodies used with their appropriate dilution factor (according to manufacturer's instructions).

Secondary antibody	**Dilution factor**
Donkey anti-mouse Cy3 (Stratech)	1:100
Donkey anti-rabbit Cy3 (Stratech)	1:50

4.2.5 Database search and bioinformatic analysis

Nuclear structures were searched for in the 'preliminary Bg genomic database'. Initially the mRNA sequence of a model organism was obtained for the target nuclear structure by searching the gene database using NCBI (http://www.ncbi.nlm.nih.gov). The mRNA sequence was then blasted against the preliminary Bg genomic database (http: //129.24. 144. 93 /blast_bg /2index. html). Contigs, supercontigs, or scaffolds with significant alignment scores (50-200) were identified and the sequences obtained from the preliminary Bg genomic database. The predicted locations and exon-intron structures of genes in the genomic sequences (obtained from the Bg database) was identified by performing a Genscan analysis (http://genes.mit.edu/GENSCAN.html). Predicted peptide sequences were then subjected to BLAST (http://blast.ncbi.nlm.nih.gov/Blast.cgi) and Clustal Omega (http://www.ebi.ac.uk/Tools/msa/clustalo/) analysis to identify any matches with the target nuclear structure and their alignment scores.

4.2.6 Preparation of Bge cell genomic DNA for suppression of repetitive sequences in the Bge cell line

Bge cells were cultured as described in the aforementioned section 4.2.1. The genomic DNA was then extracted as described in chapter 3, section 3.2.3.

4.2.7 Preparation and labelling of probes to be used in fluorescence *in situ* hybridisation

The DNA probes were prepared and labelled as described in chapter 3, section 3.2.4.

4.2.8 Preparation of slides to be used in 3-D fluorescence *in situ* hybridisation

Bge cells were cultured as previously described in section 4.2.1. For 3-D FISH, cells were grown on sterile glass Superfrost™ slides placed in quadriPERM® cell culture vessels (Sigma, UK). They were grown in Bge medium for a minimum of 48 hours.

4.2.9 Heat shock treatment of Bge cells

Bge cells grown on sterile glass slides were placed in an incubator at 32°C. They were heat treated for 1 hour and subsequently fixed in 4% PFA as described in section 4.2.10, protocol B.

4.2.10 3-D fluorescence *in situ* hybridisation on cultured Bge cells combined with immunofluorescence

The following two protocols were used to perform 3-D fluorescence in situ hybridisation combined with immunofluorescence on Bge cells:

4.2.10.a. Protocol A

This protocol was derived from Fluorescence in situ Hybridisation Protocols and Applications: 3D-FISH on Cultured Cells Combined with Immunostaining (Solovei and Cremer, 2010).

Fixation and Permeabilisation of Cells

Bge cells grown on sterile glass slides were rinsed with 1X PBS and fixed with 4% PFA in 1X PBS for 10 minutes at room temperature. During the last minute of fixation one to two drops of 0.5% Triton-X-100 in 1X PBS was added to the slides. The cells were then permeabilised with 0.5% triton-X-100 in 1X PBS for 10 minutes at room temperature and subsequently incubated in 20% glycerol (Sigma, UK) in 1X PBS, for 30 minutes at room temperature. Cells were then snap-frozen in liquid nitrogen for 15-30 seconds. The freeze-thaw process was repeated for a further 5-6 times while soaking the slides in 20% glycerol between each cycle. Excess glycerol was washed from the slides using three changes of 1X PBS / 0.05% Triton-X-100 for 5 minutes each. Cells were subsequently depurinated in 0.1N HCl for 10 minutes at room temperature. Excess acid was washed away with 1X PBS / 0.05% Triton-X-100 for 5 minutes, with three changes of the buffer. Slides were placed in 2X SSC for 5 minutes prior to incubating in 50% formamide in 2X SSC solution for 30 minutes at room temperature.

Hybridisation, Washing, and Hybrid Detection

Following the fixation and permeabilisation of the cells, 10µl of the DIG labelled probe was placed onto 18 x 18 coverslips. The slides were removed from 50% formamide solution, draining the excess fluid, and were immediately placed on the coverslips. The coverslips were then sealed using a rubber solution (Halfords), and was left to dry at room temperature. Slides were placed on a hot block at 75°C and the cellular and probe DNA was denatured simultaneously for 3 minutes. The denatured slide and probe was then left to hybridise for 24 – 48 hours in a humidified chamber at 37°C.

Following hybridisation, the rubber solution and the coverslips were removed and the slides were washed three times for 10 minutes in 2X SSC solution at 37°C. They were subsequently washed twice in 0.1X SSC for 5 minutes at 60°C and placed in 4X SSC / 0.2% Tween 20 at room temperature.

100µl of sheep anti-DIG conjugated to fluorescein (FITC) in 4X SSC / 0.2% Tween 20 (1:200 dilution, Amersham Biosciences) was added to each slide and a new coverslip applied. The slides were incubated at room temperature for 45 minutes in the dark and then washed twice for 5 minutes in 4X SSC with 0.2% Tween 20 at 37°C in the dark.

Immunostaining and Counterstaining

Following the final wash in 4X SSC with 0.2% Tween 20 (see above), slides were equilibrated in 1X PBS / 0.2% Tween 20 for 5 minutes at room temperature. 100µl of mouse primary anti-RNAP II antibody diluted in 4% BSA in 1X PBS / 0.2% Tween 20 was added to the slides and incubated in a dark humidified chamber at room temperature for 45 minutes. The slides were then washed in 1X PBS / 0.2% Tween 20 with three changes of the buffer solution for 5 minutes each. Subsequently 100µl of donkey anti-mouse secondary antibody conjugated to cyanine 3 (Cy3) (diluted in 4% BSA in 1X PBS / 0.2% Tween 20) was applied to the slides and incubated in a dark humidified chamber at room temperature for 45 minutes. The slides were then washed in 1X PBS / 0.2% Tween 20 with three changes of the buffer solution for 5 minutes each, and subsequently equilibrated in 1X PBS. Slides were post fixed in 2% PFA in 1X PBS for 10 minutes prior to counterstaining with DAPI [1.5µg/ml] (Vectorshield anti-fade mountant, Vectorlabs).

4.2.10.b. Protocol B

This protocol was an adapted version of the 3-D fluorescence in situ hybridisation protocol used by Dr D. Bolland from Babraham Institute, Cambridge Cancer Centre, University of Cambridge.

Fixation and Permeabilisation of Cells

Bge cells grown on sterile glass slides were fixed with 4% PFA in 1X PBS for 10 minutes at room temperature, and subsequently quenched in 155mM glycine (Fisher Scientific, UK) for 10 minutes at room temperature. The cells were then permeabilised with 0.1% saponin (Fisher Scientific, UK) / 0.1% Triton-X-100 in 1X PBS for 10 minutes at room temperature, and washed twice with 1X PBS for 5 minutes each. Cells were incubated in 20% glycerol (Sigma, UK) in 1X PBS, for 30 minutes at room temperature and subsequently snap-frozen in liquid nitrogen for 15-30 seconds. The freeze-thaw process was repeated for a further 6 times while soaking the slides in 20% glycerol between each freeze-thaw cycle. Excess glycerol was washed from the slides using two changes of 1X PBS for 5 minutes each and cells were depurinated in 0.1N HCl for 30 minutes at room temperature. Excess acid was washed away with 1X PBS for 5 minutes. RNase treatment was performed by adding 100µl of RNase A [100µg/ml in 2X SSC] and incubating the cells in a humidified chamber for 1 hour at 37°C. The cells were then rinsed in 2X SSC for 5 minutes followed by another rinse in 1X PBS for 5 minutes. Following this, cells were permeabilised with 0.5% saponin (Fisher Scientific, UK) / 0.5% Triton-X-100 in 1X PBS for 30 minutes at room temperature, and washed twice with 1X PBS for 5 minutes each. Slides were then incubating in 50% formamide in 2X SSC solution for 20 minutes at room temperature.

Hybridisation and Washing

Following the fixation and permeabilisation of the cells, 10µl of the DIG labelled probe was placed onto 18 x 18 coverslips. The slides were removed from 50% formamide solution draining the excess fluid, and were immediately place on the coverslips. The coverslips were then sealed using a rubber solution (Halfords), and was left to dry completely at room temperature. Slides were placed on a hot block at 78°C and the cellular and probe DNA was denatured simultaneously for exactly 2 minutes.

The denatured slide and probe was then left to hybridise for 24 – 48 hours in a humidified chamber at 37°C. Following hybridisation, the rubber solution and the coverslips were removed. Slides were washed for 15 minutes in 50% formamide / 2X SSC solution at 45°C, and subsequently transferred to 0.2X SSC solution at 63°C for 15 minutes. They were then equilibrated in 2X SSC at room temperature for 5 minutes.

Hybrid Detection, Immunostaining, and Counterstaining

100µl of blocking solution (3% BSA in 2X SSC) was applied to slides and incubated in a humidified chamber for 30 minutes at room temperature. A three-step detection system was then used to detect the hybrids and the antigens (see table 4.3). After each application of the detection antibody, slides were incubated at room temperature for 30 minutes in a humidified chamber and subsequently washed in three changes of 2X SSC / 0.1% Triton-X-100 at room temperature. Slides were rinsed in 1X PBS for 5 minutes and fixed with 2% PFA in 1X PBS for 5 minutes at room temperature. They were then quenched in 155mM glycine [w/v] for 30 minutes at room temperature, rinsed in 1X PBS for 5 minutes and subsequently counterstained with DAPI [1.5µg/ml] (Vectorshield anti-fade mountant, Vectorlabs).

Table 4.3 Antibody detection scheme used with 3-D FISH combined with immunofluorescence, protocol B. In each step the antibodies for the labelled gene probe and RNAP II were mixed in one solution.

Order of application	**Gene probe (labelled with digoxigenin-11-dUTP)**	**RNAP II**
1	Sheep anti-DIG (FITC), 1:1000 [Stratech]	Mouse anti-RNAP II, 1:200 [Chemicon]
2	Rabbit anti-sheep(FITC), 1:200 [Stratech]	Horse anti-mouse (Biotin), 1:200 [Vectorlabs]
3	Goat anti-rabbit (488), 1:200 [Stratech]	Streptavidin (Cy3), 1:100 [Invitrogen]

4.2.11 2,3-Butanedione 2-Monoxime treatment of Bge cells

The drug 2,3-Butanedione 2-Monoxime (BDM) (Calbiochem) was used to inhibit myosin polymerisation and activity in Bge cells. Cells were treated with 10mM BDM for 15 minutes (Mehta *et al.*, 2010) prior to heat shock treatment as described in section 4.2.9

4.2.12 Bge cellular fixation and slide preparation for 2-D FISH

Control, heat shocked, and BDM treated Bge cells were dislodged by firm tapping and centrifuged at 400g. The pellets were resuspended by vigorously tapping the tube, followed by the addition of hypotonic potassium chloride solution [0.05M], and subsequent fixation with 3:1 methanol-acetic acid. 20µl of the Bge cellular suspension was then applied onto a sterile glass slide and allowed to dry at room temperature.

4.2.13 2-D fluorescence *in situ* hybridisation of *B. glabrata* genes onto interphase nuclei of Bge cells

2-D FISH was performed on the Bge cell as described in chapter 3, section 3.2.5. Probes were derived from clones of *B. glabrata* bacterial artificial chromosome (BAC) libraries (BB02 and BS90 stocks) containing *ferritin,* and *hsp70* encoding sequences.

4.2.14 Image capture and analysis

Images of Bge cell nuclei stained with an antibody for immunofluorescence and 2-D FISH were observed using the Olympus BX41 fluorescence microscope and UPlanFLN 100x / 1.30 oil immersion objective. Digital images were captured using a grey scale digital camera (Digital Scientific UK) and the Smart Capture 3 software (Digital Scientific UK).

For 2-D FISH fifty images of nuclei for each gene (*ferritin,* and *hsp70*) were captured and the positions assessed using the erosion script analysis (Croft *et al.*, 1999) as described in chapter 3, section 3.3.3. Statistical analyses were performed by using unpaired, two-tailed Student's t-test.

The conserved 3-D structures of the Bge cell nuclei were observed using the Plan Apo Neofluor X100 NA 1.3 oil immersion objective on a Zeiss Axiovert 200M microscope. Image acquisition was performed with dedicated AxioVision (Zeiss) software. Digital optical sections were obtained by scanning the nuclei on z-axis at 0.5µm of thickness, creating 15-18 sections. To remove the out of focus fluorescence, image stacks were deconvolved using the inverse filter algorithm. The positions of the genes were assessed by measuring the distance between the gene signal and the nearest nuclear edge in 20 nuclei, using the Axiovision software (Zeiss). These data for gene loci were then plotted as a frequency distribution curve displaying the nuclear positioning of the genes. For co-localisation analysis, images were examined in each Z section. Gene signals were scored as associated with RNAP II transcription factories when there was no visible separation at the single pixel level between the signal and the transcription factory boundary.

4.2.15 RNA isolation and cDNA synthesis

Total ribonucleic acid (RNA) was extracted from control, heat shocked (1 hour at 32°C), and inhibitor treated (15 minute BDM treatment + 1 hour heat shock) Bge cells using RNA isolation reagent TRI® Reagent (Sigma), according to manufacturer's instructions. To purify the RNA samples from any contaminating DNA, DNase treatment was performed using DNase I AMP-D1 (Sigma, UK), according to manufacturer's instructions. RNA concentration was determined by spectrophotometric analyses using NanoDrop spectrophotometer ND-1000 (Thermo Scientific, UK). RNA (1µg) was reverse transcribed into cDNA using SuperScript® III reverse transcriptase (Invitrogen, UK) and random primers in a 21µl reaction according to manufacturer's instructions.

4.2.16 Primer construction and optimisation for qRT-PCR analysis

Primers for actin, hsp70, and 18S were obtained from collaborators from the Institute for the Environment, Brunel University. For ferritin and myoglobin, the mRNA sequence was obtained from the NCBI website (http://www.ncbi.nlm.nih.gov) and Primer3Plus software (http://primer3plus.com/cgi-bin/dev/primer3plus.cgi) was used to design the primer sequence. When designing the primers, the following criteria were considered:

- G, C content of 50-60%
- Melting temperature (Tm) between 50°C and 60°C
- Primer between 16 and 24 base pair length
- Primer amplicon size of 100 to 200 base pair lengths

The selected primer sequence was then confirmed for PCR suitability at PCR Primer Stats website (http: //www. bioinformatics.org /sms2/ pcr_primer_stats. html), according to the criteria listed above. Finally the chosen primer sequence was checked for specify for the gene by running the NCBI Basic Local Alignment Tool (BLAST). The primers were purchased from Sigma (UK), and diluted to 100µM according to manufacturer's instructions. The forward and reverse primers for each gene were then mixed and made up to 10µM working solutions. All of the primers were validated using the synthesised cDNA (see section 4.2.15) and the SsoAdvanced SYBR Green Supermix (BioRad, UK) reaction on the CFX96™ Real-Time PCR detection system (BioRad, UK). 20µl reactions were set-up and run according the manufacturer's instructions. For each primer, amplification of DNA was carried out over a temperature gradient from 50°C to 65°C to determine the best temperature for the primer.

4.2.17 Quantitative reverse transcription PCR optimisation

In order to determine the efficiency of qRT-PCR and to optimise the PCR reaction, i.e. the amount of RNA in the reaction, standard and efficiency curves were included on every plate.

cDNA samples were serially diluted from 20 to 0.016 ng/µl concentrations. 20µl reactions were then set-up and run using the synthesised cDNA (see section 4.2.15) and the SsoAdvanced SYBR Green Supermix (BioRad, UK) reaction, on the CFX96™ Real-Time PCR detection system (BioRad, UK). Template cDNA was added to each well except for the no-template controls (NTC), and the SsoAdvanced SYBR Green Supermix was excluded from the no-reaction template control (NRT) wells.

After the qRT-PCR reaction, the software CFX Manager (BioRad, UK) automatically produces the standard curve plots for the fluorescent threshold values (Ct) corresponding to the nominal concentrations of template cDNA. The slope of this curve was then used to calculate the efficiency of the qRT-PCR amplification (also calculated by the software) and to determine the optimum cDNA template concentration in the reaction.

4.2.18 Quantitative reverse transcription PCR analysis of gene transcripts

Quantitative reverse transcription PCR (qRT-PCR) was performed using SsoAdvanced SYBR Green Supermix (BioRad, UK), according to manufacturer's instructions and run by using the CFX96™ Real-Time PCR detection system (BioRad, UK). A final reaction volume of 20µl qRT-PCR mixture contained 100ng-5ng cDNA template, 200nM-500nM of each gene specific primer, and 1X SsoAdvanced SYBR Green Supermix. The primers used were: ferritin (F: 5'-CTCTCCCACACTGTACCTATC-3'; R: 5'- CGGTCTGCATCTCGTTTTC-3'), and hsp70 (F: 5'-AGGCGTCGACATTCAGGTCTA-3'; R: 5'-TGGTGATGTTGTTGGTTTTACCA-3'). A parallel reaction was performed using the constitutively expressed, housekeeping genes actin (F**:** 5'-GGAGGAGAGAGAACATGC-3'; R: 5'-CACCAATCTGCTTGATGGAC-3'), myoglobin (F: 5'-GATGTTCGCCAATGTTCCC- 3'; R: 5'-AGCGATCAAGTTTCCCCAG-3') and 18S (F: 5'-GCATGTCTAAGTTCACACTG-3'; R: 5'-TTGATAGGGCAGACATTTGA-3').

qRT-PCR reactions included an initial enzyme activation / cDNA denaturation at 95°C for 30 seconds followed by a 95°C denaturation for 5 seconds, and annealing / amplification at the optimised temperature for each primer (59°C for actin, ferritin, myoglobin and 18S, and 52°C for hsp70) for 1 minute. The fluorescent product was detected at the end of the amplification period and all amplifications were run in triplicates. As part of the qRT-PCR run, a melting curve was conducted. This involved heating the plate to 95°C, in 0.5°C increments for 5 seconds, and measuring the fluorescence of each well as the temperature increases. When the temperature reaches the specific melting temperature of a product, the product is indicated by a peak. If several peaks, which melt at different temperatures are present, this indicates the presence of other products in the sample, such as primer dimers and contamination products. The fluorescent threshold values (Ct) were determined using the CFX Manager software (BioRad, UK). The differences in gene transcript levels were also automatically calculated by the software using actin, myoglobin or 18S housekeeping genes to normalise the quantification of targets. Fold change in transcription was calculated using the following formula:

$$\text{Fold change} = 2^{-\Delta\Delta Ct}$$

$$= 2^{-\left[(Ct_{\text{gene, exposed}} - Ct_{\text{myoglobin, exposed}}) - (Ct_{\text{gene, unexposed}} - Ct_{\text{myoglobin, exposed}})\right]}$$

In order to determine the significance of differences ($P < 0.05$ or $P < 0.01$) in gene expression, the *P*-value was calculated by comparing delta-delta Ct ($\Delta\Delta Ct$) values using the Student's *t*-test between the control and treated cells.

4.2.19 *B. glabrata* stocks, heat shock and BDM treatment

Adult *B. glabrata* snails from the BB02 strain were used. Individual snails were exposed to either 1 hour heat shock at 32°C or subjected to 10mM BDM treatment for 15 minutes prior to heat shock.

Following exposure the snail ovotestes were dissected and incubated in hypotonic potassium chloride solution (0.050M) for 30 minutes, during which the tissues were macerated with a needle to obtained single cells. The cells were then centrifuged at 163g for 5 minutes, fixed with methanol - acetic acid, and spread onto glass slides as described in chapter 3, section 3.2.1.

4.2.20 2-D fluorescence *in situ* hybridisation of *B. glabrata* genes onto interphase nuclei of *B. glabrata* cells

2-D FISH was performed as described in chapter 3, sections 3.2.5 and 3.2.6 protocol B. Probes were derived from clones of *B. glabrata* bacterial artificial chromosome (BAC) libraries (BB02 and BS90 stocks) containing *hsp70* encoding sequences.

4.3 Results

Despite being a molluscan model organism, the nucleus of the freshwater snail *B. glabrata,* and the functional organisation within it is comparatively under researched. Nuclear structures have functional and regulatory roles in the nucleus. Studying these structures in the snail would enable a thorough understanding of the snail nuclear organisation as well providing an insight to the functional roles of these structures in genome organisation. In the previous chapter, repositioning of the genes after a parasitic infection was revealed. Here, by utilising the 3-D fluorescence *in situ* hybridisation technique combined with immunofluorescence, the answers to 'where', 'how', and 'why' these genes are moving are being sought. However, since this is the first time the snail nuclear structures are being investigated, these experiments were utilised in the Bge cell line.

4.3.1 Nuclear structures in Bge cells

The presence and distribution of snail nuclear structures was investigated in the Bge cells. Using antibodies raised against various model organisms, the presence of three nuclear structures have been confirmed in the Bge cells. Figure 4.1 displays the distribution patterns observed for PML bodies (A), transcription factories (B), and nuclear myosin 1β (C) in Bge cells. Using an anti-PML antibody in an indirect immunofluorescence assay, PML-like bodies were visualised in Bge cells [Fig. 4.1 A]. Conditions that cause stress are known to lead to a reduction in the number PML bodies. Therefore to further confirm that the observed structures were the Bge cell PML bodies, cells were heat shocked for 1 hour at 32˚C prior to immunofluorescence. The majority of the cells contained between 18-25 PML bodies per cell, which was reduced to 8-15 per cell following 1 hour heat shock [Fig. 4.2]. RNA polymerase II (RNAP II) transcription factories in the Bge cells were also observed [Fig. 4.2 B]. These were distributed throughout the nucleus with denser regions around the nuclear periphery. Finally, the presence of nuclear myosin 1β was also confirmed, which had a peripheral distribution forming a rim structure around the nuclear periphery, with some foci within the nucleoplasm [Fig. 4.1 C].

RNAP II transcription factories and NM1β were present in both methanol-acetone and paraformaldehyde fixation methods. However, PML bodies were only visualised when the cells were fixed with methanol-acetone. Staining with anti-coilin and anti-SC35 antibodies (to reveal Cajal bodies and nuclear speckles respectively), were unsuccessful with both fixation methods (not shown).

Figure 4.1 Representative 2-D images displaying the distribution of three nuclear structures in the Bge cells. Cells were fixed with methanol-acetone and stained for anti-PML (A), anti-RNAP II (B), and anti-myosin 1β (C). The cells were counterstained with DAPI (blue). Scale bar = 5μm.

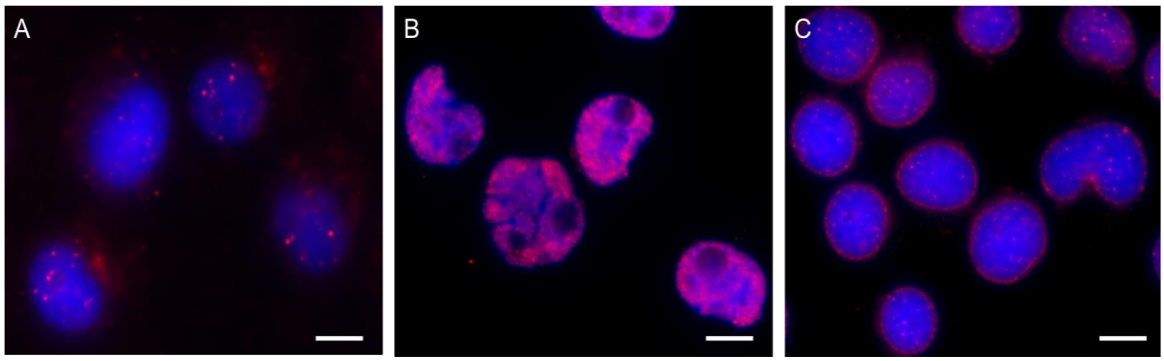

Figure 4.2 Chart showing the average number of PML bodies present in control and one hour heat shocked (at 32˚C) Bge cells; n=200. Statistically significant differences, as assessed by two-tailed Student's t-test, between control nuclei compared with heat shocked nuclei are indicated by an asterisk (P<0.05). Error bars = S.E.M.

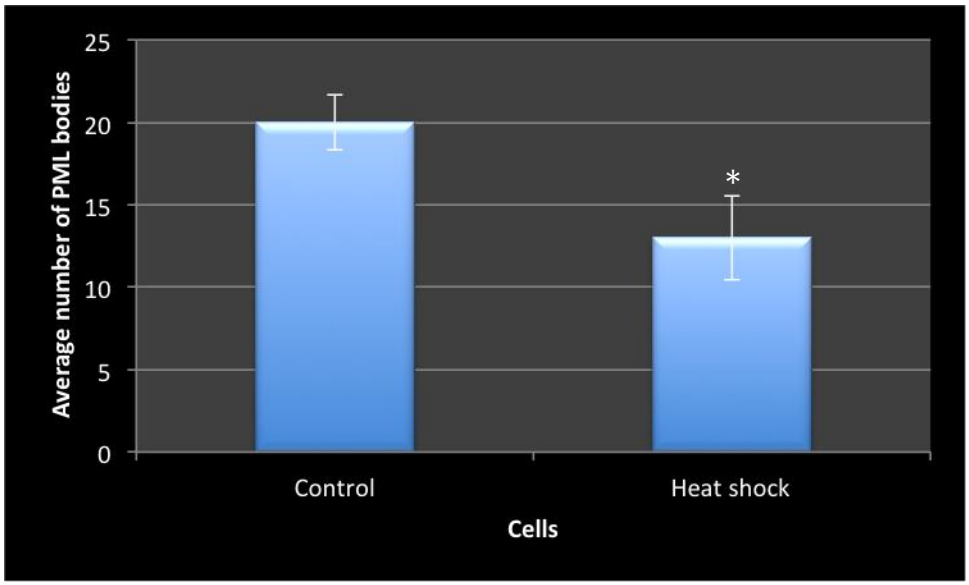

4.3.2 Bioinformatic analysis of nuclear structures in the Bge cells

To further confirm the presence of the nuclear structures identified in the Bge cells, bioinformatic analysis was performed. The mRNA sequences were obtained for RNAP II, PML, Coilin, SC35, and NM1, from various model organisms including *Homo sapiens*, mouse, and *Drosophila.* These were then blasted against the preliminary Bg genomic database. The predicted peptide sequence of RNAP II in *B. glabrata* has successfully been obtained and confirmed by BLAST and Clustal Omega analysis. Alignment of the predicted *B. glabrata* RNAP II peptide sequences with *Homo sapiens, D. melanogaster, C. elegans,* and *Mus musculus* RNAP II peptide sequences has shown 77%, 72%, 71%, and 77% sequence similarity respectively. Table 4.4 displays the results of Genscan and BLAST analysis for RNAP II in *B. glabrata*. Bioinformatic analysis for PML bodies, nuclear myosin 1, SC35 splicing speckles, and Cajal bodies in *B. glabrata* has returned no results.

Table 4.4 Predicted peptide sequence for RNA polymerase II in *B. glabrata* and BLAST results for this sequence.

Predicted peptide sequence (Genscan)	>/tmp/03_27_13-08:32:41.fasta|GENSCAN_predicted_peptide_1|1714_aa VAEEKRTTLAEEKRQKRKARPTTLAPAGITCPVYGRTFRAHSHPKMKDVISKSKGYPQKR LAHVYNLCRTRKICEGGDEMEKRKEEEEGGGENQENEAPKSHGGCGRYQPNIRRNGLELM AEWKHTNEESQEKKIQVTAERVLEIFKRITDEECIVLGMDPKYARPDWMIVTVFPVPPLP VRPAVVMFGSARNQDDLTHKLSDIVKANNQLRRNEQNGAAAHIIQEDTKMLQYHCATLVD NEIPGLPKAVQKSGRPLKSVKQRLKGKEGRVRGNLMGKRVDFSARTVITPDPNLRVDQVG VPRTIAQNMTFPELVTPFNIDRMQNLVRRGANQYPGAKYIVRDNGERIDLSVTTPYNADF DGDEMNLHLPQSLETRAEIYNLAAVPRMIITPQANRPVMGIVQDTLCAVRKMTKRDVFID RAQMMNLLMFLPTWDGRMPQPAILKPVPLWTGRVNCNRTHSTHPDSEDNGPYKWISPGDT RVLIEDAELISGIICKKALGTSAGSLVHIVFLEMGHDIAGEFYGNIQTVVNNWLLIEGHS IGIGDTIADQQTYQDIQDTIRNAKNDVIDVIEKAHNDELEPTPGNTLRQTFENQVIACVG QQNVEGKRIPFGFRYRTLPHFIKDDYGPESRGFVENSYLAGLTPSEFYFHAMGGREGLID TAVKTAETGYIQRRLIKAMESVMVKYDGTVRNQVEQLVQLRYGEDGLDACWVEFQSIPTL KPSDKAFEKRFRFDATNESNDLHPLKVIEGVRDLCRRLVIVVGEDRISYQANENATLLMK ALIRSTLCTKRVAEEHCLTSEAFEWVLGEIETKFQQAMAHPGEMVGALAAQSLGEPATQM

	TLNTFHYAGVSAKNVTLGVPRLKEIINISKKPKTPSLTVYLLGQAARDAERCKDVLCRLE HTTLRRVTANTAIYYDPDPMNTVIAEDQEWVSIYYEMPDFDASRISPWLLRIELDRKRMT DKKLTMEQISEKIQSGFGDDLNCIFNDDNAEKLVLRIRIMNSDNTKYQDEEEVVDKMEDD VFLRCIEANLLSDMSLQGIEAIAKVYMHLPNTDDKRRIHITEEGEFKAVSEWILETDGSS LTKVLSERDVDPVRTYTNDIVEVFDTLGIEAVRKAIEREMNHVISFDGSYVNYRHLALLC DVMTSKGHLMAITRHGINRQETGALARCSFEETVDILMEAASHAEIDPMKGVSENIMLGQ LAKIGTGCFELLLDAEKCKYGMEIPSQLGPGQLAGGAGTGMFFGAAGSPTSSMSPQMTPW GQVGTPGYASAWSPGVGSGMTPGGAGFSPSAASEAGYSPAYSPGWSPQPGSPGSPSSPYI PSPRGASSPGYSPSSPVYLPSSPAIATPQSPSYSPTSPSYSPSSPGYSPTSPKYSPTSPS YSPTSPSYSPTSPSYSPTSPSYSPTSPSYSPTSPSYSPTSPSYSPTSPSYSPTSPSYSPT SPSYSPTSPSYSPTSPSYSPTSPSYSPTSPSYSPTSPSYSPTSPSYSPTSPGYSPTSPSY SPSSPNYSPTSPSYSPTSPSYSPTSPSYSPSSPSYSPSSPSYSPSSPNYSPSSPSYSPSS PKYSPSSPSYSPTSPSYSPSSPQYSPSSPKYSPSSPQYSPSSPQYSPSSPSYSPSSPKYS PTSPRYSPTSPDYSPSSPHYSPTSPSYSPSSPNYSPASPTYSPSSSPKYSPTSPTSSPAS PGYSPSSPAYSPNTPHYSPTSPHYGTDLEDDDQP
BLAST results	RNA polymerase II largest subunit [Gynaikotothrips ficorum] Accession number: BAJ78670.1 DNA directed RNAP II subunit RPB1 [Mus musculus] Accession number: NP 033115.1 Largest subunit of RNAP II complex [Danaus plexippus] Accession: EHJ77617.1 RNAP II largest subunit [Homo sapiens] Accession number: CAA52862.1

4.3.3 Establishing the optimum protocol for 3-D fluorescence *in situ* hybridisation combined with immunofluorescence for Bge cells

Preserving the three dimensional structure of cells is vital to analyse the functional and structural organisation of the interphase nucleus. 3-D fluorescence *in situ* hybridisation is a widely used technique in nuclear biology, and allows the visualisation of specific DNA targets within nuclei. However as with all other techniques, the application of 3-D FISH also requires modification to suit the needs of different organisms, tissues, and cells. Here, protocols obtained from two different laboratories were utilised on the Bge cells. Protocol A was a much simpler protocol, with a single hybrid detection step.

Using this protocol gene signals were visualised in some cells, however immunofluorescence staining for nuclear structures was unsuccessful [Fig. 4.3 A]. Cells also had very high levels of background fluorescence, making it difficult to visualise the gene signals. Alternatively protocol B was a much complex protocol with additional incubations in glycine and RNase A, and had a 3-step detection scheme. Using this protocol, clear and bright gene signals were visualised in every cell with significantly reduced background fluorescence [Fig. 4.3 B]. This protocol also enabled simultaneous visualisation of gene signals and nuclear structures.

Figure 4.3 Representative 3-D images of interphase nuclei of Bge cells after 3-D FISH combined with immunofluorescence. Panels A and B are displaying interphase nuclei after 3-D FISH with protocol A and protocol B respectively. Nuclei are counterstained with DAPI (blue) and hybridised with the *actin* gene (green). Anti-RNAP II staining is shown in red. Scale bar = 5μm.

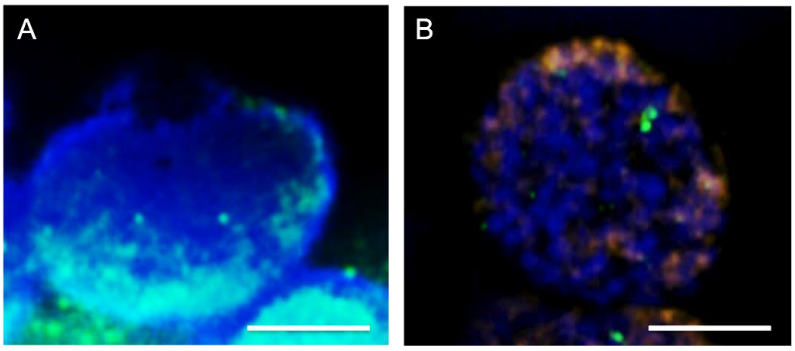

4.3.4 Non-random positioning of gene loci in interphase nuclei of Bge cells and co-localisation with transcription factories

By utilising the results attained in section 4.3.3, three genes (*actin, ferritin,* and *hsp70*) were effectively mapped in interphase nuclei of Bge cells. For each gene the distance between the gene signal and the nearest nuclear edge in x, y, and z axes were measured in 20 nuclei, using the Axiovision software (Zeiss).

These data for gene loci were then plotted as a frequency distribution curve displaying the nuclear positioning of the genes. The frequency distributions curves presented in figure 4.4 display the radial positioning of *actin, ferritin,* and *hsp70* genes in the interphase nuclei of Bge cells. All three gene loci display non-random radial positioning in Bge cells. While *actin* gene loci are located towards the nuclear interior [Fig. 4.4 A], *ferritin* and *hsp70* are located at a more peripheral position within the nucleus [Fig. 4.4 B-C].

Since PML bodies were not revealed with paraformaldehyde fixation, it was not possible to perform 3-D FISH on these cells and analyse the interaction of genes with PML bodies. RNAP II transcription factories however were visualised in both fixation methods. All three genes were found to co-localise with RNAP II transcription factories [Fig. 4.5]. 44% of the *actin* gene loci co-localised with transcription factories, and in these cells 82% was a single allele co-localisation. 12.5 % of the *ferritin* gene loci were observed to associate with transcription factories, and all were a single allele. With *hsp70,* 42% of the gene loci were found to co-localise, of which 80% was a single allele co-localisation.

Figure 4.4 Frequency distribution curves showing the radial positioning of *B. glabrata* genes in the interphase nuclei of Bge cells. Genes are non-randomly positioned in interphase nuclei of Bge cells. 20 images for each gene (A-C) were captured and the gene positions analysed by measuring the distance between the gene signal and the nearest nuclear edge, using the Axiovision software (Zeiss).

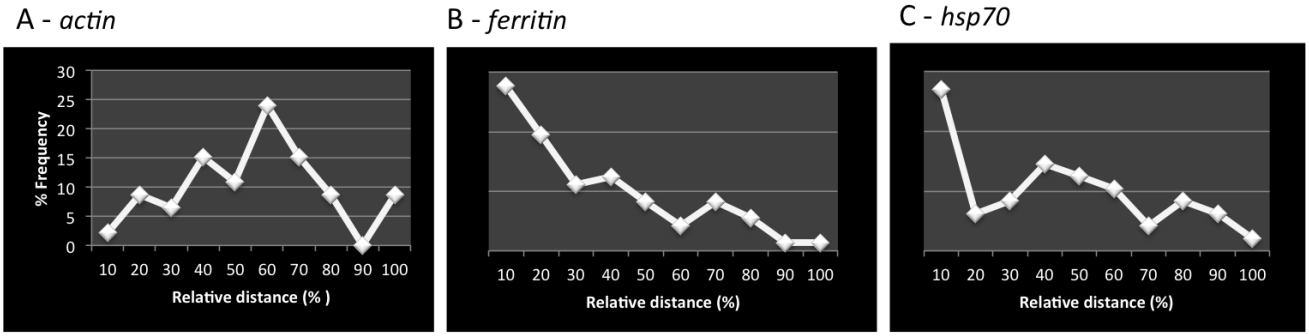

Figure 4.5 Representative images of interphase nuclei of Bge cells after 3-D FISH combined with immunofluorescence. Panels A and B are displaying gene signals not associating with transcription factories and gene signals co-localising, respectively. Nuclei are counterstained with DAPI (blue) and hybridised with the *actin* gene (green). Anti-RNAP II staining is shown in red. Scale bar = 5μm.

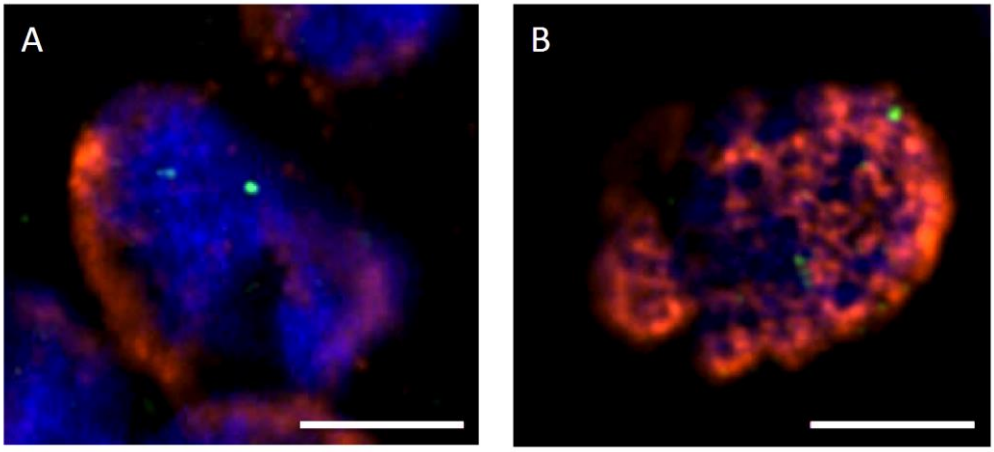

4.3.5 Gene positioning is altered in Bge cells after heat shock and this is correlated with alterations to gene expression and increased association with transcription factories

In *B. glabrata* and the Bge cell line, cellular stress induced by heat shock results in the up-regulation of certain genes including the 70kDa heat shock protein (hsp70) gene (Ittiprasert *et al.*, 2009; Laursen *et al.*, 1997). In chapter 3, induction of genes were correlated with repositioning events within the nucleus, which was also previously demonstrated in the Bge cell line after co-culture with the parasite (Knight *et al.*, 2011). In this chapter, using the Bge cell line reorganisation of the genome after an external stimulus were analysed by exposing cells to 1 hour heat shock at 32°C. To correlate the alteration in the spatial positioning with gene expression, qRT-PCR was performed using RNA isolated from heat shocked cells. By utilising the 3-D FISH combined with immunofluorescence technique, the destination of the repositioned genes was also elucidated.

4.3.5.a. *Actin* and *hsp70* gene loci repositions after heat shock and are co-localised with transcription factories

As demonstrated in section 4.3.4, *actin, ferritin,* and *hsp70* gene loci were located non-randomly within the interphase nuclei of Bge cells. Using 3-D FISH, all three genes were hybridised in interphase nuclei of Bge cells after 1 hour heat shock at 32°C. 20 images were captured for each gene and their positions analysed. Figure 4.6 displays the radial positioning of *actin, ferritin,* and *hsp70* pre and post exposure to heat shock in the Bge cells. Upon heat shock, *actin* gene loci changes position and moves from the nuclear interior towards the nuclear periphery [Fig. 4.6 A]. The *ferritin* gene has a bimodal distribution after heat shock, with the majority of the gene loci still being located towards the nuclear periphery [Fig. 4.6 B]. *Hsp70* also repositions after heat shock and the gene loci shifts from the nuclear periphery to the nuclear interior [Fig. 4.6 C]. Figure 4.7 displays the percentage co-localisation of all three gene loci with transcription factories. Following heat shock, both *actin* and *hsp70* significantly increase their percentage co-localisation with transcription factories, while the association of *ferritin* remains stable.

Figure 4.6 Charts displaying radial positioning of *B. glabrata* genes in the interphase nuclei of Bge cells pre and post exposure to heat shock at 32°C. 20 images for each gene (A-C) were captured and the gene positions analysed by measuring the distance between the gene signal and the nearest nuclear edge, using the Axiovision software (Zeiss).

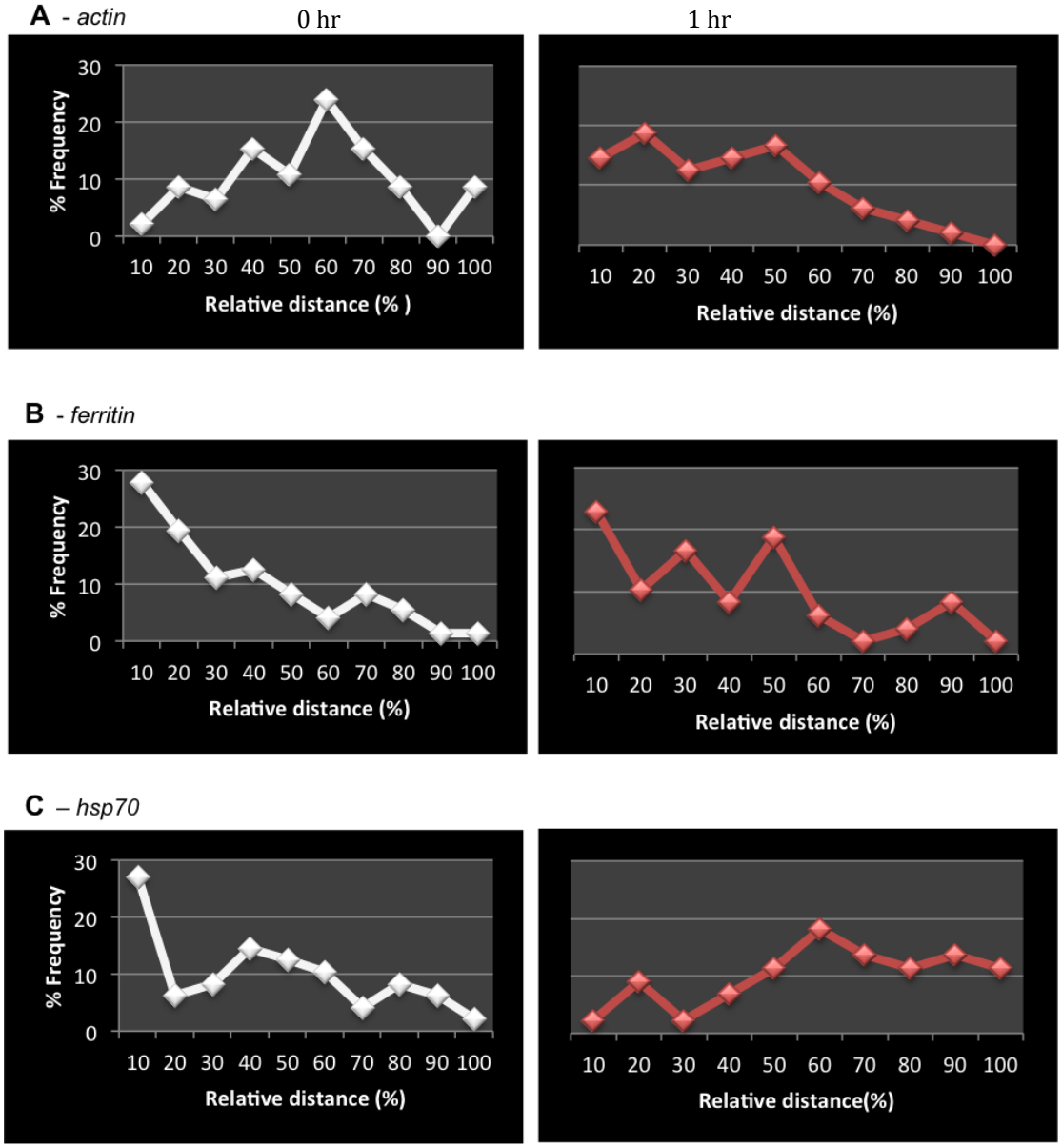

Figure 4.7 Graph and a summary table displaying percentage co-localisation of gene loci with transcription factories, in the interphase nuclei of Bge cells pre and post exposure to heat shock at 32°C. Gene signals were scored as associated with RNAP II transcription factories when there was no visible separation at the single pixel level between the signal and the transcription factory boundary. Significant *P* values of <0.05 are indicated by an asterisk to show the significance of co-localisation by using Student's *t* test.

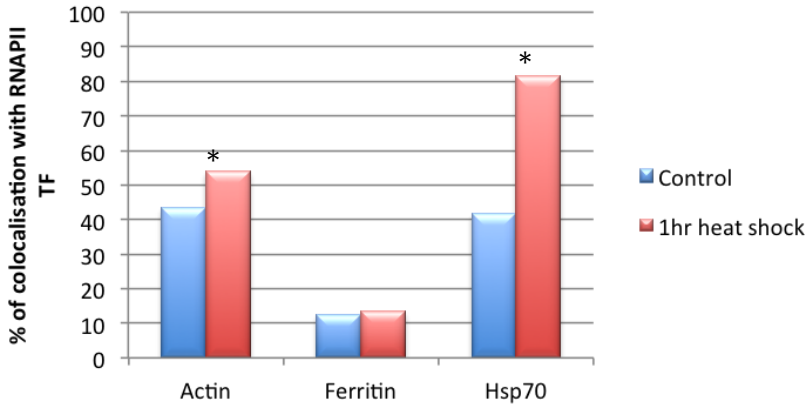

***B. glabrata* gene**	**% Co-localisation with TF's**	
	Control - [% of cells with co-localisation of both alleles]	**Heat shock – [% of cells with co-localisation of both alleles]**
Actin	43% [18%]	54% [67%]
Ferritin	12.5% [100%]	13.4% [30%]
Hsp70	41% [18%]	82% [72%]

4.3.5.b. Repositioning and co-localisation of *hsp70* gene loci with transcription factories is correlated with the up-regulation of the gene

Quantitative real time PCR was used to assess the levels of induction of *ferritin,* and *hsp70* after heat shock. A parallel reaction was performed using the constitutively expressed, housekeeping genes *actin, myoglobin,* and *18S.* However both *myoglobin* and *18S* expressions were increased after heat shock. Therefore *actin* was the housekeeping gene selected to normalise the quantification of targets when calculating the difference in gene transcript levels.

Figure 4.9 displays the results from the qRT-PCR experiments. After 1 hour heat shock at 32°C, the expression of *ferritin* is up-regulated by 1.5 fold, while *hsp70* has a dramatic up-regulation in its expression by 443 fold. The increase in the expression of *hsp70* is directly correlated with the repositioning of the gene loci to the nuclear interior and subsequent co-localisation with transcription factories. Although *actin* was also repositioned after heat shock, since it was chosen as the reference gene, and all the other genes selected have altered their expression after heat shock, it was not possible to study the expression of *actin* by qRT-PCR analysis. However, the relative quantity (RQ) of *actin* in Bge cells before and after heat shock remains stable, with no significant change.

4.3.6 Gene repositioning and subsequent expression after heat shock is blocked by a nuclear motor inhibitor in Bge cells

In an effort to elucidate the significance of gene repositioning and the effects this may have on genome organisation and function, the movement of gene loci was inhibited using a drug. Previous studies have shown nuclear motor activity in moving genomic regions within the nucleus by actin and / or myosin, and indeed Mehta *et al* had shown the involvement of NM1β in chromosome repositioning (Mehta *et al.*, 2010). Since the presence of NM1β was confirmed in the Bge cell nuclei (see section 4.3.1), an inhibitor of myosin's (BDM – also used by Mehta *et al*) was used in effort to block any gene repositioning elicited by nuclear motor activity. To correlate the alteration in the spatial positioning with gene expression, qRT-PCR was performed using RNA isolated from control, heat shocked, and BDM treated cells, and the data was normalised with the *actin* reference gene.

By utilising 2-D FISH, *hsp70* and *ferritin* genes were hybridised onto interphase nuclei derived from Bge cells pre and post exposure to BDM treatment after 1 hour heat shock at 32°C. 50 images of both gene loci were analysed using the previously mentioned erosion script analysis (Croft *et al.*, 1999). Figure 4.8 displays the radial positioning of *hsp70* and *ferritin* gene loci in control, 1 hour heat shocked, and 15 minute BDM treated cells prior to heat shock. Upon heat shock, *hsp70* moves from the nuclear periphery towards the nuclear interior. However after 15 minutes of BDM treatment prior to heat shock, the repositioning of *hsp70* gene loci was inhibited and the gene had a peripheral position, as in the control cells [Fig. 4.8 A]. The inhibition of the movement of *hsp70* gene loci also correlated with reduced levels of expression of the gene. Following 15 minute BDM treatment prior to heat shock, the expression of *hsp70* was significantly reduced from 443 fold to 109 fold [Fig. 4.9]. In contrast, the position of *ferritin* gene loci was not affected by heat shock or BDM treatment [Fig. 4.8 B], however qRT-PCR analysis has shown that its expression was down-regulated by 0.6 fold [Fig. 4.9].

Figure 4.8 Charts displaying the radial positioning of *B. glabrata* genes in the interphase nuclei of Bge cells in control (0 hr), 1 hour heat shocked at 32°C (1 hr), and 15 minute BDM treated cells prior to heat shock (BDM + 1 hr). BDM treatment inhibits gene repositioning after heat shock. Statistically significant differences, as assessed by two-tailed Student's t-test, between normalized gene signal in each shell of control nuclei compared with heat shocked and BDM treated cells are indicated by an asterisk ($P<0.05$). Error bars = S.E.M.

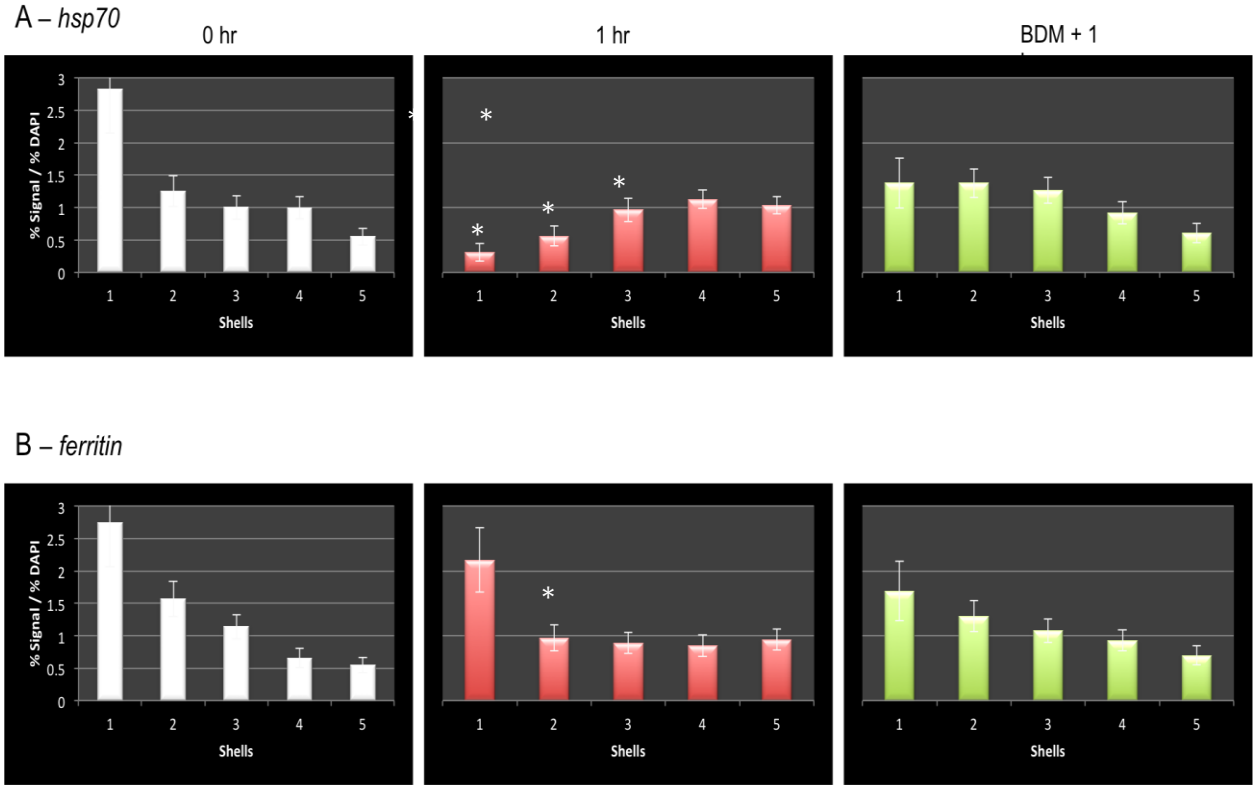

Figure 4.9 Chart displaying the real time qRT-PCR analysis of the differential gene expression of *ferritin* and *hsp70* in Bge cells pre and post exposure to 15 minute BDM treatment after 1 hour heat shock at 32°C. Fold difference of gene expression was calculated by comparative Ct method using the formula $2^{-\Delta\Delta Ct}$. Significant *P* values of <0.05 are indicated by an asterisk to show the significance of gene expression by using Student's *t* test. Error bars = S.E.M.

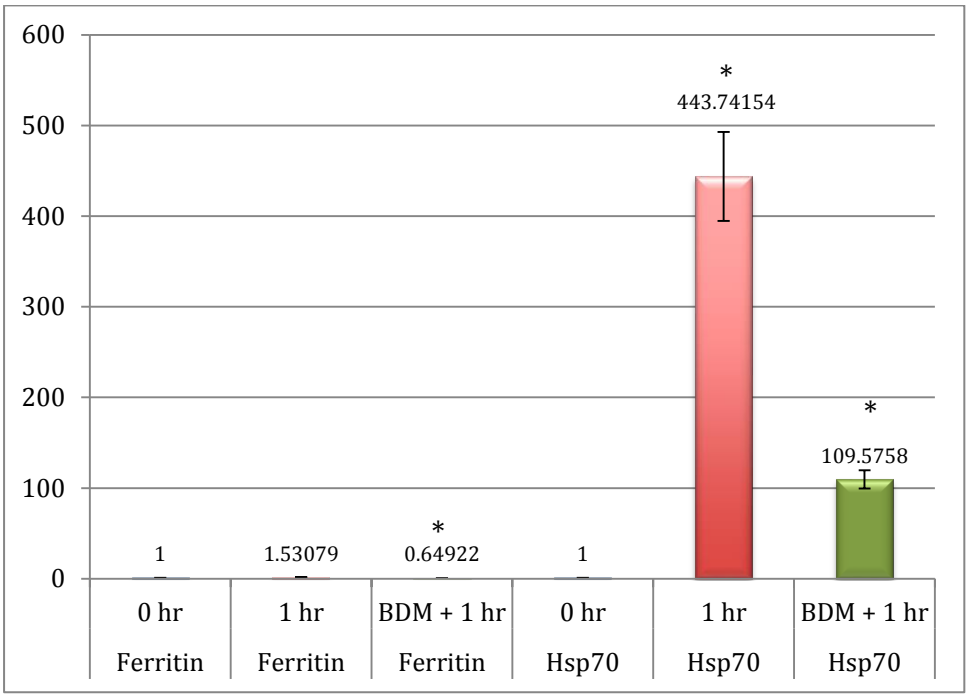

4.3.7 Distribution of NM1β is altered in Bge cells treated with BDM

As described in section 4.3.1, the presence and distribution pattern of NM1β in the Bge cells were identified. In normal cells NM1β has a peripheral distribution with a rim around the nuclear periphery, and foci within the nucleoplasm. However after treatment with BDM, this distribution pattern is altered. Figure 4.10 displays the distribution pattern of NM1β in control and BDM treated Bge cells. Following 15 minutes of BDM treatment, NM1β still has a rim structure around the nuclear periphery, however there are no foci within the nucleoplasm.

Figure 4.10 Representative 2-D images of Bge cells displaying the distribution of nuclear myosin 1β pre (A) and post (B) exposure to 15 minute BDM treatment. Cells were fixed with methanol-acetone and stained for rabbit anti-myosin 1β, and detected with anti-rabbit Cy3 (red). The cells were counterstained with DAPI (blue). Scale bar = 5μm.

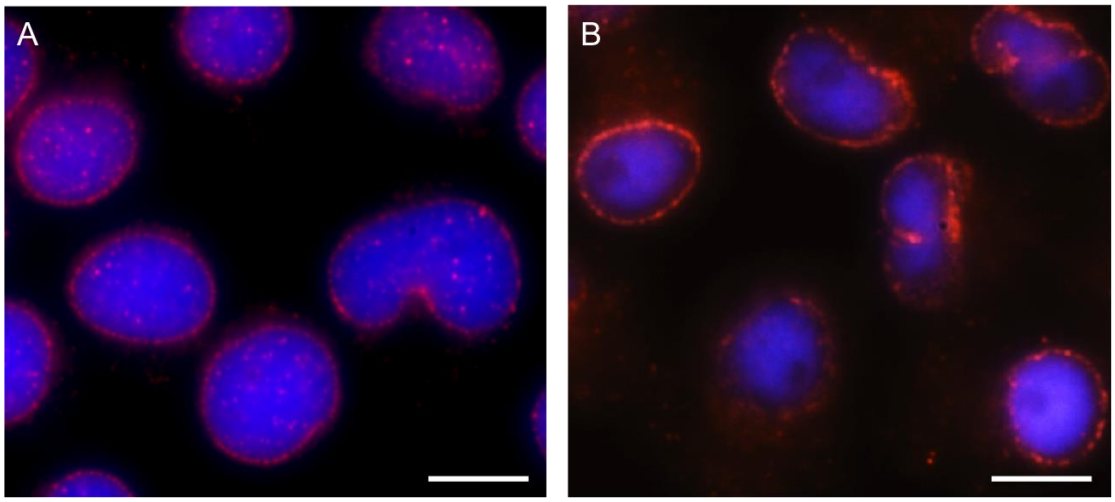

4.3.8 Gene repositioning is blocked by a nuclear motor inhibitor in the snail *Biomphalaria glabrata*

The activity of BDM to inhibit gene repositioning was also verified in the snail *B. glabrata.* Using 2-D FISH, *hsp70* gene was hybridised onto interphase nuclei derived from *B.* glabrata after 15 minute incubation in 10mM BDM solution followed by a heat shock at 32°C. Cells were also derived from control (untreated), and heat shocked snails. Figure 4.11 displays the radial positioning of *hsp70* gene loci in *B. glabrata*, following analysis using the erosion script software (Croft *et al.*, 1999). In *B. glabrata*, *hsp70* has an internal position, which is altered upon 1 hour heat shock and the gene has a peripheral position. However BDM treatment prior to heat shock inhibits the repositioning of *hsp70* after heat shock, and the gene is positioned internally within the nuclei as in the control snails.

Figure 4.11 Charts displaying radial positioning of *B. glabrata hsp70* gene in the interphase nuclei of cells derived from BB02 strain snails, pre and post exposure to BDM treatment after heat shock. BDM treatment inhibits gene repositioning in the intact snail after heat shock. Statistically significant differences, as assessed by two-tailed Student's *t* test, between normalized gene signal in each shell of control cells compared with heat shocked and BDM treated *B. glabrata* cells are indicated by an asterisk (P<0.05). Error bars = S.E.M.

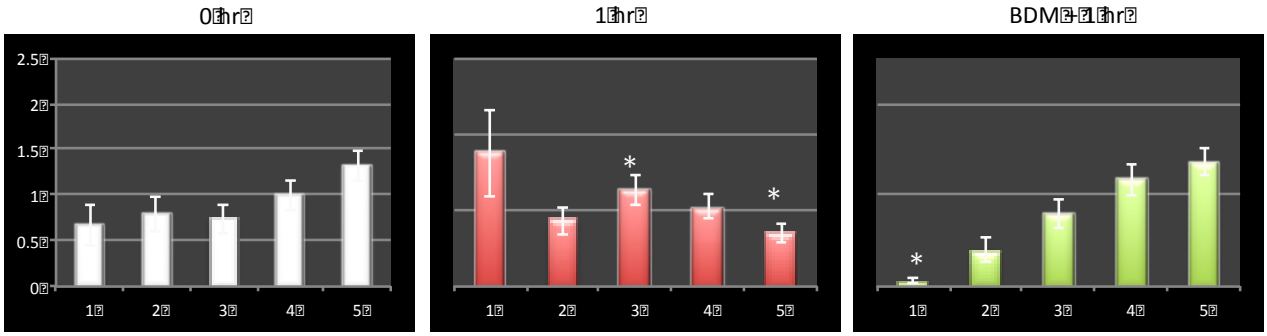

4.4 Discussion

Very little is known about the genome of the freshwater snail *B. glabrata.* Recent studies on gene positioning have shown that both in the Bge cell line (Knight *et al.*, 2011) and the intact snail (see chapter 3), gene expression occur at both the nuclear interior and nuclear periphery. Therefore this lophotrochozoan was an exceptional model system to study the involvement of different nuclear compartments in genomic regulation. Bearing this in mind, the nuclear structures of the snail were investigated. Since this was the first time the snail nuclear structures were being studied, and in order to speed the process of protocol development, the Bge cell line was utilised. Using antibodies raised against model organisms, which cross reacts with a broad range of species, the presence of three nuclear structures have been confirmed in the snail nucleus:

1. *PML bodies* – These had a similar spherical structure and distribution to PML bodies identified in other organisms (Bernardi and Pandolfi, 2007) and their numbers were reduced considerably after heat shock.

This is most likely to be due to the effects of cellular stress resulting in the detachment of smaller bodies from the main PML body (Eskiw *et al.*, 2003; Nefkens *et al.*, 2003). Different fixation methods may be required to reveal specific nuclear structures and PML bodies were visualised only by alcohol fixation of Bge cells. During this fixation cellular proteins are precipitated and aggregated, and it is a very different process from cross-linking fixatives such as paraformaldehyde used to preserve the 3-D structure of the cell.

2. *RNA polymerase II transcription factories* – Transcription factories are thought to play an important role in the organisation of the genome and have been identified in the vast majority of organisms (Razin *et al.*, 2011). The distribution pattern of these factories in the snail are similar to those observed in humans (Mitchell and Fraser, 2008), but with denser regions around the nuclear periphery.
3. *Nuclear myosin 1 β* - NM1β is the nuclear isoform of MYO1C found in vertebrates (Coluccio, 2007) and this nuclear isoform has also been identified in the snail nuclei. However NM1β has a very interesting distribution pattern in the snail nuclei, which was a combination of the staining observed in quiescent (rim) and proliferating (nucleoplasmic) human fibroblast cells (Mehta *et al.*, 2010).

Although bioinformatic analyses have only confirmed the presence of RNAP II in the genome of *B. glabrata,* it should be noted that the snail genome is still not fully complete and therefore this analysis is prone to errors. However nuclear bodies are also not very well conserved within the lower eukaryotes. PML proteins have not been found in the genomes of *S. cerevisiae, D. melanogaster,* and bacteria (Borden, 2008). Given the central role purported for the function of the PML protein and nuclear bodies, one would expect to find this protein in these organisms. Therefore the visualisation of PML like bodies in the Bge cell line by immunofluorescence assay is a promising result.

The importance of spatial positioning in regulating gene expression is now becoming an accepted concept. The interaction of genes with nuclear structures involved in essential nuclear processes, and moreover the identification of repositioned genes associating with these structures has been fundamental for studies of genome organisation and function. In this chapter, using the Bge cell line and utilising the 3-D fluorescence *in situ* hybridisation technique combined with immunofluorescence, the migration of specific gene loci to transcription factories was investigated, and the effects this has on the temporal kinetics of gene expression. A suitable variant of the 3-D FISH technique was identified for the Bge cells (protocol B), and the culmination of this technique with immunofluorescence has revealed major gene repositioning events in interphase nuclei of Bge cells. These repositioning events were directly correlated with increased association with transcription factories, and up-regulation of gene expression.

Actin, ferritin, and *hsp70* gene loci were all positioned non-randomly within the interphase nuclei of Bge cells, with *actin* having an internal position, and *ferritin* and *hsp70* having a peripheral nuclear position. These results were in complete agreement with previous 2-D FISH analysis of these gene loci in Bge cells (Knight *et al.*, 2011). After one hour heat shock at 32°C, both *actin* and *hsp70* gene loci were repositioned, with *actin* becoming more peripheral and *hsp70* more internal within the interphase nuclei of Bge cells. This is the first time the heat shock gene *hsp70* is reported to be repositioned in the Bge cells, as after co-culture experiments with *S. mansoni* parasite the gene loci was reported to be stationary (Knight *et al.*, 2011). Thus the repositioning of *hsp70* in this study is a direct effect of cellular stress caused by heat shock. These repositioning events observed after heat shock significantly correlated with increased association of *actin* (67%) and *hsp70* (82%) gene loci with transcription factories. The *ferritin* gene locus was stationary after heat shock and remained at the nuclear periphery. This was also correlated with no significant change in its association with transcription factories.

qRT-PCR analysis of *ferritin* and *hsp70* genes has also revealed that both are up-regulated following heat shock. However *hsp70* was the most significant with a substantial 443 fold increase in its expression. Although the relocation of *hsp70* gene loci to the nuclear interior and its subsequent increase in expression is in agreement with mammalian models proposing the nuclear interior as a site for transcriptionally active genes (Elcock and Bridger, 2010; Szczerbal *et al.,* 2009; Takizawa *et al.,* 2008b), the up-regulation of the *ferritin* at the nuclear periphery with no migration of the gene loci is in parallel with *Drosophila* and yeast studies (Brown and Silver, 2007). These results further add to the proposal of the snail as a unique model system to study the involvement of different nuclear compartments in genomic regulation at the phylogenetic interface between yeast/*Drosophila* and higher organisms.

The results from this chapter diverge from a previous study analysing the induction of heat shock loci in *Drosophila melanogaster*. The *hsp70* loci were shown to be immobile after heat shock in live cell analysis (Yao *et al*., 2007). Indeed Yao *et al* had observed *de novo* recruitment of RNAP II molecules to *hsp70* genes. In our study, the migration of these gene loci after heat shock has also been confirmed in the intact snail. However, further analysis would be required in the snail to elucidate whether the increased association of *hsp70* gene loci with transcription factories is a result of gene movement or *de novo* formation of these factories. Although there is evidence suggesting that transcription factories are stably maintained (Ferrai *et al.*, 2010; Papantonis, 2010; Mitchell and Fraser, 2008), the conflicting results from live cell studies indicate the necessity of further analysis.

Many studies have correlated gene repositioning with expression and co-localisation (Kang *et al.*, 2011; Szczerbal and Bridger, 2010; Sutherland and Bickmore, 2009; Mitchell and Fraser, 2008; Osborne and Eskiw, 2008; Osborne *et al.*, 2007; Osborne *et al.*, 2004), with a few suggesting actin and myosin dependent relocalisation of activated genes (Bridger, 2011; Chuang *et al.*, 2006). Other studies have also shown that migration of genes can be inhibited using various inhibitors of actin and myosin (Bridger and Mehta, 2011; Mehta *et al.*, 2010; Hu *et al.*, 2008; Chuang *et al.*, 2006).

In an effort to elucidate the purpose and the global of effects of such a motor complex in the nucleus, Bge cells were incubated with an inhibitor of nuclear myosin polymerisation (BDM), pre exposure to heat shock. The results from these experiments have revealed that the repositioning of genes after heat shock is indeed inhibited after BDM treatment in the Bge cells, which has also been confirmed in the snail *B. glabrata*. Moreover, when the expression profiles of *ferritin,* and *hsp70* were analysed by qRT-PCR, both genes were significantly down-regulated in expression. To our knowledge this is the first time the activity of a gene has shown to be manipulated by a nuclear motor activity and also demonstrates the significance of gene positioning in regulating the genome. In the previous chapter gene repositioning prior to changes in expression was revealed. Together with the findings in this chapter, repositioning of gene loci is indicated to be the initial step required prior to a change in expression. Co-localisation with transcription factories and subsequent changes in gene expression may be the steps that follow the initial gene repositioning. Whether the associations are a cause or an effect of gene expression change is yet to be discovered. Additionally, further evidence for the presence of a nuclear motor complex, and its importance in genome regulation has also been provided. Although the effects of BDM treatment on NM1β has clearly been demonstrated by immunofluorescence assay, BDM has a general effect on all cellular myosins. Therefore an siRNA experiment to suppress the levels of nuclear myosin 1β in the snail cells would be a possible experiment for future studies.

In summary, reorganisation of the genome and subsequent changes in expression has been revealed to involve a nuclear motor complex, which the activity of the motor can be constrained and the effects reversed using inhibitors of nuclear motors. This is a fundamental finding in the field of nuclear biology and could aid to bring controls measures for many debilitating diseases. In terms of the snail *B. glabrata* and the schistosomiasis disease it is involved in, these findings will be crucial when developing drugs to eliminate the disease. In this study it has been shown that drugs such as BDM can be used to inhibit gene movement in the intact snail.

Targeting susceptible specific repositioned genes after infection, such as *actin* and *hsp70* (see chapter 3), by an inhibitor of motor complexes, and investigating the effects this would have on the susceptibility of the snails would be plausible experiments for the future.

Chapter 5

General Discussion

The eukaryotic genome is highly organised with chromosome territories and genes occupying non-random locations within an interphase nucleus. This level of organisation is thought to have regulatory roles in the nucleus and is altered upon internal and external stimuli. As well as having a crucial role in cellular processes, alterations in genome organisation have many implications in life threatening diseases and infections (Knight *et al.*, 2011; Meaburn *et al.*, 2009; Li *et al.*, 2009; Meaburn and Misteli, 2008; Zink *et al.,* 2004b; Cremer *et al.*, 2003), one of which is the neglected tropical disease schistosomiasis.

Affecting over 200 million people in 78 countries, schistosomiasis is a major health concern in the tropics and subtropics. The complex life cycle of the causative agent of this disease, the schistosome parasites, has made prevention an extremely challenging goal to achieve. With the discovery that the intermediate host for these parasites, the freshwater snail *B. glabrata*, has varied susceptibility to the *S. mansoni* parasites, hopes were raised for the elimination of the disease via the displacement of susceptible snails with the resistant strains (Newton, 1953). Yet 60 years after this discovery, there still is a lack of an effective prevention scheme for schistosomiasis.

The advances in scientific techniques have lead to major breakthroughs in science. Of these, one of the first that comes to mind is the genome sequencing projects. The success of the human genome project has resulted in the leap to many other important model organisms. Also benefiting from this leap is the freshwater snail *B. glabrata,* now a model organism representing the molluscan phylum. The initiation of the snail genome project has attracted many interests to *B. glabrata* and the schistosomiasis disease, and vital information regarding snail host–parasite relationship are now being progressively revealed. However, with very limited information available on the snail nucleus, my particular interest was to exploit this area of snail-parasite studies, in particular the effects of an *S. mansoni* infection on the resistant and susceptible snail's genome organisation.

Despite the approval of the snail genome project in 2004, *B. glabrata* lacked an approved, complete karyotype. A karyotype is essential in such projects as it enables physical mapping of gene sequences and identification of their locations within the genome. Without this information, knowledge of the snail genome would be incomplete. Therefore to close this gap in the snail studies, the snail chromosomes were investigated (chapter 2). Initially a robust protocol for extracting chromosomes from whole snails was developed. Following the success of this protocol, a G-banded karyotype was constructed for *B. glabrata.* The prominent and distinctive G-bands achieved on these chromosomes enabled the identification of individual snail chromosomes and their homologs, which were organised into groups according their size, and centromere position. From this karyotype the first snail ideograms were also constructed, showing the location of the G-bands on each specific chromosome, which will be an invaluable tool for mapping studies when describing the specific location of genes on these chromosomes.

Having said that the snail karyotype was crucial for mapping studies, there also was a lack of a robust protocol for such studies to be carried out in the snail. Previously a comprehensive technique to map single copy genes to chromosomes from the Bge cell line was described (Odoemelam *et al.*, 2010). However the observed aneuploidy within this cell line shifted the route of *in vitro* snail studies to *in vivo* (Odoemelam *et al.*, 2009). Therefore adaptations to this protocol were required to suit the *in vivo* cells and chromosomes. By manipulating critical steps effecting hybridisation quality, and using state-of-the art technology, four genes were successfully mapped onto *B. glabrata* chromosomes. Therefore along with other model organisms such as humans, mice, pig, and chicken, *B. glabrata* now also has an abundant and robust protocol for routinely mapping of genes. However unlike these organisms, there exists no chromosome paints for *B. glabrata.* The development of whole chromosome paints for the snail is an exciting prospect, as it will add more depth to the characterisation of the chromosomes and the snail genome. It would also allow comparative analysis with other related organisms such as *S. mansoni,* which already has paints developed for its chromosomes (Taguchi *et al.*, 2007).

Mapping of chromosome paints of these organisms onto the genomes of each other would enable the identification of regions of synteny between the host and the parasite. This would certainly be an exciting and interesting project to further exploit the host-parasite relationship.

In this thesis, the relationship between the host snail and its parasite was studied by looking at the effects of an *S. mansoni* infection on individual genes in the *B. glabrata* genome (chapter 3). Differential response of the resistant and susceptible snail genomes to *S. mansoni* infection was observed. Not only is this a crucial finding for identification of factors influencing resistance in the snail to achieve the future goal of displacing susceptible snails for the elimination of the schistosomiasis disease, it is the first that the effects of a parasitic infection on an organisms genome has been shown. Upon infection, certain gene loci occupying non-random positions within the interphase snail nuclei were observed to reposition both towards the nuclear interior and periphery, which was in-conjunction with their up-regulation. It is apparent that the *S. mansoni* parasite is able to induce global changes in the genome of *B. glabrata.* An exciting finding was the repositioning of *actin* gene loci prior to a change in its transcriptional activity, suggesting that such reorganisation may contribute to changes in transcription, rather than being the result of a transcriptional modulation. Future work studying the physical effects of infection on other differentially expressed genes, such as the antioxidant enzyme *BgPrx4,* would further help to build the physical profile of *B. glabrata*'s genome following an infection. Indeed if repositioning of susceptible specific genes can be inhibited, which results in the reversing of this phenotype, this would be an incredible discovery in the field. The prospect of such an achievement would be exhilarating for schistosomiasis studies.

What now remains to be answered is how a parasite can cause such reorganisation in its host's genome. One possible explanation for this is the stress pathway. The presence of a foreign organism is inevitably going to cause a stress response in the host. It is also evident from RNA profiling studies that infection leads to induction of stress related genes such as hsp70.

Taken together, both the stress and the detection of the foreign organism in the host would lead to the initiation of a signalling cascade to alert the host defences. It may well be that one of these signalling pathways involve the activation of nuclear motor complexes resulting in the co-ordinated movement of the genome. However how such signals can be relayed to nuclear targets needs to be investigated. Although the question still remains of whether nuclear reorganisation has a causative role in genomic expression or it is a consequence of modulations in transcriptional activity, the findings presented in chapter 3 of this thesis provides evidence for the former. Indeed, the association of chromatin loops with nuclear bodies involved in transcriptional activities further strengthens the former hypothesis. However with still debates regarding the movement of chromatin to nuclear bodies or the *de novo* formation of these bodies in the field, further research is necessary for a better understating of these processes.

The snail cells were also used to further explore and analyse the dynamic organisation observed in the eukaryotic nucleus (chapter 4). Being a model organism with the availability of a unique cell line, *B. glabrata* is a strong candidate for such studies. Initially nuclear structures in the Bge cell line were identified, which enabled a better understanding of the snail nucleus. Although the presence of only a few of these structures was identified, with the completion of the snail genome project this would most certainly increase. Nuclear structures play a major role in the organisation of the eukaryotic genome. In this thesis, using the snail as a model system, the role of transcription factories in the genome was elucidated. Upon heat shock stimuli, gene loci were shown to co-localise with foci containing RNAP II, and this was in parallel with the up-regulation of gene expression. Using this heat shock system developed with the Bge cell line, the mechanism of gene movement and subsequent effects of its inhibition on the genome was also investigated. One of the exciting theories regarding gene and chromosome movement is the presence of an actin-myosin motor structure within the nucleus.

By using an inhibitor of myosin's (BDM), further evidence for the presence of such a motor complex has been provided. Moreover, when the movement of gene loci was inhibited using this drug, its activity was also manipulated. To our knowledge this is the first time the significance of a nuclear motor complex and gene repositioning in the nucleus has been demonstrated in regulating the genome. Both the functional significance of repositioning of genomic regions as well as the process as to how this relocation occurs is much clearer given the study presented here. This is an exciting and fundamental finding in the fields of nuclear and genome biology as well as medicine, and opens the doors to the initiation of further experiments. If the activity of specific genes can be controlled by inhibiting their movement / interaction with nuclear structures, this would be an ideal target when developing drugs for debilitating diseases such as schistosomiasis.

In summary studies in this thesis has demonstrated that *B. glabrata* can be a mutually beneficial model system for both the fields of schistosomiasis and nuclear biology. Although further research is still essential, the findings in this thesis have hopefully excavated some of the mysteries of the nucleus, as well as providing the stepping stones for the development of new control measures for a tropical disease threatening the lives of millions of people around the globe.

References

Adams, N.M. and Freemont, P.S. (2011) "Advances in Nuclear Architecture".

Adema, C.M., Hertel, L.A., Miller, R.D. and Loker, E.S. (1997) "A family of fibrinogen-related proteins that precipitates parasite-derived molecules is produced by an invertebrate after infection", *Proceedings of the National Academy of Sciences of the United States of America,* vol. **94**, no. 16, pp. 8691-8696.

Adema, C.M., Luo, M.Z., Hanelt, B., Hertel, L.A., Marshall, J.J., Zhang, S.M., DeJong, R.J., Kim, H.R., Kudrna, D., Wing, R.A., Soderlund, C., Knight, M., Lewis, F.A., Caldeira, R.L., Jannotti-Passos, L.K., Carvalho Odos, S. and Loker, E.S. (2006) "A bacterial artificial chromosome library for Biomphalaria glabrata, intermediate snail host of Schistosoma mansoni", *Memorias do Instituto Oswaldo Cruz,* vol. **101** Suppl 1, pp. 167-177.

Alberts, B. (2002) *Molecular biology of the cell,* 4th edn, Garland, New York.

Anderson, R.M., Mercer, J.G., Wilson, R.A., Carter, N.P. (1982) "Transmission of *Schistosoma mansoni* from man to snail: experimental studies of miracidial survival and infectivity in relation to larval age, water temperature, host size and host age", *Parasitology,* vol. **85**, pp. 339-360.

Barboro, P., D'Arrigo, C., Mormino, M., Coradeghini, R., Parodi, S., Patrone, E. and Balbi, C. (2003) "An intranuclear frame for chromatin compartmentalization and higher-order folding", *Journal of cellular biochemistry,* vol. **88**, no. 1, pp. 113-120.

Basch, P.F. and DiConza, J.J. (1977) "In vitro development of Schistosoma mansoni cercariae", *The Journal of parasitology,* vol. **63**, no. 2, pp. 245-249.

Bayani, J. and Squire, J.A. (2004a) "Traditional banding of chromosomes for cytogenetic analysis", Chapter 22.

Bayani, J. and Squire, J.A. (2004b) "Current Protocols in Cell Biology; Traditional Banding of Chromosomes for Cytogenetic Analysis".

Bayne, C.J., Hahn, U.K. and Bender, R.C. (2001) "Mechanisms of molluscan host resistance and of parasite strategies for survival", *Parasitology,* vol. **123** Suppl, pp. S159-67.

Bender, R.C., Broderick, E.J., Goodall, C.P. and Bayne, C.J. (2005) "Respiratory burst of Biomphalaria glabrata hemocytes: Schistosoma mansoni-resistant snails produce more extracellular H2O2 than susceptible snails", *The Journal of parasitology,* vol. **91**, no. 2, pp. 275-279.

Bender, R.C., Goodall, C.P., Blouin, M.S. and Bayne, C.J. (2007) "Variation in expression of Biomphalaria glabrata SOD1: a potential controlling factor in susceptibility/resistance to Schistosoma mansoni", *Developmental and comparative immunology,* vol. **31**, no. 9, pp. 874-878.

Bernal, S.D. and Stahel, R.A. (1985) "Cytoskeleton-associated proteins: their role as cellular integrators in the neoplastic process", *Critical reviews in oncology/hematology,* vol. **3**, no. 3, pp. 191-204.

Bernardi, R. and Pandolfi, P.P. (2007) "Structure, dynamics and functions of promyelocytic leukaemia nuclear bodies", *Nature reviews.Molecular cell biology,* vol. **8**, no. 12, pp. 1006-1016.

Berriman, M., Haas, B.J., LoVerde, P.T., Wilson, R.A., Dillon, G.P., Cerqueira, G.C., Mashiyama, S.T., Al-Lazikani, B., Andrade, L.F., Ashton, P.D., Aslett, M.A., Bartholomeu, D.C., Blandin, G., Caffrey, C.R., Coghlan, A., Coulson, R., Day, T.A., Delcher, A., DeMarco, R., Djikeng, A., Eyre, T., Gamble, J.A., Ghedin, E., Gu, Y., Hertz-Fowler, C., Hirai, H., Hirai, Y., Houston, R., Ivens, A., Johnston, D.A., Lacerda, D., Macedo, C.D., McVeigh, P., Ning, Z., Oliveira, G., Overington, J.P., Parkhill, J., Pertea, M., Pierce, R.J., Protasio, A.V., Quail, M.A., Rajandream, M., Rogers, J., Sajid, M., Salzberg, S.L., Stanke, M., Tivey, A.R., White, O., Williams, D.L., Wortman, J., Wu, W., Zamanian, M., Zerlotini, A., Fraser-Liggett, C.M., Barrell, B.G. and El-Sayed, N.M. (2009) "The genome of the blood fluke Schistosoma mansoni", *Nature,* vol. **460**, no. 7253, pp. 352-358.

Bettinger, B.T., Gilbert, D.M. and Amberg, D.C. (2004) "Actin up in the nucleus", *Nature reviews.Molecular cell biology,* vol. **5**, no. 5, pp. 410-415.

Bg_Initiative. Available at: http://biology.unm.edu/biomphalaria-genome/index.html (Accessed: 7/11/2011).

Bickmore, W.A. and van Steensel, B. (2013) "Genome Architecture: Domain Organization of Interphase Chromosomes", *Cell,* vol. **152**, no. 6, pp. 1270-1284.

Blanchard, T.J. (2004) "Schistosomiasis", *Travel medicine and infectious disease,* vol. **2**, no. 1, pp. 5-11.

Bolzer, A., Kreth, G., Solovei, I., Koehler, D., Saracoglu, K., Fauth, C., Muller, S., Eils, R., Cremer, C., Speicher, M.R. and Cremer, T. (2005) "Three-dimensional maps of all chromosomes in human male fibroblast nuclei and prometaphase rosettes", *PLoS biology,* vol. **3**, no. 5, pp. e157.

Borden, K.L. (2008) "Pondering the puzzle of PML (promyelocytic leukemia) nuclear bodies: can we fit the pieces together using an RNA regulon?", *Biochimica et biophysica acta,* vol. **1783**, no. 11, pp. 2145-2154.

Bourne, G., Moir, C., Bikkul, U., Ahmed, M.H., Kill, I.R., Eskiw, C.H., Tosi, S. and Bridger, J.M. (2013) "Human Interphase Chromosomes; Interphase Chromosome Behavior in Normal and Diseased Cells", pp. 9-33.

Boveri, T. (1909) "Die Blastomerenkerne von*Ascaris megalocephala* und die Theorie der Chromosomenindividualitat", *Arch Zellforsch,* vol. **3**, pp. 181-268.

Boyle, S., Gilchrist, S., Bridger, J.M., Mahy, N.L., Ellis, J.A. and Bickmore, W.A. (2001) "The spatial organization of human chromosomes within the nuclei of normal and emerin-mutant cells", *Human molecular genetics,* vol. **10**, no. 3, pp. 211-219.

Brickner, J.H. and Walter, P. (2004) "Gene Recruitment of the Activated INO1 Locus to the Nuclear Membrane", *PLoS Biology,* vol. **2**, no. 11, pp. e342.

Bridger, J.M. (2011) "Chromobility: the rapid movement of chromosomes in interphase nuclei", *Biochemical Society transactions,* vol. **39**, no. 6, pp. 1747-1751.

Bridger, J.M. and Bickmore, W.A. (1998) "Putting the genome on the map", *Trends in genetics : TIG,* vol. 14, no. 10, pp. 403-409.

Bridger, J.M., Boyle, S., Kill, I.R. and Bickmore, W.A. (2000) "Re-modelling of nuclear architecture in quiescent and senescent human fibroblasts", *Current biology : CB,* vol. **10**, no. 3, pp. 149-152.

Bridger, J.M., Kill, I.R., O'Farrell, M. and Hutchison, C.J. (1993) "Internal lamin structures within G1 nuclei of human dermal fibroblasts", *Journal of cell science,* vol. **104**, no. Pt 2, pp. 297-306.

Bridger, J.M. and Mehta, I.S. (2011) "Advances in Nuclear Architecture; Nuclear Molecular Motors for Active, Directed Chromatin Movement in Interphase Nuclei", pp. 149-172.

Brown, C.R., Kennedy, C.J., Delmar, V.A., Forbes, D.J. and Silver, P.A. (2008a) "Global histone acetylation induces functional genomic reorganization at mammalian nuclear pore complexes", *Genes & development,* vol. **22**, no. 5, pp. 627-639.

Brown, C.R. and Silver, P.A. (2007) "Transcriptional regulation at the nuclear pore complex", *Current opinion in genetics & development,* vol. **17**, no. 2, pp. 100-106.

Brown, J.M., Green, J., das Neves, R.P., Wallace, H.A.C., Smith, A.J.H., Hughes, J., Gray, N., Taylor, S., Wood, W.G., Higgs, D.R., Iborra, F.J. and Buckle, V.J. (2008b) "Association between active genes occurs at nuclear speckles and is modulated by chromatin environment", *The Journal of cell biology,* vol. **182**, no. 6, pp. 1083-1097.

Brown, J.M., Leach, J., Reittie, J.E., Atzberger, A., Lee-Prudhoe, J., Wood, W.G., Higgs, D.R., Iborra, F.J. and Buckle, V.J. (2006) "Coregulated human globin genes are frequently in spatial proximity when active", *The Journal of cell biology,* vol. **172**, no. 2, pp. 177-187.

Brown, K.E., Baxter, J., Graf, D., Merkenschlager, M. and Fisher, A.G. (1999) "Dynamic repositioning of genes in the nucleus of lymphocytes preparing for cell division", *Molecular cell,* vol. **3**, no. 2, pp. 207-217.

Brown, K.E., Guest, S.S., Smale, S.T., Hahm, K., Merkenschlager, M. and Fisher, A.G. (1997) "Association of transcriptionally silent genes with Ikaros complexes at centromeric heterochromatin", *Cell,* vol. **91**, no. 6, pp. 845-854.

Burch, J.B. (1960) "Chromosome numbers of schistosome vector snails", *Zeitschrift fur Tropenmedizin und Parasitologie,* vol. **11**, pp. 442-449.

Burke, B. and Gerace, L. (1986) "A cell free system to study reassembly of the nuclear envelope at the end of mitosis", *Cell,* vol. **44**, no. 4, pp. 639-652.

Bystricky, K., Laroche, T., van Houwe, G., Blaszczyk, M. and Gasser, S.M. (2005) "Chromosome looping in yeast: telomere pairing and coordinated movement reflect anchoring efficiency and territorial organization", *The Journal of cell biology,* vol. 1**68**, no. 3, pp. 375-387.

Casolari, J.M., Brown, C.R., Drubin, D.A., Rando, O.J. and Silver, P.A. (2005) "Developmentally induced changes in transcriptional program alter spatial organization across chromosomes", *Genes & development,* vol. **19**, no. 10, pp. 1188-1198.

Casolari, J.M., Brown, C.R., Komili, S., West, J., Hieronymus, H. and Silver, P.A. (2004) "Genome-wide localization of the nuclear transport machinery couples transcriptional status and nuclear organization", *Cell,* vol. **117**, no. 4, pp. 427-439.

Castillo, M.G. and Yoshino, T.P. (2002) "Carbohydrate inhibition of Biomphalaria glabrata embryonic (Bge) cell adhesion to primary sporocysts of Schistosoma mansoni", *Parasitology,* vol. **125**, no. Pt 6, pp. 513-525.

Chambeyron, S. and Bickmore, W.A. (2004) "Chromatin decondensation and nuclear reorganization of the HoxB locus upon induction of transcription", *Genes & development,* vol. **18**, no. 10, pp. 1119-1130.

Chambeyron, S., Da Silva, N.R., Lawson, K.A. and Bickmore, W.A. (2005) "Nuclear re-organisation of the Hoxb complex during mouse embryonic development", *Development (Cambridge, England),* vol. **132**, no. 9, pp. 2215-2223.

Cheever, A.W., Lenzi, J.A., Lenzi, H.L. and Andrade, Z.A. (2002) "Experimental models of Schistosoma mansoni infection", *Memorias do Instituto Oswaldo Cruz,* vol. **97**, no. 7, pp. 917-940.

Chuang, C.H., Carpenter, A.E., Fuchsova, B., Johnson, T., de Lanerolle, P. and Belmont, A.S. (2006) "Long-range directional movement of an interphase chromosome site", *Current biology : CB,* vol. **16**, no. 8, pp. 825-831.

Coluccio, L.M. (2007) *Myosins: A Superfamily of Molecular Motors (Proteins and Cell Regulation) (Proteins and Cell Regulation),* Springer.

Cook, G.C. and Zumla, A.I. (2003) *Manson's Tropical Diseases: Expert Consult,* Saunders Ltd.

Couturier-Turpin, M.H., Couturier, D., Nepveux, P., Louvel, A., Chapuis, Y. and Guerre, J. (1982) "Human chromosome analysis in 24 cases of primary carcinoma of the large intestine: contribution of the G-banding technique", *British journal of cancer,* vol. **46**, no. 6, pp. 856-869.

Cremer, C., Zorn, C. and Cremer, T. (1974) "An ultraviolet laser microbeam for 257 nm", *Microscopica acta,* vol. 75, no. 4, pp. 331-337.

Cremer, M., Kupper, K., Wagler, B., Wizelman, L., von Hase, J., Weiland, Y., Kreja, L., Diebold, J., Speicher, M.R. and Cremer, T. (2003) "Inheritance of gene density-related higher order chromatin arrangements in normal and tumor cell nuclei", *The Journal of cell biology,* vol. **162**, no. 5, pp. 809-820.

Cremer, M., von Hase, J., Volm, T., Brero, A., Kreth, G., Walter, J., Fischer, C., Solovei, I., Cremer, C. and Cremer, T. (2001) "Non-random radial higher-order chromatin arrangements in nuclei of diploid human cells", *Chromosome research : an international journal on the molecular, supramolecular and evolutionary aspects of chromosome biology,* vol. **9**, no. 7, pp. 541-567.

Cremer, T. and Cremer, C. (2006a) "Rise, fall and resurrection of chromosome territories: a historical perspective. Part I. The rise of chromosome territories", *European journal of histochemistry : EJH,* vol. **50**, no. 3, pp. 161-176.

Cremer, T. and Cremer, C. (2006b) "Rise, fall and resurrection of chromosome territories: a historical perspective. Part II. Fall and resurrection of chromosome territories during the 1950s to 1980s. Part III. Chromosome territories and the functional nuclear architecture: experiments and models from the 1990s to the present", *European journal of histochemistry : EJH,* vol. **50**, no. 4, pp. 223-272.

Cremer, T. and Cremer, C. (2001) "Chromosome territories, nuclear architecture and gene regulation in mammalian cells", *Nature reviews.Genetics,* vol. **2**, no. 4, pp. 292-301.

Croft, J.A., Bridger, J.M., Boyle, S., Perry, P., Teague, P. and Bickmore, W.A. (1999) "Differences in the localization and morphology of chromosomes in the human nucleus", *The Journal of cell biology,* vol. **145**, no. 6, pp. 1119-1131.

Dalzell, P., Miles, L.G., Isberg, S.R., Glenn, T.C., King, C., Murtagh, V. and Moran, C. (2009) "Standardized reference ideogram for physical mapping in the saltwater crocodile (Crocodylus porosus)", *Cytogenetic and genome research,* vol. **127**, no. 2-4, pp. 204-212.

Damian, R.T. (1989) "Molecular mimicry: parasite evasion and host defense", *Current topics in microbiology and immunology,* vol. **145**, pp. 101-115.

DeJong, R.J., Emery, A.M. and Adema, C.M. (2004) "The mitochondrial genome of Biomphalaria glabrata (Gastropoda: Basommatophora), intermediate host of Schistosoma mansoni", *The Journal of parasitology,* vol. **90**, no. 5, pp. 991-997.

Deng, W., Lee, J., Wang, H., Miller, J., Reik, A., Gregory, P.D., Dean, A. and Blobel, G.A. (2012) "Controlling long-range genomic interactions at a native locus by targeted tethering of a looping factor", *Cell,* vol. **149**, no. 6, pp. 1233-1244.

Deniaud, E. and Bickmore, W.A. (2009) "Transcription and the nuclear periphery: edge of darkness?", *Current opinion in genetics & development,* vol. **19**, no. 2, pp. 187-191.

Dhar, S.S., Ongwijitwat, S. and Wong-Riley, M.T.T. (2009) "Chromosome Conformation Capture of All 13 Genomic Loci in the Transcriptional Regulation of the Multisubunit Bigenomic Cytochrome c Oxidase in Neurons", *Journal of Biological Chemistry,* vol. **284**, no. 28, pp. 18644-18650.

Dissous, C., Grzych, J.M. and Capron, A. (1986) "Schistosoma mansoni shares a protective oligosaccharide epitope with freshwater and marine snails", *Nature,* vol. **323**, no. 6087, pp. 443-445.

Doenhoff, M.J., Kusel, J.R., Coles, G.C. and Cioli, D. (2002) "Resistance of Schistosoma mansoni to praziquantel: is there a problem?", *Transactions of the Royal Society of Tropical Medicine and Hygiene,* vol. **96**, no. 5, pp. 465-469.

Dong, F. and Jiang, J. (1998) "Non-Rabl patterns of centromere and telomere distribution in the interphase nuclei of plant cells", *Chromosome research : an international journal on the molecular, supramolecular and evolutionary aspects of chromosome biology,* vol. **6**, no. 7, pp. 551-558.

Dundr, M., Ospina, J.K., Sung, M.H., John, S., Upender, M., Ried, T., Hager, G.L. and Matera, A.G. (2007) "Actin-dependent intranuclear repositioning of an active gene locus in vivo", *The Journal of cell biology,* vol. **179**, no. 6, pp. 1095-1103.

Duraisingh, M.T., Voss, T.S., Marty, A.J., Duffy, M.F., Good, R.T., Thompson, J.K., Freitas-Junior, L.H., Scherf, A., Crabb, B.S. and Cowman, A.F. (2005) "Heterochromatin silencing and locus repositioning linked to regulation of virulence genes in Plasmodium falciparum", *Cell,* vol. **121**, no. 1, pp. 13-24.

Edelman, L.B. and Fraser, P. (2012) "Transcription factories: genetic programming in three dimensions", *Current opinion in genetics & development,* vol. **22**, no. 2, pp. 110-114.

Elcock, L.S. and Bridger, J.M. (2010) "Exploring the relationship between interphase gene positioning, transcriptional regulation and the nuclear matrix", *Biochemical Society transactions,* vol. **38**, no. Pt 1, pp. 263-267.

Ellegren, H. (2011) "Sex-chromosome evolution: recent progress and the influence of male and female heterogamety", *Nature reviews.Genetics,* vol. **12**, no. 3, pp. 157-166.

Eskiw, C.H., Cope, N.F., Clay, I., Schoenfelder, S., Nagano, T. and Fraser, P. (2010) "Transcription factories and nuclear organization of the genome", *Cold Spring Harbor symposia on quantitative biology,* vol. **75**, pp. 501-506.

Eskiw, C.H., Dellaire, G. and Bazett-Jones, D.P. (2004) "Chromatin contributes to structural integrity of promyelocytic leukemia bodies through a SUMO-1-independent mechanism", *The Journal of biological chemistry,* vol. **279**, no. 10, pp. 9577-9585.

Eskiw, C.H., Dellaire, G., Mymryk, J.S. and Bazett-Jones, D.P. (2003) "Size, position and dynamic behavior of PML nuclear bodies following cell stress as a paradigm for supramolecular trafficking and assembly", *Journal of cell science,* vol. **116**, no. Pt 21, pp. 4455-4466.

Everett, R.D. and Chelbi-Alix, M.K. (2007) "PML and PML nuclear bodies: implications in antiviral defence", *Biochimie,* vol. **89**, no. 6-7, pp. 819-830.

Federico, C., Saccone, S., Andreozzi, L., Motta, S., Russo, V., Carels, N. and Bernardi, G. (2004) "The pig genome: compositional analysis and identification of the gene-richest regions in chromosomes and nuclei", *Gene,* vol. **343**, no. 2, pp. 245-251.

Ferrai, C., Xie, S.Q., Luraghi, P., Munari, D., Ramirez, F., Branco, M.R., Pombo, A. and Crippa, M.P. (2010) "Poised transcription factories prime silent uPA gene prior to activation", *PLoS biology,* vol. **8**, no. 1, pp. e1000270.

Ferreira, J., Paolella, G., Ramos, C. and Lamond, A.I. (1997) "Spatial organization of large-scale chromatin domains in the nucleus: a magnified view of single chromosome territories", *The Journal of cell biology,* vol. **139**, no. 7, pp. 1597-1610.

Fomproix, N. and Percipalle, P. (2004) "An actin-myosin complex on actively transcribing genes", *Exp.Cell Res,* vol. **294**, no. 1, pp. 140-148.

Foster, H.A., Abeydeera, L.R., Griffin, D.K. and Bridger, J.M. (2005) "Non-random chromosome positioning in mammalian sperm nuclei, with migration of the sex chromosomes during late spermatogenesis", *Journal of cell science,* vol. **118**, no. Pt 9, pp. 1811-1820.

Foster, H.A. and Bridger, J.M. (2005) "The genome and the nucleus: a marriage made by evolution. Genome organisation and nuclear architecture", *Chromosoma,* vol. **114**, no. 4, pp. 212-229.

Foster, H., Griffin, D. and Bridger, J. (2012) "Interphase chromosome positioning in in vitro porcine cells and ex vivo porcine tissues", *BMC Cell Biology,* pp. 30.

Fraga de Azevedo, J. and Goncalves, M.M. (1956) "Ensaios sobre o estudo da numeracao cromosomica de algumas especies de moluscos de agua doce", *An. Inst. Med. Trpo.* vol. **13**, no. 4, pp. 569-577.

Francke, U. and Oliver, N. (1978) "Quantitative analysis of high-resolution trypsin-giemsa bands on human prometaphase chromosomes", *Human genetics,* vol. **45**, no. 2, pp. 137-165.

Fraser, P. and Bickmore, W. (2007) "Nuclear organization of the genome and the potential for gene regulation", *Nature,* vol. **447**, no. 7143, pp. 413-417.

Frey, M.R., Bailey, A.D., Weiner, A.M. and Gregory Matera, A. (1999) "Association of snRNA genes with coiled bodies is mediated by nascent snRNA transcripts", *Current Biology,* vol. **9**, no. 3, pp. 126-136.

Galinier, R. (2013) "Biomphalysin, a New ß Pore-forming Toxin Involved in Biomphalaria glabrata Immune Defense against Schistosoma mansoni", *Pathogens*.

Gall, J.G. (2003) "The centennial of the Cajal body", *Nature reviews.Molecular cell biology,* vol. **4**, no. 12, pp. 975-980.

Gall, J.G. and Pardue, M.L. (1969) "Formation and detection of RNA-DNA hybrid molecules in cytological preparations", *Proceedings of the National Academy of Sciences of the United States of America,* vol. **63**, no. 2, pp. 378-383.

Garcia, A.B. (2010) "Involvement of the Cytokine MIF in the Snail Host Immune Response to the Parasite Schistosoma mansoni", *Pathogens*.

Gardner, R.J.M., Sutherland, G.R. and Shaffer, L.G. (2011) "Chromosome Abnormalities and Genetic Counseling".

Garimberti, E. and Tosi, S. (2010) "Fluorescence in situ Hybridization (FISH), Basic Principles and Methodology", *Methods in molecular biology (Clifton, N.J.),* vol. **659**, pp. 3-20.

Genome: Biomphalaria glabrata *Genome: Biomphalaria glabrata*. Available at: http://genome.wustl.edu/genomes/detail/biomphalaria-glabrata/ (Accessed: 4/26/2013 2013).

Geyer, P.K., Vitalini, M.W. and Wallrath, L.L. (2011) "Nuclear organization: taking a position on gene expression", *Current opinion in cell biology*.

Goldman, M.A. (1983) "Nucleolar organizer regions in Biomphalaria and Bulinus snails", *Experientia,* vol. **39**, no. 8, pp. 911.

Goldman, A.E., Moir, R.D., Montag-Lowy, M., Stewart, M. and Goldman, R.D. (1992) "Pathway of incorporation of microinjected lamin A into the nuclear envelope", *The Journal of cell biology,* vol. **119**, no. 4, pp. 725-735.

Goldman, M.A., Loverde, P.T., Chrisman, C.L. and Franklin, D.A. (1984) "Chromosomal Evolution in Planorbid Snails of the Genera Bulinus and Biomphalaria", *Malacologia,* vol. **25**, no. 2, pp. 427-446.

Goldman, R.D., Gruenbaum, Y., Moir, R.D., Shumaker, D.K. and Spann, T.P. (2002) "Nuclear lamins: building blocks of nuclear architecture", *Genes & development,* vol. **16**, no. 5, pp. 533-547.

Gondor, A. and Ohlsson, R. (2009) "Chromosome crosstalk in three dimensions", *Nature,* vol. **461**, no. 7261, pp. 212-217.

Gonsior, S., Platz, S., Buchmeier, S., Scheer, U., Jockusch, B. and Hinssen, H. (1999) "Conformational difference between nuclear and cytoplasmic actin as detected by a monoclonal antobidy", *J.Cell.Sci.,* vol. **112**, pp. 797-809.

Goodall, C.P., Bender, R.C., Broderick, E.J. and Bayne, C.J. (2004) "Constitutive differences in Cu/Zn superoxide dismutase mRNA levels and activity in hemocytes of Biomphalaria glabrata (Mollusca) that are either susceptible or resistant to Schistosoma mansoni (Trematoda)", *Molecular and biochemical parasitology,* vol. **137**, no. 2, pp. 321-328.

Goodall, C.P., Bender, R.C., Brooks, J.K. and Bayne, C.J. (2006) "Biomphalaria glabrata cytosolic copper/zinc superoxide dismutase (SOD1) gene: association of SOD1 alleles with resistance/susceptibility to Schistosoma mansoni", *Molecular and biochemical parasitology,* vol. **147**, no. 2, pp. 207-210.

Green, E.M., Jiang, Y., Joyner, R. and Weis, K. (2012) "A negative feedback loop at the nuclear periphery regulates GAL gene expression", *Molecular biology of the cell,* vol. **23**, no. 7, pp. 1367-1375.

Grevelding, C.G. (2004) "Schistosoma", *Current biology : CB,* vol. **14**, no. 14, pp. R545.

Gryseels, B., Polman, K., Clerinx, J. and Kestens, L. (2006) "Human schistosomiasis", *The Lancet,* vol. **368**, no. 9541, pp. 1106-1118.

Guelen, L., Pagie, L., Brasset, E., Meuleman, W., Faza, M.B., Talhout, W., Eussen, B.H., de Klein, A., Wessels, L., de Laat, W. and van Steensel, B. (2008) "Domain organization of human chromosomes revealed by mapping of nuclear lamina interactions", *Nature,* vol. **453**, no. 7197, pp. 948-951.

Habermann, F.A., Cremer, M., Walter, J., Kreth, G., von Hase, J., Bauer, K., Wienberg, J., Cremer, C., Cremer, T. and Solovei, I. (2001) "Arrangements of macro- and microchromosomes in chicken cells", *Chromosome research : an international journal on the molecular, supramolecular and evolutionary aspects of chromosome biology,* vol. **9**, no. 7, pp. 569-584.

Hagen, S.J., Kiehart, D.P., Kaiser, D.A. and Pollard, T.D. (1986) "Characterization of monoclonal antibodies to Acanthamoeba myosin-I that cross-react with both myosin-II and low molecular mass nuclear proteins", *J.Cell Biol.,* vol. **103**, no. 6, pp. 2121-2128.

Haines, J.L., Korf, B.R., Morton, C.C., Seidman, C.E., Seidman, J.G. and Smith, D.R. (2001) "Current Protocols in Human Genetics".

Handwerger, K.E. and Gall, J.G. (2006) "Subnuclear organelles: new insights into form and function", *Trends in cell biology,* vol. **16**, no. 1, pp. 19-26.

Hanelt, B., Lun, C.M. and Adema, C.M. (2008) "Comparative ORESTES-sampling of transcriptomes of immune-challenged Biomphalaria glabrata snails", *Journal of invertebrate pathology,* vol. **99**, no. 2, pp. 192-203.

Hanington, P.C., Forys, M.A. and Loker, E.S. (2012) "A Somatically Diversified Defense Factor, FREP3, Is a Determinant of Snail Resistance to Schistosome Infection", *PLoS neglected tropical diseases,* vol. **6**, no. 3, pp. e1591.

Hanington, P.C., Lun, C.M., Adema, C.M. and Loker, E.S. (2010) "Time series analysis of the transcriptional responses of Biomphalaria glabrata throughout the course of intramolluscan development of Schistosoma mansoni and Echinostoma paraensei", *International journal for parasitology,* vol. **40**, no. 7, pp. 819-831.

Hansen, E.L. (1979) "Initiating a cell line from embryos of the snail*Biomphalaria glabrata*", *Method in Cell Science,* vol. **5**, no. 1, pp. 1009-1014.

Harris, H. (1999) *The birth of the cell,* Yale University Press, New Haven, Conn; London.

Hartman, M.A. and Spudich, J.A. (2012) "The myosin superfamily at a glance", *J.Cell.Sci,* vol. **125**, no. 7, pp. 1627-1632.

Helleberg, M. and Thybo, S. (2010) "High rate of failure in treatment of imported schistosomiasis", *Journal of travel medicine,* vol. **17**, no. 2, pp. 94-99.

Herman, R.K. (2005) "Introduction to sex determination", *WormBook,* The *C. elegans* research community.

Hertel, L.A., Adema, C.M. and Loker, E.S. (2005) "Differential expression of FREP genes in two strains of Biomphalaria glabrata following exposure to the digenetic trematodes Schistosoma mansoni and Echinostoma paraensei", *Developmental and comparative immunology,* vol. **29**, no. 4, pp. 295-303.

Hewitt, S.L., High, F.A., Reiner, S.L., Fisher, A.G. and Merkenschlager, M. (2004) "Nuclear repositioning marks the selective exclusion of lineage-inappropriate transcription factor loci during T helper cell differentiation", *European journal of immunology,* vol. **34**, no. 12, pp. 3604-3613.

Hodgkin, J. (1987) "Primary sex determination in the nematode *C. elegans*" *Development,* pp. 5-17.

Hoffmann, K.F. and Dunne, D.W. (2003) "Characterization of the Schistosoma transcriptome opens up the world of helminth genomics", *Genome biology,* vol. **5**, no. 1, pp. 203.

Hofmann, W.A., Johnson, T., Klapczynski, M., Fan, J.L. and de Lanerolle, P. (2006) "From transcription to transport: emerging roles for nuclear myosin I", *Biochemistry and cell biology = Biochimie et biologie cellulaire,* vol. **84**, no. 4, pp. 418-426.

Holwerda, S. and de Laat, W. (2012) "Chromatin loops, gene positioning, and gene expression", *Frontiers in genetics,* vol. **3**, pp. 217.

Hozak, P., Sasseville, A.M., Raymond, Y. and Cook, P.R. (1995) "Lamin proteins form an internal nucleoskeleton as well as a peripheral lamina in human cells", *Journal of cell science,* vol. **108**, no. Pt 2, pp. 635-644.

Hu, Q., Kwon, Y.S., Nunez, E., Cardamone, M.D., Hutt, K.R., Ohgi, K.A., Garcia-Bassets, I., Rose, D.W., Glass, C.K., Rosenfeld, M.G. and Fu, X.D. (2008) "Enhancing nuclear receptor-induced transcription requires nuclear motor and LSD1-dependent gene networking in interchromatin granules", *Proceedings of the National Academy of Sciences of the United States of America,* vol. **105**, no. 49, pp. 19199-19204.

Hu, Y., Kireev, I., Plutz, M., Ashourian, N. and Belmont, A.S. (2009) "Large-scale chromatin structure of inducible genes: transcription on a condensed, linear template", *The Journal of cell biology,* vol. **185**, no. 1, pp. 87-100.

Humphries, J.E. (2003) "Cellular Receptors and Signal Transduction in Molluscan Hemocytes: Connections with the Innate Immune System of Vertebrates", *Integrative and Comparative Biology,* vol. **43**, no. 2, pp. 305-312.

Humphries, J.E. and Yoshino, T.P. (2008) "Regulation of hydrogen peroxide release in circulating hemocytes of the planorbid snail Biomphalaria glabrata", *Developmental and comparative immunology,* vol. **32**, no. 5, pp. 554-562.

Iborra, F.J., Pombo, A., Jackson, D.A. and Cook, P.R. (1996) "Active RNA polymerases are localized within discrete transcription "factories' in human nuclei", *Journal of cell science,* vol. **109**, no. Pt 6, pp. 1427-1436.

Ittiprasert, W. and Knight, M. (2012) "Reversing the resistance phenotype of the Biomphalaria glabrata snail host Schistosoma mansoni infection by temperature modulation", *PLoS pathogens,* vol. **8**, no. 4, pp. e1002677.

Ittiprasert, W., Miller, A., Myers, J., Nene, V., El-Sayed, N.M. and Knight, M. (2010) "Identification of immediate response genes dominantly expressed in juvenile resistant and susceptible Biomphalaria glabrata snails upon exposure to Schistosoma mansoni", *Molecular and biochemical parasitology,* vol. 169, no. **1**, pp. 27-39.

Ittiprasert, W., Nene, R., Miller, A., Raghavan, N., Lewis, F., Hodgson, J. and Knight, M. (2009) "Schistosoma mansoni infection of juvenile Biomphalaria glabrata induces a differential stress response between resistant and susceptible snails", *Experimental parasitology,* vol. **123**, no. 3, pp. 203-211.

Jackson, D.A., Hassan, A.B., Errington, R.J. and Cook, P.R. (1993) "Visualization of focal sites of transcription within human nuclei", *The EMBO journal,* vol. **12**, no. 3, pp. 1059-1065.

Jeong, K.H., Lie, K.j., Heyneman, D. (1983) "The ultrastructure of the amebocyte-producing organ in *Biompgalaria glabrata*" *Developmental and comparative immunology* , vol. **7**, no. 2, pp. 217-228.

Jin, S., Xu, R., Wei, Y. and Goodwin, P.H. (1999) "Increased expression of a plant actin gene during a biotrophic interaction between round-leaved mallow, Malva pusilla, and Colletotrichum gloeosporioides f. sp. malvae", *Planta,* vol. **209**, no. 4, pp. 487-494.

Jockusch, B.M., Schoenenberger, C.A., Stetefeld, J. and Aebi, U. (2006) "Tracking down the different forms of nuclear actin", *Trends Cell Biol.,* vol. **16**, no. 8, pp. 391-396.

Kang, J., Xu, B., Yao, Y., Lin, W., Hennessy, C., Fraser, P. and Feng, J. (2011) "A dynamical model reveals gene co-localizations in nucleus", *PLoS computational biology,* vol. **7**, no. 7, pp. e1002094.

Kawano, T., Simoes, L.C.G. and Foresti de Almeida Toledo, L. (1987) "Nucleolar oganizer regions in three species of the genus*Bimophalaria* (mollusca, gastropoda)", *Brazillian journal of genetics,* vol. **4**, pp. 695-707.

Kim, S.H., McQueen, P.G., Lichtman, M.K., Shevach, E.M., Parada, L.A. and Misteli, T. (2004) "Spatial genome organization during T-cell differentiation", *Cytogenetic and genome research,* vol. **105**, no. 2-4, pp. 292-301.

King, C.H., Sturrock, R.F., Kariuki, H.C. and Hamburger, J. (2006) "Transmission control for schistosomiasis - why it matters now", *Trends in parasitology,* vol. **22**, no. 12, pp. 575-582.

Knight, M., Adema, C.M., Raghavan, N., Loker, E.S., Lewis, F.A. and Tettelin, H. (2002) "Obtaining the genome sequence of the mollusc Biomphalaria glabrata: a major intermediate host for the parasite causing human schistosomiasis", *Biomedical Research Institute (BRI)*.

Knight, M., Ittiprasert, W., Odoemelam, E.C., Adema, C.M., Miller, A., Raghavan, N. and Bridger, J.M. (2011a) "Non-random organization of the Biomphalaria glabrata genome in interphase Bge cells and the spatial repositioning of activated genes in cells co-cultured with Schistosoma mansoni", *International journal for parasitology,* vol. **41**, no. 1, pp. 61-70.

Knight, M., Miller, A., Liu, Y., Scaria, P., Woodle, M. and Ittiprasert, W. (2011b) "Polyethyleneimine (PEI) Mediated siRNA Gene Silencing in the Schistosoma mansoni Snail Host, Biomphalaria glabrata", *PLoS neglected tropical diseases,* vol. **5**, no. 7, pp. e1212.

Knight, M., Miller, A.N., Patterson, C.N., Rowe, C.G., Michaels, G., Carr, D., Richards, C.S. and Lewis, F.A. (1999) "The identification of markers segregating with resistance to Schistosoma mansoni infection in the snail Biomphalaria glabrata", *Proceedings of the National Academy of Sciences of the United States of America,* vol. **96**, no. 4, pp. 1510-1515.

Knight, M., Raghavan, N., Goodall, C., Cousin, C., Ittiprasert, W., Sayed, A., Miller, A., Williams, D.L. and Bayne, C.J. (2009) "Biomphalaria glabrata peroxiredoxin: Effect of Schistosoma mansoni infection on differential gene regulation", *Molecular and biochemical parasitology,* vol. **167**, no. 1, pp. 20-31.

Kumar, P.P., Bischof, O., Purbey, P.K., Notani, D., Urlaub, H., Dejean, A. and Galande, S. (2007) "Functional interaction between PML and SATB1 regulates chromatin-loop architecture and transcription of the MHC class I locus", *Nature cell biology,* vol. **9**, no. 1, pp. 45-56.

Kumaran, R.I. and Spector, D.L. (2008) "A genetic locus targeted to the nuclear periphery in living cells maintains its transcriptional competence", *The Journal of cell biology,* vol. **180**, no. 1, pp. 51-65.

Lamond, A.I. and Spector, D.L. (2003) "Nuclear speckles: a model for nuclear organelles", *Nature reviews. Molecular cell biology,* vol. **4**, no. 8, pp. 605-612.

Lane, N. (1969) "Intranuclear fibrillar bodies in actinomycin D-treated oocytes", *J.Cell Biology,* no. 40, pp. 286-291.

Langer, P.R., Waldrop, A.A. and Ward, D.C. (1981) "Enzymatic synthesis of biotin-labeled polynucleotides: novel nucleic acid affinity probes", *Proceedings of the National Academy of Sciences of the United States of America,* vol. **78**, no. 11, pp. 6633-6637.

Laursen, J.R., di Liu, H., Wu, X.J. and Yoshino, T.P. (1997) "Heat-shock response in a molluscan cell line: characterization of the response and cloning of an inducible HSP70 cDNA", *Journal of invertebrate pathology,* vol. **70**, no. 3, pp. 226-233.

Lehr, T., Frank, S., Natsuka, S., Geyer, H., Beuerlein, K., Doenhoff, M.J., Hase, S. and Geyer, R. (2010) "N-Glycosylation patterns of hemolymph glycoproteins from Biomphalaria glabrata strains expressing different susceptibility to Schistosoma mansoni infection", *Experimental parasitology,* vol. **126**, no. 4, pp. 592-602.

Lewis, F.A., Stirewalt, M.A., Souza, C.P. and Gazzinelli, G. (1986) "Large-scale laboratory maintenance of Schistosoma mansoni, with observations on three schistosome/snail host combinations", *The Journal of parasitology,* vol. **72**, no. 6, pp. 813-829.

Li, C., Shi, Z., Zhang, L., Huang, Y., Liu, A., Jin, Y., Yu, Y., Bai, J., Chen, D., Gendron, C., Liu, X. and Fu, S. (2009) "Dynamic changes of territories 17 and 18 during EBV-infection of human lymphocytes", *Molecular biology reports,* vol. **37**, no. 5, pp. 2347-2354.

Lindquist, S. (1986) "The heat-shock response", *Annual Review of Biochemistry,* vol. **55**, pp. 1151-1191.

Lindquist, S. and Craig, E.A. (1988) "The heat-shock proteins", *Annual Review of Genetics,* vol. **22**, pp. 631-677.

Liu, J.L., Murphy, C., Buszczak, M., Clatterbuck, S., Goodman, R. and Gall, J.G. (2006) "The Drosophila melanogaster Cajal body", *The Journal of cell biology,* vol. **172**, no. 6, pp. 875-884.

Livak, K.J. and Schmittgen, T.D. (2001) "Analysis of relative gene expression data using real-time quantitative PCR and the 2(-Delta Delta C(T)) Method", *Methods (San Diego, Calif.),* vol. **25**, no. 4, pp. 402-408.

Lockyer, A.E., Emery, A.M., Kane, R.A., Walker, A.J., Mayer, C.D., Mitta, G., Coustau, C., Adema, C.M., Hanelt, B., Rollinson, D., Noble, L.R. and Jones, C.S. (2012) "Early differential gene expression in haemocytes from resistant and susceptible Biomphalaria glabrata strains in response to Schistosoma mansoni", *PloS one,* vol. **7**, no. 12, pp. e51102.

Lockyer, A.E., Noble, L.R., Rollinson, D. and Jones, C.S. (2004) "Schistosoma mansoni: resistant specific infection-induced gene expression in Biomphalaria glabrata identified by fluorescent-based differential display", *Experimental parasitology,* vol. **107**, no. 1-2, pp. 97-104.

Lockyer, A.E., Spinks, J., Kane, R.A., Hoffmann, K.F., Fitzpatrick, J.M., Rollinson, D., Noble, L.R. and Jones, C.S. (2008) "Biomphalaria glabrata transcriptome: cDNA microarray profiling identifies resistant- and susceptible-specific gene expression in haemocytes from snail strains exposed to Schistosoma mansoni", *BMC genomics,* vol. **9**, pp. 634.

Lockyer, A.E., Spinks, J., Noble, L.R., Rollinson, D. and Jones, C.S. (2007) "Identification of genes involved in interactions between Biomphalaria glabrata and Schistosoma mansoni by suppression subtractive hybridization", *Molecular and biochemical parasitology,* vol. **151**, no. 1, pp. 18-27.

Lyons, N.F., Green, C.R., Gordon, D.H. and Walters, C.R. (1977) "G-banding chromosome analysis of Praomys natalensis (Smith) (Rodentia muridae) from Rhodesia", *Heredity,* vol. **38**, no. 2, pp. 197-200.

Manuelidis, L. and Borden, J. (1988) "Reproducible compartmentalization of individual chromosome domains in human CNS cells revealed by in situ hybridization and three-dimensional reconstruction", *Chromosoma,* vol. **96**, no. 6, pp. 397-410.

Marshall, W.F., Dernburg, A.F., Harmon, B., Agard, D.A. and Sedat, J.W. (1996) "Specific interactions of chromatin with the nuclear envelope: positional determination within the nucleus in Drosophila melanogaster", *Molecular biology of the cell,* vol. **7**, no. 5, pp. 825-842.

Matera, A.G. (1999) "Nuclear bodies: multifaceted subdomains of the interchromatin space", *Trends in cell biology,* vol. **9**, no. 8, pp. 302-309.

Mayer, R., Brero, A., von Hase, J., Schroeder, T., Cremer, T. and Dietzel, S. (2005) "Common themes and cell type specific variations of higher order chromatin arrangements in the mouse", *BMC cell biology,* vol. **6**, pp. 44.

McDonald, D., Carrero, G., Andrin, C., de Vries, G. and Hendzel, M. (2006) "Nucleoplasmic beta-actin exists in a dynamic equilibrium between low-mobility polymeric species and rapidly diffusing populations", *J.Cell Biology,* vol. **172**, no. 4, pp. 541-552.

Meaburn, K.J., Cabuy, E., Bonne, G., Levy, N., Morris, G.E., Novelli, G., Kill, I.R. and Bridger, J.M. (2007) "Primary laminopathy fibroblasts display altered genome organization and apoptosis", *Aging cell,* vol. **6**, no. 2, pp. 139-153.

Meaburn, K.J., Gudla, P.R., Khan, S., Lockett, S.J. and Misteli, T. (2009) "Disease-specific gene repositioning in breast cancer", *The Journal of cell biology,* vol. **187**, no. 6, pp. 801-812.

Meaburn, K.J. and Misteli, T. (2008) "Locus-specific and activity-independent gene repositioning during early tumorigenesis", *The Journal of cell biology,* vol. **180**, no. 1, pp. 39-50.

Meaburn, K.J. and Misteli, T. (2007a) "Cell biology: chromosome territories", *Nature,* vol. **445**, no. 7126, pp. 379-781.

Meaburn, K.J., Misteli, T. and Soutoglou, E. (2007b) "Spatial genome organization in the formation of chromosomal translocations", *Seminars in cancer biology,* vol. **17**, no. 1, pp. 80-90.

Mehta, I.S., Amira, M., Harvey, A.J. and Bridger, J.M. (2010) "Rapid chromosome territory relocation by nuclear motor activity in response to serum removal in primary human fibroblasts", *Genome biology,* vol. **11**, no. 1, pp. R5.

Mehta, I.S., Elcock, L.S., Amira, M., Kill, I.R. and Bridger, J.M. (2008) "Nuclear motors and nuclear structures containing A-type lamins and emerin: is there a functional link?", *Biochemical Society transactions,* vol. **36**, no. Pt 6, pp. 1384-1388.

Mehta, I., Eskiw, C., Arican, H., Kill, I. and Bridger, J. (2011) "Farnesyltransferase inhibitor treatment restores chromosome territory positions and active chromosome dynamics in Hutchinson-Gilford Progeria syndrome cells", *Genome biology,* vol. **12**, pp. R74.

Meister, P., Towbin, B.D., Pike, B.L., Ponti, A. and Gasser, S.M. (2010) "The spatial dynamics of tissue-specific promoters during C. elegans development", *Genes & development,* vol. **24**, no. 8, pp. 766-782.

Meltzer, E. and Schwartz, E. (2013) "Schistosomiasis: Current Epidemiology and Management in Travelers", *Current infectious disease reports*.

Mendjan, S., Taipale, M., Kind, J., Holz, H., Gebhardt, P., Schelder, M., Vermeulen, M., Buscaino, A., Duncan, K., Mueller, J., Wilm, M., Stunnenberg, H.G., Saumweber, H. and Akhtar, A. (2006) "Nuclear pore components are involved in the transcriptional regulation of dosage compensation in Drosophila", *Molecular cell,* vol. **21**, no. 6, pp. 811-823.

Mermall, V., Post, P.L. and Mooseker, M.S. (1998) "Unconventional myosins in cell movement, membrane traffic, and signal transduction", *Science,* vol. **279**, no. 5350, pp. 527-533.

Miller, A.N., Raghavan, N., FitzGerald, P.C., Lewis, F.A. and Knight, M. (2001) "Differential gene expression in haemocytes of the snail Biomphalaria glabrata: effects of Schistosoma mansoni infection", *International journal for parasitology,* vol. **31**, no. 7, pp. 687-696.

Misteli, T. (2005) "Concepts in nuclear architecture", *BioEssays : news and reviews in molecular, cellular and developmental biology,* vol. **27**, no. 5, pp. 477-487.

Mitchell, J.A. and Fraser, P. (2008) "Transcription factories are nuclear subcompartments that remain in the absence of transcription", *Genes & development,* vol. **22**, no. 1, pp. 20-25.

Mitta, G., Galinier, R., Tisseyre, P., Allienne, J.F., Girerd-Chambaz, Y., Guillou, F., Bouchut, A. and Coustau, C. (2005) "Gene discovery and expression analysis of immune-relevant genes from Biomphalaria glabrata hemocytes", *Developmental and comparative immunology,* vol. **29**, no. 5, pp. 393-407.

Moralli, D. and Monaco, Z.L. (2010) "Simultaneous Visualization of FISH Signals and Bromo-deoxyuridine Incorporation by Formamide-Free DNA Denaturation", *Methods in molecular biology (Clifton, N.J.),* vol. **659**, pp. 203-218.

Morey, C., Da Silva, N.R., Perry, P. and Bickmore, W.A. (2007) "Nuclear reorganisation and chromatin decondensation are conserved, but distinct, mechanisms linked to Hox gene activation", *Development (Cambridge, England),* vol. **134**, no. 5, pp. 909-919.

Morris, G.E. (2008) "The Cajal body", *Biochimica et biophysica acta,* vol. **1783**, no. 11, pp. 2108-2115.

Nakayasu, H. and Ueda, K. (1985) "Ultrastructural localization of actin in nuclear matrices from mouse leukemia L5178Y cells", *Cell structure and function,* vol. **10**, no. 3, pp. 305-309.

Narang, N. (1974) "Chromosomal studies during spermatogenesis and the radiatin induced chromosomal aberrations in*Biomphalaria glabrata.*", *Revista brasileira de pesquisas edicas e biologicas,* vol. **7**, no. 4, pp. 419-425.

Nefkens, I., Negorev, D.G., Ishov, A.M., Michaelson, J.S., Yeh, E.T., Tanguay, R.M., Muller, W.E. and Maul, G.G. (2003) "Heat shock and Cd2+ exposure regulate PML and Daxx release from ND10 by independent mechanisms that modify the induction of heat-shock proteins 70 and 25 differently", *Journal of cell science,* vol. **116**, no. Pt 3, pp. 513-524.

Newton, W.L. (1953) "The inheritance of susceptibility to infection with Schistosoma mansoni in Australorbis glabratus", *Experimental parasitology,* vol. **2**, no. 3, pp. 242-257.

Obrdlik, A., Louvet, E., Kukalev, A., Naschekin, D., Kiseleva, E., Fahrenkrog, B. and Percipalle, P. (2010) "Nuclear myosin 1 is in complex with mature rRNA transcripts and associates with the nuclear pore basket", *FASEB journal : official publication of the Federation of American Societies for Experimental Biology,* vol. **24**, no. 1, pp. 146-157.

Odoemelam, E., Raghavan, N., Miller, A., Bridger, J.M. and Knight, M. (2009) "Revised karyotyping and gene mapping of the Biomphalaria glabrata embryonic (Bge) cell line", *International journal for parasitology,* vol. **39**, no. 6, pp. 675-681.

Odoemelam, E.C., Raghavan, N., Ittiprasert, W., Miller, A., Bridger, J.M. and Knight, M. (2010) "FISH on Chromosomes Derived from the Snail Model Organism Biomphalaria glabrata", *Methods in molecular biology (Clifton, N.J.),* vol. **659**, pp. 379-388.

Osborne, C.S., Chakalova, L., Brown, K.E., Carter, D., Horton, A., Debrand, E., Goyenechea, B., Mitchell, J.A., Lopes, S., Reik, W. and Fraser, P. (2004) "Active genes dynamically colocalize to shared sites of ongoing transcription", *Nature genetics,* vol. **36**, no. 10, pp. 1065-1071.

Osborne, C.S., Chakalova, L., Mitchell, J.A., Horton, A., Wood, A.L., Bolland, D.J., Corcoran, A.E. and Fraser, P. (2007) "Myc dynamically and preferentially relocates to a transcription factory occupied by Igh", *PLoS biology,* vol. **5**, no. 8, pp. e192.

Osborne, C.S. and Eskiw, C.H. (2008) "Where shall we meet? A role for genome organisation and nuclear sub-compartments in mediating interchromosomal interactions", *Journal of cellular biochemistry,* vol. **104**, no. 5, pp. 1553-1561.

Papantonis, A. (2010) "Active RNA Polymerases: Mobile or Immobile Molecular Machines?", *Biology*.

Parada, L. and Misteli, T. (2002) "Chromosome positioning in the interphase nucleus", *Trends in cell biology,* vol. **12**, no. 9, pp. 425-432.

Pearce, E.J. (2003) "Progress towards a vaccine for schistosomiasis", *Acta Tropica,* vol. **86**, no. 2-3, pp. 309-313.

Pederson, T. and Aebi, U. (2002) "Actin in the nucleus: what form and what for?", *Journal of structural biology,* vol. **140**, no. 1-3, pp. 3-9.

Pestic-Dragovich, L., Stojiljkovic, L., Philimonenko, A.A., Nowak, G., Ke, Y., Settlage, R.E., Shabanowitz, J., Hunt, D.F., Hozak, P. and de Lanerolle, P. (2000) "A myosin I isoform in the nucleus", *Science (New York, N.Y.),* vol. **290**, no. 5490, pp. 337-341.

Philimonenko, V.V., Zhao, J., Iben, S., Dingová, H., Kyselá, K., Kahle, M., Zentgraf, H., Hofmann, W.A., de Lanerolle, P., Hozák, P. and Grummt, I. (2004) "Nuclear actin and myosin I are required for RNA polymerase I transcription", *Nat.Cell Biol.,* vol. **6**, no. 12, pp. 1165-1172.

Pickersgill, H., Kalverda, B., de Wit, E., Talhout, W., Fornerod, M. and van Steensel, B. (2006) "Characterization of the Drosophila melanogaster genome at the nuclear lamina", *Nature genetics,* vol. **38**, no. 9, pp. 1005-1014.

Pranchevicius, M.C., Baqui, M.M., Ishikawa-Ankerhold, H.C., Lourenco, E.V., Leao, R.M., Banzi, S.R., dos Santos, C.T., Roque-Barreira, M.C., Espreafico, E.M. and Larson, R.E. (2008) "Myosin Va phosphorylated on Ser1650 is found in nuclear speckles and redistributes to nucleoli upon inhibition of transcription", *Cell motility and the cytoskeleton,* vol. **65**, no. 6, pp. 441-456.

Rabl, K. (1885) "Uber Zelltheilung", *Gegenbaurs Morphol Jahrb,* vol. **10**, pp. 214-330.

Rafael Toledo and Fried, B. (2011) *Biomphalaria Snails and Larval Trematodes,* Springer Science.

Raghavan, N. and Knight, M. (2006) "The snail (Biomphalaria glabrata) genome project", *Trends in parasitology,* vol. **22**, no. 4, pp. 148-151.

Raghavan, N., Miller, A.N., Gardner, M., FitzGerald, P.C., Kerlavage, A.R., Johnston, D.A., Lewis, F.A. and Knight, M. (2003) "Comparative gene analysis of Biomphalaria glabrata hemocytes pre- and post-exposure to miracidia of Schistosoma mansoni", *Molecular and biochemical parasitology,* vol. **126**, no. 2, pp. 181-191.

Raghavan, N., Tettelin, H., Miller, A., Hostetler, J., Tallon, L. and Knight, M. (2007) "Nimbus (BgI): an active non-LTR retrotransposon of the Schistosoma mansoni snail host Biomphalaria glabrata", *International journal for parasitology,* vol. **37**, no. 12, pp. 1307-1318.

Raghunathan, L. (1976) "The karyotype of Biomphalaria glabrata, the snail vector of Schistosoma mansoni", *Malacologia,* vol. **15**, no. 2, pp. 447-450.

Ragoczy, T., Bender, M.A., Telling, A., Byron, R. and Groudine, M. (2006) "The locus control region is required for association of the murine beta-globin locus with engaged transcription factories during erythroid maturation", *Genes & development,* vol. **20**, no. 11, pp. 1447-1457.

Rangel, N.M. (1951) "Nota previa sobre o numero cromossomico de*Australorbis glabratus*", *Ciencia e cultura,* vol. **3**, pp. 284.

Razin, S.V., Gavrilov, A.A., Pichugin, A., Lipinski, M., Iarovaia, O.V. and Vassetzky, Y.S. (2011) "Transcription factories in the context of the nuclear and genome organization", *Nucleic acids research,* vol. **39**, no. 21, pp. 9085-9092.

Richards, C.S. (1973) "Susceptibility of adult Biomphalaria glabrata to Schistosoma mansoni infection", *American Journal of Tropical Medicine and Hygiene,* vol. **22**, no. 6.

Richards, C.S., Knight, M. and Lewis, F.A. (1992) "Genetics of Biomphalaria glabrata and its effect on the outcome of Schistosoma mansoni infection", *Parasitology today (Personal ed.),* vol. **8**, no. 5, pp. 171-174.

Richards, C.S. and Minchella, D.J. (1987) "Transient non-susceptibility to Schistosoma mansoni associated with atrial amoebocytic accumulations in the snail host Biomphalaria glabrata", *Parasitology,* vol. **95**, no. Pt 3, pp. 499-505.

Richards, C.S. and Shade, P.C. (1987) "The genetic variation of compatibility in Biomphalaria glabrata and Schistosoma mansoni", *The Journal of parasitology,* vol. **73**, no. 6, pp. 1146-1151.

Richter, K., Haslbeck, M. and Buchner, J. (2010) "The heat shock response: life on the verge of death", *Molecular cell,* vol. **40**, no. 2, pp. 253-266.

Rieder, C.L. and Palazzo, R.E. (1992) "Colcemid and the mitotic cycle", *Journal of cell science,* vol. **102**, no. Pt 3, pp. 387-392.

Rohner, S., Kalck, V., Wang, X., Ikegami, K., Lieb, J.D., Gasser, S.M. and Meister, P. (2013) "Promoter- and RNA polymerase II-dependent hsp-16 gene association with nuclear pores in Caenorhabditis elegans", *The Journal of cell biology,* vol. **200**, no. 5, pp. 589-604.

Rollinson, D., Webster, J.P., Webster, B., Nyakaana, S., Jorgensen, A. and Stothard, J.R. (2009) "Genetic diversity of schistosomes and snails: implications for control", *Parasitology,* vol. **136**, no. 13, pp. 1801-1811.

Ronne, M. (1989) "Chromosome preparation and high resolution banding techniques. A review", *Journal of dairy science,* vol. **72**, no. 5, pp. 1363-1377.

Schirmer, E.C., Florens, L., Guan, T., Yates, J.R.,3rd and Gerace, L. (2003) "Nuclear membrane proteins with potential disease links found by subtractive proteomics", *Science (New York, N.Y.),* vol. **301**, no. 5638, pp. 1380-1382.

Schirmer, E.C. and Foisner, R. (2007) "Proteins that associate with lamins: many faces, many functions", *Experimental cell research,* vol. **313**, no. 10, pp. 2167-2179.

Schistosoma japonicum Genome Sequencing and Functional Analysis Consortium (2009) "The Schistosoma japonicum genome reveals features of host-parasite interplay", *Nature,* vol. **460**, no. 7253, pp. 345-351.

Schoenenberger, C.A., Buchmeier, S., Boerries, M., Sutterlin, R., Aebi, U. and Jockusch, B.M. (2005) "Conformation-specific antibodies reveal distinct actin structures in the nucleus and the cytoplasm", *Journal of structural biology,* vol. **152**, no. 3, pp. 157-168.

Schoenfelder, S., Sexton, T., Chakalova, L., Cope, N.F., Horton, A., Andrews, S., Kurukuti, S., Mitchell, J.A., Umlauf, D., Dimitrova, D.S., Eskiw, C.H., Luo, Y., Wei, C., Ruan, Y., Bieker, J.J. and Fraser, P. (2010) "Preferential associations between co-regulated genes reveal a transcriptional interactome in erythroid cells", *Nature genetics,* vol. **42**, no. 1, pp. 53-61.

Schul, W., Adelaar, B., van Driel, R. and de Jong, L. (1999) "Coiled bodies are predisposed to a spatial association with genes that contain snoRNA sequences in their introns", *Journal of cellular biochemistry,* vol. **75**, no. 3, pp. 393-403.

Shaffer, L.R., Marilyn L. Slovak and Lynda J. Campbell (2009) *ISCN 2009: An International System for Human Cytogenetic Nomenclature (2009): Recommendations of the International Standing Committee on Human Cytogenetic Nomenc,* S. Karger AG (Switzerland).

Shaklai, S., Amariglio, N., Rechavi, G. and Simon, A.J. (2007) "Gene silencing at the nuclear periphery", *The FEBS journal,* vol. **274**, no. 6, pp. 1383-1392.

Shiels, C., Islam, S.A., Vatcheva, R., Sasieni, P., Sternberg, M.J., Freemont, P.S. and Sheer, D. (2001) "PML bodies associate specifically with the MHC gene cluster in interphase nuclei", *Journal of cell science,* vol. **114**, no. Pt 20, pp. 3705-3716.

Shopland, L.S., Johnson, C.V., Byron, M., McNeil, J. and Lawrence, J.B. (2003) "Clustering of multiple specific genes and gene-rich R-bands around SC-35 domains: evidence for local euchromatic neighborhoods", *The Journal of cell biology,* vol. **162**, no. 6, pp. 981-990.

Siddiqui, A.A., Siddiqui, B.A. and Ganley-Leal, L. (2011) "Schistosomiasis vaccines", *Human Vaccines,* vol. **7**, no. 11, pp. 1192-1197.

Solovei, I. and Cremer, M. (2010) "3D-FISH on Cultured Cells Combined with Immunostaining", *Methods in molecular biology (Clifton, N.J.),* vol. **659**, pp. 117-126.

Solovei, I., Kreysing, M., Lanctot, C., Kosem, S., Peichl, L., Cremer, T., Guck, J. and Joffe, B. (2009) "Nuclear architecture of rod photoreceptor cells adapts to vision in mammalian evolution", *Cell,* vol. **137**, no. 2, pp. 356-368.

Spector, D.L. (2006) "SnapShot: Cellular bodies", *Cell,* vol. **127**, no. 5, pp. 1071.

Spector, D.L. (2001) "Nuclear domains", *Journal of cell science,* vol. **114**, no. Pt 16, pp. 2891-2893.

Spector, D.L. and Lamond, A.I. (2010) "Nuclear Speckles", *Cold Spring Harbor Perspectives in Biology,* vol. **3**, no. 2, pp. a000646-a000646.

Stack, S.M., Brown, D.B. and Dewey, W.C. (1977) "Visualization of interphase chromosomes", *Journal of cell science,* vol. **26**, pp. 281-299.

Strouboulis, J. and Wolffe, A.P. (1996) "Functional compartmentalization of the nucleus", *Journal of cell science,* vol. **109**, no. Pt 8, pp. 1991-2000.

Sutherland, H. and Bickmore, W.A. (2009) "Transcription factories: gene expression in unions?", *Nature reviews.Genetics,* vol. **10**, no. 7, pp. 457-466.

Szczerbal, I. and Bridger, J.M. (2010) "Association of adipogenic genes with SC-35 domains during porcine adipogenesis", *Chromosome research : an international journal on the molecular, supramolecular and evolutionary aspects of chromosome biology,* vol. **18**, no. 8, pp. 887-895.

Szczerbal, I., Foster, H.A. and Bridger, J.M. (2009) "The spatial repositioning of adipogenesis genes is correlated with their expression status in a porcine mesenchymal stem cell adipogenesis model system", *Chromosoma,* vol. **118**, no. 5, pp. 647-663.

Taddei, A., Van Houwe, G., Hediger, F., Kalck, V., Cubizolles, F., Schober, H. and Gasser, S.M. (2006) "Nuclear pore association confers optimal expression levels for an inducible yeast gene", *Nature,* vol. **441**, no. 7094, pp. 774-778.

Taguchi, T., Hirai, Y., LoVerde, P.T., Tominaga, A. and Hirai, H. (2007) "DNA probes for identifying chromosomes 5, 6, and 7 of Schistosoma mansoni", *The Journal of parasitology,* vol. **93**, no. 3, pp. 724-726.

Takizawa, T., Gudla, P.R., Guo, L., Lockett, S. and Misteli, T. (2008a) "Allele-specific nuclear positioning of the monoallelically expressed astrocyte marker GFAP", *Genes & development,* vol. **22**, no. 4, pp. 489-498.

Takizawa, T., Meaburn, K.J. and Misteli, T. (2008b) "The meaning of gene positioning", *Cell,* vol. **135**, no. 1, pp. 9-13.

Toivola, D.M., Strnad, P., Habtezion, A. and Omary, M.B. (2009) "Intermediate filaments take the heat as stress proteins", *Trends in cell biology*.

Venter, J.C., Adams, M.D., Myers, E.W., Li, P.W., Mural, R.J., Sutton, G.G., Smith, H.O., Yandell, M., Evans, C.A., Holt, R.A., Gocayne, J.D., Amanatides, P., Ballew, R.M., Huson, D.H., Wortman, J.R., Zhang, Q., Kodira, C.D., Zheng, X.H., Chen, L., Skupski, M., Subramanian, G., Thomas, P.D., Zhang, J., Gabor Miklos, G.L., Nelson, C., Broder, S., Clark, A.G., Nadeau, J., McKusick, V.A., Zinder, N., Levine, A.J., Roberts, R.J., Simon, M., Slayman, C., Hunkapiller, M., Bolanos, R., Delcher, A., Dew, I., Fasulo, D., Flanigan, M., Florea, L., Halpern, A., Hannenhalli, S., Kravitz, S., Levy, S., Mobarry, C., Reinert, K., Remington, K., Abu-Threideh, J., Beasley, E., Biddick, K., Bonazzi, V., Brandon, R., Cargill, M.,

Chandramouliswaran, I., Charlab, R., Chaturvedi, K., Deng, Z., Di Francesco, V., Dunn, P., Eilbeck, K., Evangelista, C., Gabrielian, A.E., Gan, W., Ge, W., Gong, F., Gu, Z., Guan, P., Heiman, T.J., Higgins, M.E., Ji, R.R., Ke, Z., Ketchum, K.A., Lai, Z., Lei, Y., Li, Z., Li, J., Liang, Y., Lin, X., Lu, F., Merkulov, G.V., Milshina, N., Moore, H.M., Naik, A.K., Narayan, V.A., Neelam, B., Nusskern, D., Rusch, D.B., Salzberg, S., Shao, W., Shue, B., Sun, J., Wang, Z., Wang, A., Wang, X., Wang, J., Wei, M., Wides, R., Xiao, C., Yan, C., Yao, A., Ye, J., Zhan, M., Zhang, W., Zhang, H., Zhao, Q., Zheng, L., Zhong, F., Zhong, W., Zhu, S., Zhao, S., Gilbert, D., Baumhueter, S., Spier, G., Carter, C., Cravchik, A., Woodage, T., Ali, F., An, H., Awe, A., Baldwin, D., Baden, H., Barnstead, M., Barrow, I., Beeson, K., Busam, D., Carver, A., Center, A., Cheng, M.L., Curry, L., Danaher, S., Davenport, L., Desilets, R., Dietz, S., Dodson, K., Doup, L., Ferriera, S., Garg, N., Gluecksmann, A., Hart, B., Haynes, J., Haynes, C., Heiner, C., Hladun, S., Hostin, D., Houck, J., Howland, T., Ibegwam, C., Johnson, J., Kalush, F., Kline, L., Koduru, S., Love, A., Mann, F., May, D., McCawley, S., McIntosh, T., McMullen, I., Moy, M., Moy, L., Murphy, B., Nelson, K., Pfannkoch, C., Pratts, E., Puri, V., Qureshi, H., Reardon, M., Rodriguez, R., Rogers, Y.H., Romblad, D., Ruhfel, B., Scott, R., Sitter, C., Smallwood, M., Stewart, E., Strong, R., Suh, E., Thomas, R., Tint, N.N., Tse, S., Vech, C., Wang, G., Wetter, J., Williams, S., Williams, M., Windsor, S., Winn-Deen, E., Wolfe, K., Zaveri, J., Zaveri, K., Abril, J.F., Guigo, R., Campbell, M.J., Sjolander, K.V., Karlak, B., Kejariwal, A., Mi, H., Lazareva, B., Hatton, T., Narechania, A., Diemer, K., Muruganujan, A., Guo, N., Sato, S., Bafna, V., Istrail, S., Lippert, R., Schwartz, R., Walenz, B., Yooseph, S., Allen, D., Basu, A., Baxendale, J., Blick, L., Caminha, M., Carnes-Stine, J., Caulk, P., Chiang, Y.H., Coyne, M., Dahlke, C., Mays, A., Dombroski, M., Donnelly, M., Ely, D., Esparham, S., Fosler, C., Gire, H., Glanowski, S., Glasser, K., Glodek, A., Gorokhov, M., Graham, K., Gropman, B., Harris, M., Heil, J., Henderson, S., Hoover, J., Jennings, D., Jordan, C., Jordan, J., Kasha, J., Kagan, L., Kraft, C., Levitsky, A., Lewis, M., Liu, X., Lopez, J., Ma, D., Majoros, W., McDaniel, J., Murphy, S., Newman, M., Nguyen, T., Nguyen, N., Nodell, M., Pan, S., Peck, J., Peterson, M., Rowe, W., Sanders, R., Scott, J., Simpson, M., Smith, T., Sprague, A., Stockwell, T., Turner, R., Venter, E., Wang, M., Wen, M., Wu, D., Wu, M., Xia, A., Zandieh, A. and Zhu, X. (2001) "The sequence of the human genome", *Science (New York, N.Y.),* vol. **291**, no. 5507, pp. 1304-1351.

Verheggen, C., Lafontaine, D.L., Samarsky, D., Mouaikel, J., Blanchard, J.M., Bordonne, R. and Bertrand, E. (2002) "Mammalian and yeast U3 snoRNPs are matured in specific and related nuclear compartments", *The EMBO journal,* vol. **21**, no. 11, pp. 2736-2745.

Volpi, E.V. and Bridger, J.M. (2008) "FISH glossary: an overview of the fluorescence in situ hybridization technique", *BioTechniques,* vol. **45**, no. 4, pp. 385-390.

Volpi, E.V., Chevret, E., Jones, T., Vatcheva, R., Williamson, J., Beck, S., Campbell, R.D., Goldsworthy, M., Powis, S.H., Ragoussis, J., Trowsdale, J. and Sheer, D. (2000) "Large-scale chromatin organization of the major histocompatibility complex and other regions of human chromosome 6 and its response to interferon in interphase nuclei", *Journal of cell science,* vol. **113**, no. Pt 9, pp. 1565-1576.

Vreugde, S., Ferrai, C., Miluzio, A., Hauben, E., Marchisio, P.C., Crippa, M.P., Bussi, M. and Biffo, S. (2006) "Nuclear myosin VI enhances RNA polymerase II-dependent transcription", *Molecular cell,* vol. **23**, no. 5, pp. 749-755.

Walker, A.J. (2011) "Insights into the functional biology of schistosomes", *Parasites & vectors,* vol. **4**, no. 1, pp. 203.

Walker, A.J. (2006) "Do trematode parasites disrupt defence-cell signalling in their snail hosts?", *Trends in parasitology,* vol. **22**, no. 4, pp. 154-159.

Wang, J., Shiels, C., Sasieni, P., Wu, P.J., Islam, S.A., Freemont, P.S. and Sheer, D. (2004) "Promyelocytic leukemia nuclear bodies associate with transcriptionally active genomic regions", *The Journal of cell biology,* vol. **164**, no. 4, pp. 515-526.

Wang, S.H. and Elgin, S.C. (2011) "Drosophila Piwi functions downstream of piRNA production mediating a chromatin-based transposon silencing mechanism in female germ line", *Proceedings of the National Academy of Sciences of the United States of America,* vol. **108**, no. 52, pp. 21164-21169.

Wansink, D.G., Schul, W., van der Kraan, I., van Steensel, B., van Driel, R. and de Jong, L. (1993) "Fluorescent labeling of nascent RNA reveals transcription by RNA polymerase II in domains scattered throughout the nucleus", *The Journal of cell biology,* vol. **122**, no. 2, pp. 283-293.

Welch, W.J. and Suhan, J.P. (1985) "Morphological study of the mammalian stress response: characterization of changes in cytoplasmic organelles, cytoskeleton, and nucleoli, and appearance of intranuclear actin filaments in rat fibroblasts after heat-shock treatment", *The Journal of cell biology,* vol. **101**, no. 4, pp. 1198-1211.

WHO. *Schistosomiasis*. Available at: http://www.who.int/schistosomiasis/en/ (Accessed: 04/10/2008 2008).

Williams, R.R., Azuara, V., Perry, P., Sauer, S., Dvorkina, M., Jorgensen, H., Roix, J., McQueen, P., Misteli, T., Merkenschlager, M. and Fisher, A.G. (2006) "Neural induction promotes large-scale chromatin reorganisation of the Mash1 locus", *Journal of cell science,* vol. **119**, no. Pt 1, pp. 132-140.

Wright, B., Lacchini, A.H., Davies, A.J. and Walker, A.J. (2006) "Regulation of nitric oxide production in snail (Lymnaea stagnalis) defence cells: a role for PKC and ERK signalling pathways", *Biology of the cell / under the auspices of the European Cell Biology Organization,* vol. **98**, no. 5, pp. 265-278.

Xu, M. and Cook, P.R. (2008) "Similar active genes cluster in specialized transcription factories", *The Journal of cell biology,* vol. **181**, no. 4, pp. 615-623.

Yao, J., Ardehali, M.B., Fecko, C.J., Webb, W.W. and Lis, J.T. (2007) "Intranuclear distribution and local dynamics of RNA polymerase II during transcription activation", *Molecular cell,* vol. **28**, no. 6, pp. 978-990.

Yoshino, T.P. and Bayne, C.J. (1983) "Mimicry of snail host antigens by miracidia and primary sporocysts of Schistosoma mansoni", *Parasite immunology,* vol. **5**, no. 3, pp. 317-328.

Yoshino, T.P. and Laursen, J.R. (1995) "Production of Schistosoma mansoni daughter sporocysts from mother sporocysts maintained in synxenic culture with Biomphalaria glabrata embryonic (Bge) cells", *The Journal of parasitology,* vol. **81**, no. 5, pp. 714-722.

Yoshino, T.P. (2012) "Glycotope Sharing between Snail Hemolymph and Larval Schistosomes: Larval Transformation Products Alter Shared Glycan Patterns of Plasma Proteins", *Neglected Tropical Diseases.*

Yoshino, T.P. and Coustau, C. (2011) "Biomphalaria Snails and Larval Trematodes; Immunobiology of Biomphalaria–Trematode Interactions", pp. 159-189.

Young, N.D., Jex, A.R., Li, B., Liu, S., Yang, L., Xiong, Z., Li, Y., Cantacessi, C., Hall, R.S., Xu, X., Chen, F., Wu, X., Zerlotini, A., Oliveira, G., Hofmann, A., Zhang, G., Fang, X., Kang, Y., Campbell, B.E., Loukas, A., Ranganathan, S., Rollinson, D., Rinaldi, G., Brindley, P.J., Yang, H., Wang, J., Wang, J. and Gasser, R.B. (2012) "Whole-genome sequence of Schistosoma haematobium", *Nature genetics,* vol. **44**, no. 2, pp. 221-225.

Zahoor, Z., Davies, A.J., Kirk, R.S., Rollinson, D. and Walker, A.J. (2008) "Disruption of ERK signalling in Biomphalaria glabrata defence cells by Schistosoma mansoni: Implications for parasite survival in the snail host", *Developmental and comparative immunology,* vol. **32**, no. 12, pp. 1561-1571.

Zahoor, Z., Davies, A.J., Kirk, R.S., Rollinson, D. and Walker, A.J. (2009) "Nitric oxide production by Biomphalaria glabrata haemocytes: effects of Schistosoma mansoni ESPs and regulation through the extracellular signal-regulated kinase pathway", *Parasites & Vectors,* vol. **2**, no. 1, pp. 18.

Zahoor, Z., Davies, A.J., Kirk, R.S., Rollinson, D. and Walker, A.J. (2010) "Larval excretory-secretory products from the parasite Schistosoma mansoni modulate HSP70 protein expression in defence cells of its snail host, Biomphalaria glabrata", *Cell Stress and Chaperones*.

Zhang, S.M., Zeng, Y. and Loker, E.S. (2008) "Expression profiling and binding properties of fibrinogen-related proteins (FREPs), plasma proteins from the schistosome snail host Biomphalaria glabrata", *Innate immunity,* vol. **14**, no. 3, pp. 175-189.

Zhao, K., Wang, W., Rando, O., Xue, Y., Swiderek, K., Kuo, A. and Crabtree, G. (1998) "Rapid and phosphoinositol-dependent binding of the SWI/SNF-like BAF complex to chromatin after T lymphocyte receptor signaling", *Cell,* vol. **95**, no. 5, pp. 625-636.

Zhao, R., Bodnar, M.S. and Spector, D.L. (2009) "Nuclear neighborhoods and gene expression", *Current opinion in genetics & development,* vol. **19**, no. 2, pp. 172-179.

Zimber, A., Nguyen, Q.D. and Gespach, C. (2004) "Nuclear bodies and compartments: functional roles and cellular signalling in health and disease", *Cellular signalling,* vol. **16**, no. 10, pp. 1085-1104.

Zink, D., Amaral, M.D., Englmann, A., Lang, S., Clarke, L.A., Rudolph, C., Alt, F., Luther, K., Braz, C., Sadoni, N., Rosenecker, J. and Schindelhauer, D. (2004a) "Transcription-dependent spatial arrangements of CFTR and adjacent genes in human cell nuclei", *The Journal of cell biology,* vol. **166**, no. 6, pp. 815-825.

Zink, D., Fischer, A.H. and Nickerson, J.A. (2004b) "Nuclear structure in cancer cells", *Nature reviews.Cancer,* vol. **4**, no. 9, pp. 677-687.

Appendix I

List of publications:

Joanna M. Bridger; **Halime D. Arican-Goktas**; Helen A. Foster; Lauren S. Godwin; Amanda Harvey; Ian R. Kill; Matty Knight; Ishita S. Mehta; Mai Hassan Ahmed. (2013, book chapter) The non-random repositioning of whole chromosomes and individual gene loci in interphase nuclei and its relevance in disease, infection, aging and cancer: Cancer and the nuclear envelope. Edited by Eric Schirmer and Jose de las Heras. *Springer.*

Mehta, I.S., Eskiw, C.H., **Arican, H.D.**, Kill, I.R. and Bridger, J.M. (2011) Farnesyltransferase inhibitor treatment restores chromosome territory positions and active chromosome dynamics in Hutchinson-Gilford Progeria syndrome cells. *Genome Biology.* **12.** R74.

Halime D. Arican, Matty Knight, Joanna M. Bridger. (2011, published abstract) Parasitic influences on the host genome using the molluscan model organism Biomphalaria glabrata. *The Malacologist.* **56**. 3.

Joanna M. Bridger, Edwin C. Odoemelam, **Halime D. Arican**, Ishita S. Mehta, Nithya Raghavan, Wannaporn Ittiprasert, Andre Miller, Matty Knight. (2009, published abstract) Spatial repositioning of gene loci in the interphase nuclei of Bge cells co-cultured with *Schistosoma mansoni* parasite. *The American Society of Tropical Medicine and Hygiene.* 321.

Publications:

Joanna M. Bridger, Edwin C. Odoemelam, **Halime D. Arican**, Ishita S. Mehta, Nithya Raghavan, Wannaporn Ittiprasert, Andre Miller, Matty Knight. (2009, published abstract) Spatial repositioning of gene loci in the interphase nuclei of Bge cells co-cultured with *Schistosoma mansoni* parasite. *The American Society of Tropical Medicine and Hygiene.* 321.

The genome of mammals is highly organized when packed into interphase cell nuclei. Individual chromosomes are located in their own nuclear areas with minimal intermingling, termed chromosome territories. These chromosome territories are non-randomly positioned within cell nuclei, as are gene loci. We have found that snails are no exception and organise their genome in chromosome territories in interphase nuclei and exhibit specific nuclear radial locations for gene loci.

The nuclear interior is associated with active gene expression whereas the nuclear periphery is a repressive environment with respect to transcription. Indeed, gene loci nuclear positioning has been correlated with gene expression regulation in a number of different animal species. Bge cells are a cell-line derived from an embryonic Biomphalaria glabrata snail in the 1970s. The cells can be infected with parasite *in vitro* and so provide a good model system in which to assess cellular and genomic responses to schistosoma infection. We have found that gene loci that are up regulated after infection have become repositioned in the nuclei of the infected cells, into a significantly more interior location, whereas a control gene is relocated more to the nuclear periphery. This leads us to postulate that upon parasite infection there is a major reorganization of the host genome that may be involved in controlling host gene expression. In support of this we have observed measurable and significant differences in global chromatin/histone methylation soon after parasitic infection of whole snails, as revealed by specific antibodies. The mechanism through which genome behaviour and dynamics are controlled and respond to parasitic infection could be a target to control infection.

Halime D. Arican, Matty Knight, Joanna M. Bridger. (2011, published abstract) Parasitic influences on the host genome using the molluscan model organism Biomphalaria glabrata. *The Malacologist.* **56**. 3.

The freshwater snail Biomphalaria glabrata is an intermediate host for *Schistosoma mansoni* parasites, causing one of the most prevalent parasitic infections in mammals, known as schistosomiasis (*Bilharzia*). Due to its importance in the spread of the disease and to develop new control measures *B. glabrata* has been selected for whole genome sequencing and thus a molluscan model organism.

This study will investigate the influence on genome behaviour in the snail by the parasite and ways we can interfere with this host -parasite interaction. For the first time responsive genes have been positioned in the interphase nuclei of ex vivo cells from the whole snail. We are also developing protocols for the genome sequencing project and have successfully developed a robust chromosome spreading procedure for *B. glabrata* chromosomes derived from the ovotestis.

Joanna M. Bridger; **Halime D. Arican-Goktas**; Helen A. Foster; Lauren S. Godwin; Amanda Harvey; Ian R. Kill; Matty Knight; Ishita S. Mehta; Mai Hassan Ahmed. (2013, book chapter) The non-random repositioning of whole chromosomes and individual gene loci in interphase nuclei and its relevance in disease, infection, aging and cancer: Cancer and the nuclear envelope. Edited by Eric Schirmer and Jose de las Heras. *Springer.*

The genomes of a wide range of different organisms are non-randomly organized within interphase nuclei. Chromosomes and genes can be moved rapidly, with direction, to new non-random locations within nuclei upon a stimulus such as a signal to initiate differentiation, quiescence or senescence, or also the application of heat or an infection with a pathogen. It is now becoming increasingly obvious that chromosome and gene position can be altered in diseases such as cancer and other syndromes that are affected by changes to nuclear architecture such as the laminopathies. This repositioning seems to affect gene expression in these cells and may play a role in progression of the disease. We have some evidence in breast cancer cells and in the premature ageing disease Hutchinson-Gilford Progeria that an aberrant nuclear envelope may lead to genome repositioning and correction of these nuclear envelope defects can restore proper gene positioning and expression in both disease situations.

Although spatial positioning of the genome probably does not entirely control expression of genes, it appears that spatio-epigenetics may enhance the control over gene expression globally and/or is deeply involved in regulating specific sets of genes. A deviation from normal spatial positioning of the genome for a particular cell type could lead to changes that affect the future health of the cell or even an individual.